UNIVERSITE DES SCIENCES ET TECHNOLOGIES DE LILLE

ECOLE DOCTORALE DE BIOLOGIE-SANTE

THESE DE DOCTORAT

En vue de l'obtention du grade de docteur en sciences de l'université des sciences et technologies de Lille

Présenté par

Flore HERVE

Development of an LTP-MS system for breast cancer diagnosis based on volatilomics analysis

A Lille le 20 octobre 2020

Présenté devant le jury compose de:

Rapporteur	Mme Christine ENJALBAL	Professeur (Montpellier)
Rapporteur	Mr Stéphane Le CALVÉ	Docteur (Directeur de recherche au CNRS de Strasbourg)
Examinateur	Mr Régis MATRAN	Professeur (CHR de lille)
Directrice de thèse	Mme Isabelle FOURNIER	Professeur (Université de Lille)
Co-encadrant de thèse	Mr Julien FRANCK	Maitre de conférences (Université de Lille)

Acknowledgement

Je tiens à remercier les professeurs Michel SALZET, directeur du laboratoire et Isabelle FOURNIER co-directrice et encadrante de ma thèse pour m'avoir permis de réaliser cette thèse ambitieuse au sein de leur laboratoire avec le degré de liberté qui m'a été accordé.

Je remercie également mon co-encadrant, le Dr Julien FRANCK, pour le temps et son investissement qu'il m'a accordé tout au long de ma thèse.

Je remercie particulièrement les professeurs Christine ENJALBAL, Stéphane Le CALVÉ et Régis MATRAN qui m'ont fait l'honneur d'accepter d'être jurys et examinateurs de mon travail.

Merci à tous les collaborateurs qui m'ont fourni de nombreux échantillons précieux dont le Dr Nawal HAJAJI et le Dr Sébastien OLIVIER

Je souhaite faire un clin d'œil à tous mes collègues ayant partagés ou non mon bureau et les remercier pour tous les bon moments partagés.
Un grand merci à Jean Pascal GIMENOT qui toujours été là pour m'aider à travers mes nombreuses installations et difficultés.
Merci aussi à Philippe SAUDEMONT, pour son aide précieuse dans le design et impression 3D. Merci également à Maya pour son savoir-faire et réactivité dans le soufflage des nombreux prototypes en verres.

Evidemment, je remercie énormément mes deux compères Mélanie et Lauranne d'avoir partagé, vécu ces trois années avec moi et qui sont devenus bien plus des amis que des collègues. Sans aucun doute, vous avez été mes repères au sein du laboratoire ; nous avons traversé avec engouement, tristesse, énervement et joie cette dure épreuve mais toujours en une seul unité. Ces discussions improbable parfois trop animées, idées si prometteuses et habitudes que nous avons eu ensemble me manquerons inévitablement.

Merci à mon frère jumeau formidable qui m'a fait devenir cette personne manuelle et ingénieuse. Sans nos constantes constructions et innovations je n'aurais pas pu mettre à bien ce projet.

Un immense merci à mes parents qui m’ont toujours inculqués et donnés la volonté de toujours mieux faire. C’est grâce à vous si je suis arrivée ici.

Table of contents

List of abbreviations

ADH: Alcohol dehydrogenase

ALDH Aldehyde dehydrogenase

APCI: Atmospheric pressure chemical ionization

API: Atmospheric pressure ionization

APNP: Atmospheric pressure non-equilibrium plasma

APPI: Atmospheric pressure Photo ionization

AS: Active sampling

BC: Breast cancer

Bp: Boiling point

CAR: Carboxen 2,6-diphenyl-p-phenylene oxide polymer

CD: Corona discharge

CI: Chemical ionisation

CNT gas sensor: Carbon nanotubes gas sensors

COD: Cancer odor database

CP: Liquid acceptor phase

CYP: Cythochrome

DART: Direct analysis in real time

DBD: Dielectric barrier discharge

DE: Double electrode

DFE: Dielectric free electrode

DHS: Dynamic headspace sampling

DIMS: Direction injection mass spectrometry

DNA: Dexoribose nucleic acid

DS: Direct systeme

DVB: Divinylbenzene

EI: Electric impact ionization

EPA: Environmental protection agency

ER: Oestrogen receptor

ESI: Electrospray ionisation

FP: Filter paper

FTMS: Fournier transformation mass spectrometer

GC: Gas chromatography

GP: Gas phase

HMDB: Human metabolome database

HS: Headspace

IMS: Ion mobility mass spectrometry

IS: Indirect system

ISF: Interstitial fluids

IT: Ion trap

LC: Liquid chromatography

LDA: Linear discriminative analysis

LIT: Linear ion trap

LOD: Limit of detection

LPO: lipid peroxidation

LTE: Local thermal plasma, or thermal plasma

LTP: Low temperature plasma

MALDI: Matrix assisted laser desorption

MEMS: Micro-electro-mechanical system

MIMS: Membrane introduction mass spectrometry

MOS gas sensor: Metal oxide semiconductor

MS: Mass spectrometer

MWAS: Metabolome-wide association studies

NaCl: Sodium chlorur

NMR: Nuclear magnetic resonance

NTD: Needle trap device

NTP: Non-thermal plasma

OMIC: Field of study in biology ending in *–omics*

OS: Oxidative stress

P&T: Purge and trap

PA: Probe angle

PA: Proton affinity

PCA: Principal component analysis

PDMS : Polydimethylsiloxane

PDMS: Polydimetyl siloxane

PE: Probe to the edge of the slide

PM: Probe to the inlet of mass spectrometer

Ppb; parts per billion

Ppm parts per million

Ppt: partis per trillion

PR: Progesterone receptor

PS: Passive sampling

PS: Probe to the sample

PTR: Proton transfer reaction

PUFA: Poly- saturated fatty acids

Q: Quad

QCM acoustic sensor: Qartz crystal micro-balance acoustic sensor

ROS: Reactive oxygen species

Rpm: Rotation per minute

SAW das sensor: Surface acoustic wave gas sensor

SE: Single electrode

SHS: Static headspace sampling

SIFT: Selected ion Fournier transformation

SPME: Solid phase micro extraction

SvDHS: Static- vacuum based Dynamic headspace sampling

TA: Tube angle

TD: Thermal desorption

TM: Tube to the inlet of mass spectrometer

TOF: Time of flight

TX: Tenax

vDHS: vacuum based Dynamic headspace sampling

VOC: Volatile organic compound

Vp: Vapor pressure

VVOC: Very volatile

λb: a : Blood: air partition coefficient

λf:b: fat: Blood partition coefficient

General introduction

Despite public health efforts and focus on prevention, the constant rise of cancer has led to 18.1 million new cases and 9.6 million deaths in 2018[1]. Worldwide, one in six women develops cancer during their lifetime, and one in eleven women dies from it. Breast cancer (BC) is the leading cancer in women[2] in both developed and developing countries. There were about 2,088,849 (11.6%) newly diagnosed female BC cases in 2018 and a total of 626,679 (6.6%) women died. This increase is due to several factors, including population growth and ageing as well as the changing prevalence of certain causes of cancer linked to social and economic development. The majority of women with BC are diagnosed in the late stages and the overall five-year survival rate is very low, with a range of 10−40%. On the other hand, the five-year survival rate for early localized BC exceeds 80% in settings where early detection and basic treatment are available and accessible.

In order to improve BC outcomes, enhance survival and minimize recurrence, early detection and early diagnosis is critical[3]. Early detection is only possible through early screening, thereby early diagnosis stems from early screening

Screening involves the systematic application of a screening test to identify cancers before any symptoms appear; at an early stage when it can be treated and may be cured. Various methods have been evaluated as BC screening tools, including mammography[4], magnetic resonance imaging (MRI)[5] and ultrasound[6]. Each of these techniques has several drawbacks[7] due to their invasiveness (X-ray, contrast agent), cost, accuracy, sensitivity and specificity.

The strategies of early screening and detection focus on providing timely access to cancer treatment by improving access to effective diagnosis services and reducing barriers to care. The goal is to increase the proportion of breast cancers identified at an early stage, allowing for more effective treatment to be used and reducing the risks of death from BC.

In this context extensive effort were made to highlight biological characteristic consider as an indicator of a normal biological and pathological process or response to a therapeutic intervention called biomarker[8]. Biomarkers are powerful tools for early cancer detection and selection of therapeutic strategy, thus improving the outcome of cancer treatment and reducing cancer-related mortalities.

The purpose of OMIC science[9] (Figure 1) (genomics, transcriptomic, proteomics and metabolomics) in cancer research relies on the identification of cancer-specific biomarkers[10] based on untargeted analysis.

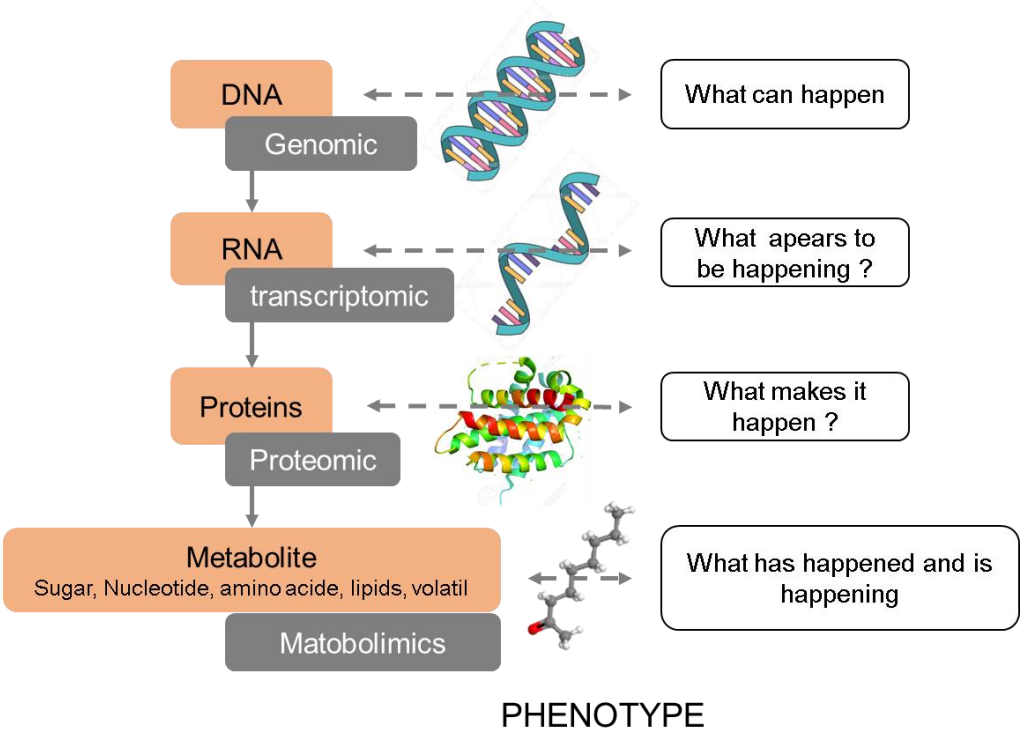

Figure 1: The OMICs' cascade. Interrelations and interactions between genomics, transcriptomics, proteomics and metabolomics

The recent advances in OMICs approaches allow the development of analytical tools and approaches, that can screen, decode phenotype variations and processes occurring in the metabolism of an organism. In the case of BC, several biomarkers are currently used for diagnosis and prognosis[11]. The most common BC markers are the oestrogen receptor (ER)[12] and the progesterone receptor (PR). Recent researches were focused on genetic markers arising from somatic or germline mutations (ER-positive and –negative) while others on serum markers for diagnosis of systematic recurrence (cancer antigen and carcinoembryonic antigen levels). Even though these biomarkers help to characterize, diagnose and prognose cancer, the genetic and proteomic approaches suffer from a lack of sensitive molecular readout often associated with disease and stages. Additionally, the technologies associated with these approaches are often expensive and unavailable in many medical facilities.

To overcome these drawbacks, the metabolites [10] present in cells, tissue or fluids, have been the focus of biomarker discovery studies for a long time[10]. Metabolites are

products of cellular processes, mediated by proteins. Therefore, changes in metabolites are presumed to be reflective of changes in function of the mediating enzymes and proteins[13]. Thereby, metabolite composition marks a biological endpoint that reflects the genetic, epigenetic and proteomic profile specific to a physiological and physio-pathological environment. Metabolites are considered as a source of cancer biomarkers and can be used as a fingerprint to detect and classify pathologies. In this context, large scale metabolomics, untargeted approach[14] (Figure 2) is now becoming a suitable tool for providing pattern recognition procedures for diagnosis and for the assessment of robust etiological pathways[15].

Metabolites (lipids, nucleotides, amino acid, saccharides and volatile compounds) are small molecules (<1500Da) which can be classified according to their properties including polarity and volatility. Metabolomics research[16] has recently focused on the detection of Volatile Organic Compounds (VOCs); a promising approach to achieve accurate, time-efficient and non-invasive screening[17].

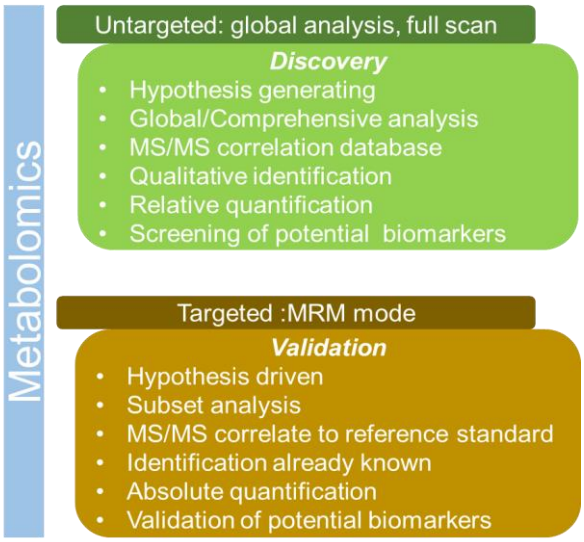

Figure 2: Targeted and untargeted approaches in metabolomics

Part of the metabolome, VOCs are rapidly emerging as an alternative source of biomarkers. Initially introduced for alcohol breath test detection, volatolomics analysis has continued to expand due to widespread applications as cancer detection[18]. VOCs are released during cellular metabolic processes and therefore they can be detected in body fluids and can be exhaled via the exchange of gas/blood. It can be assumed that different phenotypes of cancer including BC can be distinguished by the examination of VOCs[18]. Due to their characteristic, untargeted VOC analysis[19] (Figure

3) can discriminate groups (healthy vs diseases) based on the molecular fingerprint and can be used to identify biomarkers. Subsequently, the selected marks (fingerprint or biomarker) are used as reference for cancer screening. In early studies, some selected VOC based biomarkers were found to be promising in accurate discrimination of cancer patients[20]. VOCs based cancer-screening methods (fingerprint or biomarker) open new frontiers in accurate and non-invasive monitoring of human body[21]. Furthermore VOCs screening can offer real time and quasi real time analysis.

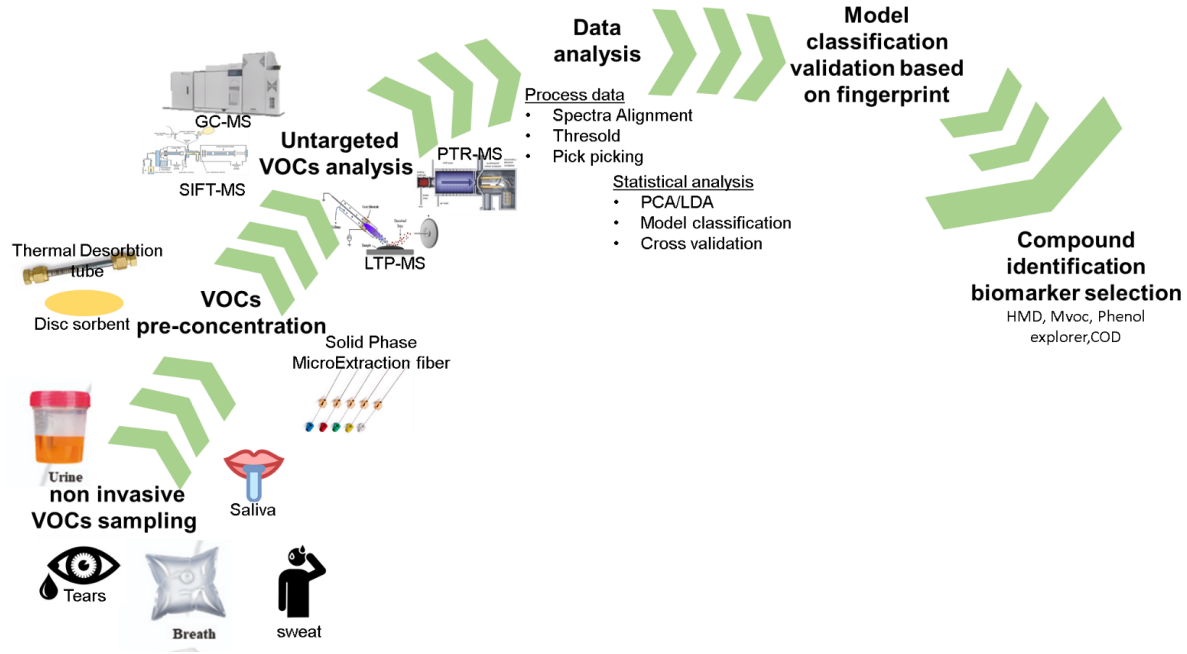

Figure 3: Workflow of untargeted volatolomic analysis for model discrimination.

VOCs based non-invasive screening can be achieved by numerous separative and non-separative MS methods. The gold standard method of VOCs analysis is based on separative gas chromatography-mass spectrometer method. Meanwhile, Low Temperature Plasma coupled to mass spectrometry (LTP-MS) is the most versatile non-separative method[22]. This analytical system can detect VOCs from different sources (e.g. liquid, solid, gas) at ambient pressure and temperature and can ensure real-time and quasi-real-time non-invasive analysis with possible portability and miniaturization.

Consequently, a LTP-MS system will be designed for the diagnosis of BC based on the detection of VOCs adsorbed onto a disc membrane; in order to respond to the demand of non-invasive, rapid, cost-effective diagnosis. The design system will be then applied on biofluids from human cohort in SNOOP-I project context. SNOOP-I

project aim to diagnosed BC though VOC from multiple biofluids (e.g. breath, saliva, tears, skin/sweat urine).

The manuscript is composed of three parts. The first section is meant to present the implantation of metabolite focusing in volatilomics studies in clinics. All the analytical methods, sampling methods and pre-concentrated methods will be discussed.

The second part is dedicated to the development of a LTP-MS system focusing on analytical and sampling method. All these development have led to the selection of an optimal vacuum based dynamic headspace sampling and a system coupling thermal desorption, and desorption and ionization from LTP.

The final chapter is the application of the developed systems to discriminate group (healthy and cancer) by their VOCs from cell lines, urine, saliva, tears and skin/sweat after multivariate statistical analysis.

Part one: State of art

Chapter I: Metabolomics in clinic

Metabolomics is the study of small molecule (<1500Da) within cells, biofluids (e.g. serum, plasma, cerebrospinal fluid, urine), tissue or organism in a biological system. This last OMIC tool is an evolving field to exhaustively identify and quantify products of cellular processes and metabolites processes. The metabolome; set of all metabolites, is a synergy of exogenously introduced and endogenously generated product and some of which interfere together. The classes of small molecules detected by metabolomics include lipids, amino acids, carbohydrates, hormonals steroids, vitamins, peptides, nucleic acids, organic acid, volatile organic molecule and xenobiotics obtained from the diet, environmental exposure, and pharmacotherapy. The composition of endogenous compounds is affected by environmental factors, lifestyle factors (age, gender, race, diet, drugs, and exercise) and by upstream influence of the proteome, transcriptome and genome which directly impact the physical and chemical complexity of the metabolome. Unlike genomics, transcriptomics and proteomics, metabolomics defines in real-time the metabolic phenotype expressed by an organism, resulting from the ongoing pathophysiological changes at a given moment. This accurate cell phenotype reflection makes metabolomics the most suitable omic's tool[15] to appreciate modulation between health and disease molecular phenotype. Furthermore, changes in metabolism related to cancer are now increasingly well understood especially its involvement in hallmark of cancer[23].

For the two past decay, metabolomics and metabonomics analysis (quantitative measurement of the global , dynamic metabolic responses of living systems to biological stimuli or genetic modification)[24] has been extensively applied in clinics[25] in particularly for precision/personalized medicine, single cell analysis, epidemiologic population studies, metabolic phenotyping and metabolome-wide association studies (MWAS), precision metabolomics and in combination with other omics disciplines as integrative omics. Clinical metabolomics (e.g. research and testing) have been employed to drive fundamental discovery, gain insight into mechanism of action,

identify biomarkers and stratify patient groups. Clinical research is based on statistical comparisons between groups to identify areas of metabolism that differ or to find biomarkers that distinguish between groups.

Contrary to targeted metabolomic workflow[26], the analysis of a set of pre-selected metabolites; untargeted metabolomics workflow is used to obtain a full scan of the metabolome, pattern identification for the global classification of phenotypes. Global approaches make the identification of all detected compound impractical but lead to the identification of metabolites/biomarkers that has the potential to discriminate between samples obtained from healthy subjects and diseased patients. Successful research metabolomics is linked to optimal study design. It includes the population that will be part in the study and also the determination of the conditions that are relevant for the hypothesis in investigation, namely the sample (e.g. type, compound class, preparation, extraction); randomization (e.g. uniform subject demographics, site of collection, collection method, storage, control groups and condition) and the choice of instrumentation to guarantee maximal metabolites detection, minimum variability and reproducible experiment.

Nevertheless, each metabolomics study could only focused on one group of metabolites at time. The extraction of targeted molecule is conditioned by the sample preparation, enrichment strategies and the analytical system used. Indeed considering the diverse nature of metabolites (polar, apolar, ionic specie), no single analytical method could offers a “one-size-fits-all' solution especially with the rapid variation of the metabolome making hard to capture biological time point of interest.

The two main technologies used for metabolomics (Table 1) are nuclear magnetic resonance (NMR) and mass spectrometry (MS).

NMR is used for fingerprinting or full scan of specific changes rather than for elucidating the total metabolome of a matrix (detect 50–200 metabolites). NMR is advantageous for compounds that are difficult to ionize and can be used to determine structures of unknown compounds as metabolome don’t drive from gene expression and therefore no structural prediction is possible. In addition, NMR based metabolomics research do not have access to the large spectral libraries commonly found within the MS-based metabolomics community. Furthermore, NMR is relatively less sensitive compared to MS (NMR: µmol, MS: pmol) and very expensive.

On the contrary, MS provides excellent sensitivity and an ability to rapidly resolve and identify individual metabolites in complex mixtures with simple extraction methods. These advantages made MS an ideal tool for global high throughput precision metabolomics of clinical sample (Table 1).

Table 1: Summary of metabolomics studies performed in breast cancer biomarker discovery in different biological matrices

	Biological sample	Aim	Anlytical approaches	Main conclusion	References
Cell line	BC cell line (MCF7)	therapy response/ to develop a robust and highy sensitive plateform to identify endogenous estrones in clinical specimens	MALDI-MS, LC-MS	MALDI-MS based quantitative aproche can be a broad method for the ketone (estrone) containing metabolites target analysis thus replacing the clinicl stage	27
	BC (MDA-MB-468, SKBR3, MCF-7)	Diagnostic biomarkers/ To quantify specific metabolites in BC cell extracts	NMR	Significantly differences were observed between cell lines, namely in the concentrations of 15 metabolites	28
	BC cell line (ZR-75-1, T-74D, MCF7, MDA-MB-231, MDA-MB-453, MDA-MB-468, SK-BR-3, BT-474, BT-549), Control (MCF10A)	Diagnostic Biomarker/ To compare the differences in the lipidomic compositions of human cell lines derived from normal and BC tissues, and tumor vs. normal tissues obtained after the surgery of BC patients	LC-MS/MS, GC-MS	23 lipids were identified, and a differentiation was observed for MDA cell	29
Tissus	tissus from 267 BC patient	therapy reponse/ identify cancer vs noncancerous tissue, gene silencing experiment as experimental proof of revelance of lipid metabolism	LC-MS	Membrane phospolipids , sach as palmitate containing PtdCho-s, ere inceased in tumor vs normal breast tissus	30
	tissus from OC (84 peritoneal, 11 pleural), 10 BC (7 pleural, 2 peritoneal, 1 pericardial), and 10 malignant mesothelioma s (6 peritoneal, 4 pleural)	Diagnostic Biomarker/ To identify the metabolic differences between ovarian serous carcinoma effusions obtained pre- and post-chemotherapy and compare ovarian carcinoma (OC) effusions with breast carcinoma and malignant	1H-NMR	Differences in metabolic profiles of different malignant effusions were detected , metabolic characterization by NMR can be a technique to additional knowledge the mechanisms of effusion development	31

		mesothelioma specimen			
	tissus from BC patients (n = 271)	therapy reponse /To establish metabolic signatures for ER+ vs. ER− BC	GC-TOFMS	Some metabolites levels were increased in ER− subtype, such as, beta-alanine, glutamate and xanthine	12
Blood , plasma, serum	Metastatic BC patients (n = 95), Early-stage BC patients (n = 80)	Diagnostic biomarker/ To explore whether serum metabolomic spectra could distinguish between early and metastatic BC patients and predict disease relapse	NMR	Disease relapse was linked with lower and higher levels of histidine and glucose, respectively	32
	BC patients (n = 27), control (n = 30)	Diagnostic biomarker/To apply 1H NMR and DART-MS for the metabolomics analysis of serum samples from BC patients and healthy controls.	NMR, DART-MS	disease classification and the biochemical validation useful to identify the mechanisms associated to BC development	33
	BC patients (n= 132), Control (n= 76)	Diagnostic Biomarker/ To develop a new computational method using personalized pathway dysregulation scores for disease diagnosis	LC-TOF-MS, GC-TOF-MS	determinationof important metabolic pathways signature for BC diagnosis, representing a suitable tool for diagnostic and therapeutic interventions	34
Saliva	BC patients (primary, n = 8; relapse, n = 22) and healthy volunteers (n = 14)	Diagnostic biomarkers/ To quantify specific polyamines in BC	LC-MS	The levels of several N-acetylpolyamines, including Ac-PUT, Ac-SPD, Ac-SPM, DAc-SPD, and DAc-SPM, were higher in breast cancer patients than in healthy volunteers	35
Urine	BC patients (n = 31), Control (n = 29)	Therapy reponse/ To identify metabolites which can be helpful in the understanding of metabolic alterations driven by BC as well as their potential usage as biomarkers	LC-MS, GC-MS	The analytical multiplatform approach enabled a wide coverage of urine metabolites revealing significant alterations in BC samples	36

Due to broad area of experimentation, a subset of the metabolomics, the volatile omics was recently introduced as a rapid non-invasive approach that constitutes the study of the volatile organic compounds (VOCs) that are emitted by the metabolome.

Volatolomics

Volatolomics, the study of VOCs includes endogenous, exogenous and metabolized VOCs produced and emitted by living organisms (plant, animals, bacteria, fungus). VOCs are carbon-based stable chemical compounds (odorous or not) at low molecular weight (< 500Da), which can be transmitted from the liquid phase into the gaseous phase at room temperature (25 °C) and pressure of 760 mmHg. They can be categorised in a wide range of groups depending on their volatility (e.g. very VOCs, VOCs and semi-VOCs), their origin (e.g. endogenous or exogenous) and their emission source (e.g. outdoor, indoor, industrial, material, building). Volatolomics is applied in a broad range of applications[37] including toxicological analysis (e.g. exposure tool to environmental pollutants, toxic and hazardous chemical environments, industrial accidents), molecular communications, forensics, safety, security (e.g. search and rescue operations) and clinical research (e.g. biomarker discovery, disease diagnostic tools, personalised healthcare).

In the human body, VOCs are produced by various metabolic processes, released into the blood, transported in the bloodstream and/or passed onto the airway[38]. Finally, the VOCs are exhaled in the breath or emanated from skin, urine, faeces, tears and sweat. Their chemical properties (e.g. volatility, partition coefficient), metabolism (e.g. origin, biogenesis) and emission source (e.g. breath, urine, saliva, tears, sweat feces, tissues) permit to classify them. It has been proposed that pathological processes such as cancer metabolic disorders, can produce new VOCs or change the ratio between the VOCs that are produced normally by the body (fluid and tissue). This volatile chemical fingerprint provides rapid non-invasive phenotype information on metabolic disorders.

I. Physiochemical property

a. Volatility

The volatility characterizes the tendency of a substance to evaporate at a given temperature. The volatility is a feature which can be defined by the vapor pressure and the boiling point. The vapor pressure (Vp) of a substance is the pressure at which its gaseous phase is in equilibrium with its liquid or solid phase. Vp depends very strongly on the intermolecular forces and the temperature. It increases non-linearly with

temperature according to the Clausius–Clapeyron relation (Equation 1) or the Raoult's law (Figure 4).

$$\ln\left(\frac{P_1}{P_2}\right)=\frac{\Delta H_{vap}}{R}\left(\frac{1}{T_2}-\frac{1}{T_1}\right)$$

Equation 1: equation of Clausius-Clapeyron. Ln: natural log, P_1:vapor pressure at temperature T_1, P_2:Vapor pressure at temperature T2, ΔH_{vap}: enthalpy of vaporization for substance, R:8.314j/molK

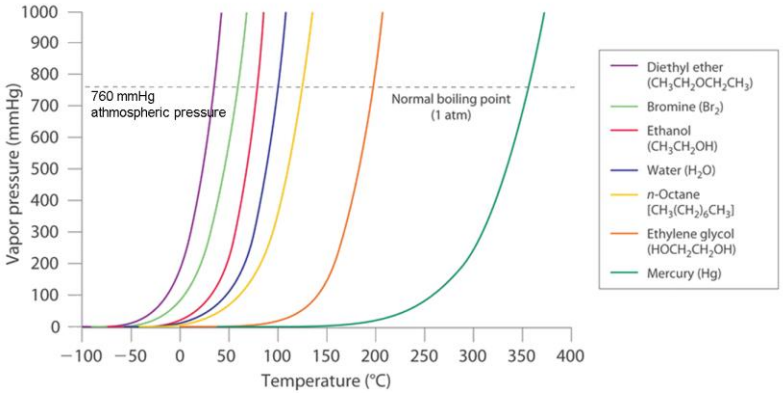

Figure 4: Vapour pressure of several liquids as a function of temperature. The point at which the Vp curve crosses the line of atmospheric pressure is the normal boiling point of the liquid.

A substance with a higher vapor pressure will turn in a gaseous phase more readily than a substance with lower vapor pressure. Moreover, intramolecular forces such as hydrogen bonds can influence the Vp. Strong intramolecular forces lead to relatively low Vp and weak intramolecular forces lead to a relatively high Vp.

The boiling point (Bp) of a substance is the temperature at which the Vp of a liquid equals the pressure surrounding the liquid. It's also the temperature at which the liquid state changes from a liquid to a gas phase. That temperature is very commonly referred to as the liquid's normal boiling point at 1 atm.

Any substance with a high Vp at room temperature (20-25°c) is considered to be volatile. Volatile molecules have low Bp and relatively weak intermolecular interactions. In contrast, non-volatile substances have high Bp and relatively strong intermolecular interactions.

Therefore, VOCs are a diverse group of carbon-based chemicals presenting a high Vp at room temperature which is is a consequence of a low Bp. VOCs can be classified on the basis of their Bp which ranges from 30 °C to 260 °C.

The compounds having low Bp (<0°C °to 50-100°C) are called very volatile organic compounds (VVOCs). Their Bp makes them difficult to measure because there are found almost entirely as gases.
The second class of VOCs have their Bp comprise between 100°C and 240°ccalled volatile.
The third class called semi-volatile organic compounds (SVOCs) have a Bp between 240 - 260°C to 380-400°C. A molecule with a Bp beyond <380°C are name organic matter (PM). As rule, the lower Bp is, the greater the compound volatility is.

b. Partition coefficient

The area regarding volatolomics which remains the least understood is the behavior and metabolic pathways of these molecules. With this in mind, knowledge of the fundamental physicochemical parameters of identified markers and distribution in the human organism is highly desirable. Fundamental physicochemical parameters based on the partition coefficient[39] blood: air (λb:a) and fat: blood (λf:b) govern the behavior and fate of VOCs in the human body[40,41].

The blood: air partition coefficient (λb:a) is a paramount determinant of pulmonary gas exchange. Depending on the λb:a some gases exchange in the airways, rather than in the alveoli. Gases with low blood solubility, mainly apolar VOCs (λb/a < 10), exchange almost only in the alveoli. Polar VOCs (λb/a > 100) exchange in the airways. In this case they are not respiratory gases but solvent gases with high water and blood solubility. VOCs with 10 < λb/a < 100 interact significantly both with the airways and with the alveoli.

The fat: blood partition coefficient (λf:b) governs the distribution of VOCs between the blood compartment and fat tissue and lipophilic cell membranes. Volatiles with high coefficients (λf:b) tend to accumulate in lipid membranes, or the fat compartment, whereas compounds with low λf:b leave lipophilic cell membranes directly and drain into the blood.

Together, λf:b and λb:a design the uptake, distribution, and elimination of VOCs in the human organism and govern the equilibrium concentration of a compound between fat, blood and breath. This means, for example, that species having comparable levels in exhaled breath can exhibit disparate concentrations in blood and fat. With a

maximum of 12 orders of magnitude, this heterogeneous distribution explains the differences in concentration between different compartments (e.g. blood, fat and muscle) and in the different body-fluid (e.g. breath, saliva, sweat and urine). For instance 112 VOCs are identical represented in exhaled breath whereas huge variability are present in blood and fat, meaning that different compounds may be stored (or exist in equilibrium) in different compartments of the body.

It is now well established that cancer-related VOCs have very different physicochemical properties with different λb:a and λf:b. implying that VOC are inhomogeneous represented within the compartments (blood, fat, muscle, etc). Furthermore the release of these compounds from their 'main storage' compartment depends on the blood flow through this compartment during sampling. It becomes clear that the knowledge of reliable λb:a and λf:b of VOCs observed in the human volatilome is important for the understanding of their behaviour in the human body, identification of their underlying biochemical pathways and assessment of their applicability in diagnosis and therapy monitoring. To gain a more comprehensive understanding on the cancer- related VOCs, combined information on appearance and concentration of these VOCs in breath and blood, or in breath and urine or saliva, is critical.

For a simple point of care screening tool, knowing the exhalation kinetics and optimized the sampling procedure is capital. Their exhalation kinetics depends on one or a combination of the following factors: (i) the partition coefficients between tissue(s), blood and air, (ii) the VOC concentrations in different parts of the body; (iii) the VOCs' diffusion constants and the VOC synthesis and metabolism rates.

II. Metabolism of VOCs

a. Origin of VOCs

The volatilome originates molecules from exogenous (due to external conditions) and endogenous (due to bio-function) sources.
Exogenous sources comprise inspiratory air, smoking, dermal absorption, drugs and nutrients. After adsorption, absorption or ingestion, the exogenous VOCs are metabolized, released though the blood and finally excreted.

Endogenous VOCs are metabolites naturally produced by an organism, through normal and abnormal metabolic processes occurring in the body under the influence of drug metabolism, environmental pollution, UV light or cigarette smoke. The most common reason for VOC generation is the destruction of cells from direct or indirect oxidative stress and inflammation of the human body.

Following their production, VOCs are emitted and can be found in body-fluids including blood, breath, skin, urine, saliva and feces.

b. VOC biogenesis

i. Exogenous VOCs

The exogenous VOCs absorbed from food and drink are mostly metabolized in the liver and are disseminated through blood. The inhaled VOCs may bind/dissolve in hemoglobin and be stored in body compartments and later exhaled or excreted through urine.

Human skin allows the entrance of adsorbed VOC through passive diffusion (simple diffusion and facilitated diffusion) without the consumption of chemical energy. The adsorbed VOCs considered as pollutants and drugs will be more or less readily taken up depending on their property (e.g. hydrophobic or polar) by metabolizing enzyme as defense reaction (Figure 5). In the liver, exogenous uptake consists of three phases.

- Phase I: Bioactivation usually by the cytochrome p450 enzyme catalysed oxido-reduction and hydrolyse reaction.
- Phase II: Activation by glutahione-S-transferase (GST) which catalyse the glutathione conjugation and increase the solubility of molecule.
- Phase III: Molecules are expelled by other enzyme systems, including GST, sulfotransferases, and N-acetyltransferases.

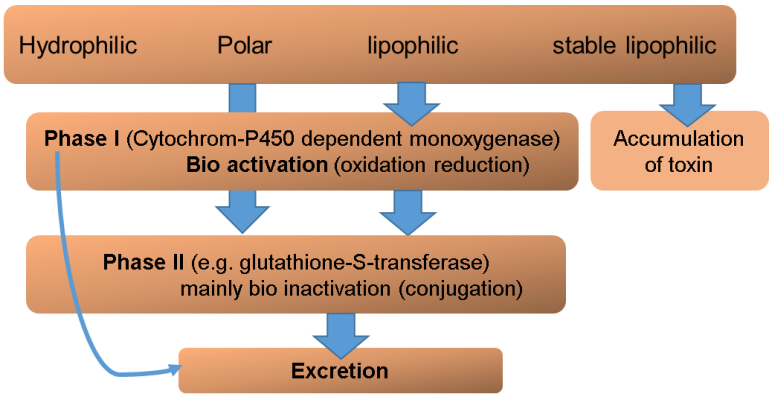

Figure 5: Uptake mechanism of endogenous VOCs

ii. Endogenous VOC

Naturally produced during the cellular respiration process in the mitochondria, cells release a group of compounds called reactive oxygen species (ROS) such the superoxide anion, O2- or the hydroxyl radical OH•. ROS are generated by activated granulocyte and can potentially damage any cellular structure. A balance between the formation and deactivation of ROS and free radicals is maintained within the human body through homeostasis. This balance determines the oxidative stress[42] (OS) within the body.

Oxidative stress:

Any accumulation of ROS[43] due to pathologies and/or external environment (e.g. diet, drug) leads to OS (Figure 6). Overexpression of ROS results in DNA damage, protein oxidation and lipid peroxidation particularly of poly-saturated fatty acids (PUFA).

Lipid peroxidation (LPO) represents the oxidative degradation of lipids usually containing double carbon bonds. Cell membrane polyunsaturated fatty acids (PUFAs) contain reactive hydrogens bound to methylen groups and are important targets for LPO with ROS accumulation (OH•). LPO is initiated by the formation of (L•) by abstracting a hydrogen atom from a PUFA; further (L•) reacts with O2 and forms (LOO•) a peroxide radical in the propagation step. Next, the peroxyl radical forms a hydroxiperoxide (LOOH) in a reinitiation reaction by abstracting hydrogen from a polyunsaturated fatty acid (LH). LOOH is then converted into an alkoxyl radical (LO•).

DNA damage/ protein oxidation: Different ROS have varying affinities for their target substrates, DNA bases, namely pyrimidine and purine and these bases can be

damaged by the hydroxyl radical. ROS-mediated protein oxidation can potentially target any amino-acid in the peptide chain but it preferentially damages methionine and cysteine. Protein damage occurs following exposure to superoxide/hydroxyl radicals.

The end products of these chemical interactions (e.g. LPO, damage and oxidation) are usually hydrocarbons such as ethane, pentane or 2-hydroxy-nonenal.

A better understanding of the interconnection between oxidative stress and the release of VOCs from target substrates would greatly help in identifying precisely the origin of VOC compounds in various diseases.

Environmental risk:

Several cytochrome p450 (CYP)[44] mixed oxidases are activated by exposure to environmental toxins such as tobacco smoke, air pollution. These environement exposures may raise the risk of cancer by increased conversion of precursors to carcinogens. An altered pattern of CYP p450 could potentially modulate and upregulated the catabolism of endogenous VOC products of oxidative stress and then generate an altered pattern of VOCs.

This enzyme family is overexpressed in abnormal conditions, such as human breast cancer tissue, through enzymes such as aromatase, which synthesizes oestrogens.

The overexpression of CYP leads to lipid peroxidation of PUFA in cell membranes and results in increased generation of volatile alkanes and alkane-derivatives in the breath, and potentially affects the abundance of VOCs (Figure 6).

The VOCs biogenesis linked to cancer development is the association of oxidative stress and the induction of cytochrome p-450 enzymes (CYP450) (Figure 6). In this setting, free radicals and reactive oxygen species (ROS), characterized by an unpaired electron in the outer shell originating from endogenous as well as exogenous sources (i.e., cigarette smoke) is accumulated leading to cell damage. The interaction with protein and fatty acids lead to the production of VOCs (Figure 6).

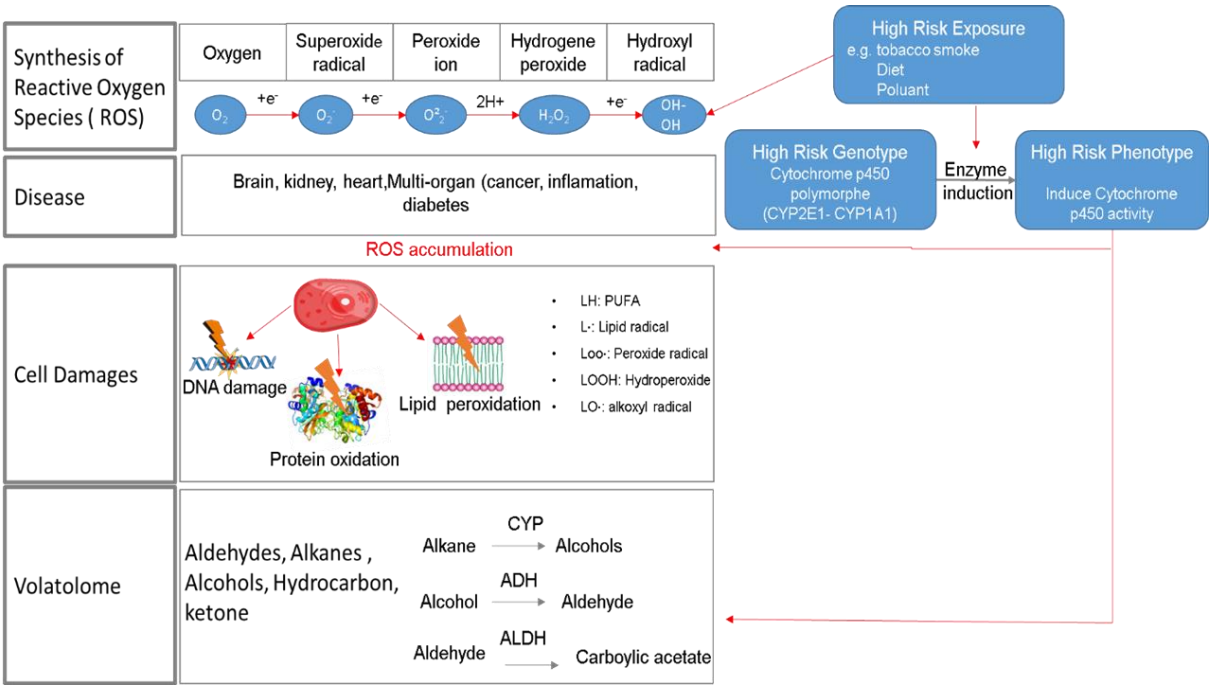

Figure 6: Interplay between VOCs - OS in local and systemic diseases. Metabolic pathways leading to the generation of VOCs. Oxidative stress through the activation of cytochrome p450 determines the specific pattern of VOCs. Genotype and phenotype risk could be increasing by external exposure risk. All the stress induce the CYP450 activity. The accumulation of OS lead to the ROS accumulation and thus cell damages. ROS, reactive oxygen species; PUFA, polyunsaturated fatty acid; VOC, volatile organic compound.

III. Pathway biosynthesis

Class of volatile could be separate into: nitrogen containing, sulfur containing, ethers, esters, hydrocarbons, aldehydes, alkanes, alkenes, ketones. acids and aromatic. All these coumpound derived from different metabolic process (Figure 6).

Hydrocarbon are stable end products of lipid peroxidation and protein oxidation. Different hydrocarbons generated during OS process may further oxidize and therefore produce different kinds of alcohols, aldehydes, and alkane. During carcinogenesis, cytochrome p450 (CYP) enzymes are induced and result in the hydroxylation of several VOCs such as Alkane to alcohol.

Alcohol mostly originates from food and alcohol beverages and absorbed from all parts of the gastrointestinal tract, largely by simple diffusion into the blood. Alcohols is also derived from the metabolism of hydrocarbons. These alcohols are metabolized in the body from alkane into aldehydes by enzymes, such as alcohol dehydrogenase (ADH) and cytochrome p450 (CYP2E1), which mostly operates in the liver. A small fraction of alcohol are removed through breath, urine, sweat, feces, breast milk, and saliva.

Aldehydes originate from several sources in the body. The first relates to metabolized alcohol in the body. Aldehydes formed in the body are oxidized by aldehyde dehydrogenase (ALDH), an enzyme which oxidizes aldehydes into carboxylic acids. Cells with high activity of ALDH are likely to be “cancer stem cells” (CSC). The second source for the aldehydes relates to the reduction of hydroperoxide by cytochrome p450 as a secondary product of lipid peroxidation. Cigarettes represent a third source of aldehydes.

Ketone compounds are produced by the liver from fatty acids such as acetone and oxidized in the Krebs cycle by peripheral tissue. Acetone (one of the most abundant VOC in humans) is produced by the liver by the decarboxylation of acetoacetate from excess acetyl-CoA. Ketone levels in the blood are also influenced by diet and rise as fat or protein metabolism increases.

Aromatic and nitril compounds are considered exogenous pollutants originating from exposure to cigarette smoke, alcohol, pollution, and radiation. Since these molecules are highly reactive, they leak into the cytoplasm, attacking organs or organelles in the body and causing peroxidative damage to proteins, PUFA, and DNA. This damage accumulates during life and is assumed to lead to age-dependent diseases.

VOCs: A non-invasisive source of biomarkers for diagnosis

VOCs reflect changes in cell chemistry, as they are bio-products of metabolic and pathological processes at the cellular and tissue level. Due to extensive analysis[4517,46], over 1,800 VOCs have been found in different biofluids; including blood, interstitial fluids (ISF), breath, sweat, saliva, urine, serum, breast milk, tears and faeces. In healthy subjects, breath and skin are the main sources of VOCs representing 54% of the total amount, whereas they are present in faeces, saliva, urine, and blood, 15%, 14%, 11%, and 6% respectively (Figure 7). Furthermore, due to the increasing interest VOCs studies, several metabolomics/volatolomic databases have emerged to facilitate VOCs identification including the Human metabolome database (HMDB) (microbial, yeast, human), the Human volatilome database (HVDB), the mVOC (http://bioinformatics.charite.de/mvoc) and the Cancer Odor Database (COD).

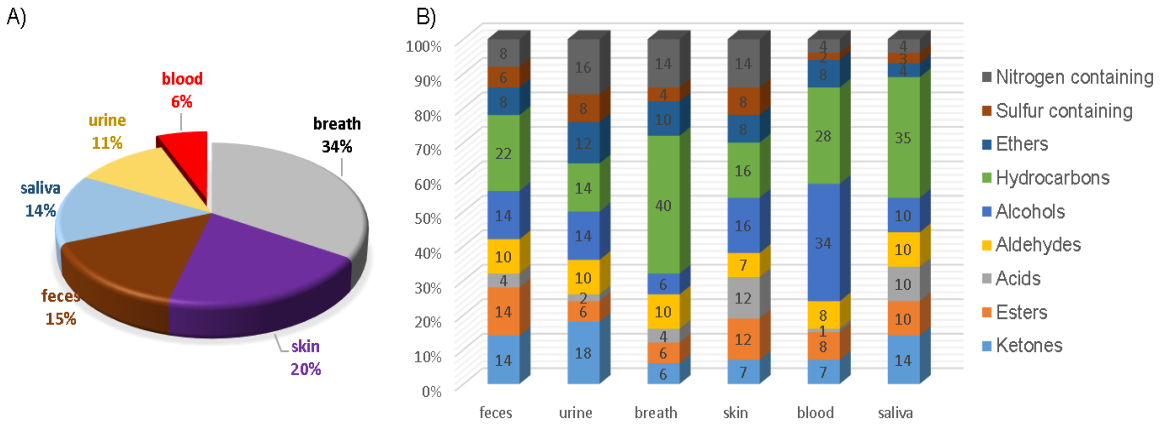

Figure 7: VOC abundance within the body. A) VOC percentages in different biofluids following the data of healthy human adapted from wiley and al. B) relative number of compounds in each chemical class detected in the volatilome.

It has been shown that a pathology leads to alteration of the cell metabolism inducing modification in the VOCs releasing, ending product of the biochemical reactions. Moreover, each disease has its own unique volatolome pattern giving the possibility of differentiating diseases based on VOCs discrimination. This increasing interest lead VOC analysis becoming an expending field in clinical research as biomarker diagnosis (Figure 7**Erreur ! Source du renvoi introuvable.**). The current clinical diagnosis including fluorescence in situ hybridization (FISH), in situ hybridization (ISH), Enzyme-Linked Immuno Sorbent Assay (ELISA) are used to evaluate the HER2 gene copy number (SISH, FISH)[47], to measure and quantify BCAR1, BCRA 2 (ELISA) in extracts of human breast cancer tissue. The consider gold standard of gene copy HER2 is

FISH. Immunohistochemistry[48] is the most frequently used method to study the expression of C-erbB-2 in breast cancer. Nevertheless, Immuno-histochemical staining results are easily affected by the variations of the method such as variations due to the storage conditions of the tissue samples, the specifications of the fixative used, duration of fixation and the antibody used. The FISH technique is more quantitative compared to immunohistochemistry and reflected by the identification of the HER2 gene count associated with the copy of the chromosome 17 centromere. On the opposite of previous method, VOCs based diagnosis is expected to be less expensive while allowing (i) screening of high-risk population (ii) early detection of diseases (iii) monitoring and follow up of therapy efficiency.

VOC diagnosis is especially head towards to non-invasive diagnosis. Consequently, blood and ISF are not used in this purpose on contrary of tears, cerumen, saliva, sweat, urine and faeces (Table 2). All these different non-invasive source of biomarker will be present. The gold standard of VOCs diagnosis in clinics is the GC-MS.

Table 2: Recapitulative table of VOC analysis

	Dease	Sample type	Sampling	Analytical method	Aim	Detected VOCs	References
Cerumen	healty	(N = 8 Caucasians, average age = 35 ± 5; and N = 8 East Asians, average age = 28 ± 3)	SHS-SPME	GC/MS	To compare VOCs cerumen production of ethnic groups	The relative amounts of VOCs greater in the Caucasian cerumen (yellow cerumen) compared to the East Asian (dry cerumen)/ Dry cerumen phenotype correlate with a decreased production of axillary odorants cerumen.	49
Breath	BC	total exhaled breath of BC patient (n=101)	sorbent trap/portable breath collection	TD-GC-MS	Diagnsotic biomarker/ To provide a sensitive and specific set of biomarkers for breast cancer.	Higher expression of Nonane; Tridecane, 5-methyl Undecane, 3-methyl Pentadecane, 6-methyl Propane, 2-methyl	50

	BC	totale exhaled breath of BC patient (n=30) Control (n=30)	Desorption tube	GC-MS	Diagnostic biomarker/ to provide sebsivtive Volatile metabolomic signature of human breast cancer cell lines	increase: 1,1,2-trichloroethene , decrease: 3-methylhexane , (E)-dec-2-ene, naphthalene . Five specific breast cancer-VOCs were identified	51
Saliva	head and neck cancer (HNC)	HNC (n=− 32), Control (n=27)	SHS-SPME	GC-MS	Diagnosis biomarker/ To address the effects of HNC on saliva	48 VOCs identified and quantified and 15 discriminative with four higly sensitive: 1,4-Dichlorobenzene; 1,2-Decanediol; 1-dimethylethyl, phenol; Decen-2-ol	52
	BC	BC (n = 66), Control (n =40)	HS-SPME	GC-MS	Diagnosis biomarker/ To explore the potential of the volatile composition of saliva samples as biosignatures for BC	5 VOCs discriminative: acetophenone; 1-hexanol-2-ethyl-; 2,4-dimethyl-1-heptene and hexadecane	53
	oral squamous cell carcinoma (OSCC)	control group (n=50) and oral cancer group (n=24),	ZSM-5/PDMS hybrid thin films microextraction/ Liquid extraction	GC–MS	Diagnosis biomarker/ to distinguish biomarker and establish metabolomic patterns of salivaryVOCs.	38 VOCs detected from the oral cancer group and 35 VOCs that overlapped between the healthy	54
Skin	Healty	wrist, ankle,sweat sample from 2 healty male	PDMS passive samplig	GC-GC-MS	to investigate the skin microbiome and interactions with anthropophilic mosquito	88 compounds detects	55

					disease vectors		
	Healty	axillary sweat (n=197, 89 males, 108 females, ages 18–91, mean 44 year)	PDMS passive sampling	SBSE-GC-MS	To highlight the chemical basis of individual and sex-specific odours	axillary sweat is richer in volatiles and semi-volatiles than saliva or urine/characteristic peaks distinguish the sexes	[56]
Urinary	BC	BC (n=26) control(n =21)	SHS-SPME	GC-MS	Diagnosis fingerprint / To provide a simple sensitive solvent free method SPME coupled to GC–QMS for the establishment of urinary volatile metabolomic pattern characteristic for breast cancer patients and normal subjects	decrease of :butanal-3-methyl-, butanal-2-methyl-, benzaldehyde, benzophenone, dodecane, tetradecane, in cancer patient	[57]
	BC	BC (n = 30), CC (n = 30), control (n=30)	SHS - NTME	GC-MS	Diagnosis fingerprint/ To discriminate di erent types ofcancer based on urinary volatomic biosignature	pentadecane, nonane-5-methyl-5-propyl-, dodecane-4,6-dimethyl-, 2,4-di-tetra-butylphenol)	[58]
Faeces	Colorectal cancer	31 high risk patients and 31 low risk or non-cancer controls	Nalophan bag	SIFT-MS	Diagnosis biomarker/ To predict whether someone is going to have or get colorectal cancer	Discriminant VOCs: Ammonia; Hydrogen Sulphide; Pyrrole m/z 53; Pyridine; Heptanal; Octanal; propanoic acid; Isopropylamine, Dimethylami	[59]

I. Exhaled Breath

Breath metabolomics analysis (breathomics)[60,61], holds great promise for general diagnostic and bio-monitoring application by providing non-invasive and continuous information on the metabolic and physiological state of an individual Moreover, environmental exposure, diet, and lifestyle (e.g. alcohol consumption) of individuals influence the concentration of VOCs in their breath. The combination of internal and external exposure are called exposome. Exhaled air comprises a mixture of dead-space air and alveolar air. The dead-space air consists of roughly 150 ml air from the upper airway where no gaseous exchange between blood and breath air is facilitated. Consequently, this part of the exhaled air displays a high resemblance to the previously inspired air. In contrast, alveolar air originates from the lower airways where gaseous exchange between blood and breath air results in concentrations of endogenous compounds that are two to three-fold higher than those observed in the dead-space air. To date, 874 VOCs have been found in breath samples, thus making it the most examined source of VOCs. Exhaled breath is predominantly composed (Figure 7, B) of nitrogen, oxygen, carbon dioxide, and argon. However, determining exogenous contaminant compounds from those produced endogenously remains challenging due to the difficulty to determine which one comes from internal or external or from an interaction of both of them. Recently, a new breathomic database is available HBDB (https://hbdb.cmdm.tw) providing 2766 related references, 913 compounds and 60 diseases associated with human breathomics. In the case of breast cancer, investigation was made based on total exhaled breath and highlight some discriminative VOCs such as nonane; tridecane, 5-methyl Undecane, 3-methyl pentadecane and 1,1,2-trichloroethene (Table 2).

II. Saliva

VOCs in saliva are mostly transferred from blood to saliva through passive diffusion. They reflect biochemical information about the blood and contain additional VOCs resulting from serum, gingival exudate, the nasal cavity, gastrointestinal reflux, food debris, oral cavity microorganisms, commercial products, and environmental pollution. With the possibility to collect a large volume of saliva samples, this biofluid is promising

for continuous and real-time monitoring of different diseases[62,63] and could provide an accurate reflection of the VOCs present in the blood. Saliva is known to contain 360 different kinds of exogenous and endogenous VOCs. Major VOCs in saliva include (Figure 7, B) acetic acid, ester, acetonitrile, mercaptan, methyl sulfide, different alkanes, diene, different aromatic compounds (e.g. benzene, toluene and xylene), polycyclic hydrocarbons (e.g. carane, copaene, etc.), alcohols (ethanol, propanol, butanol, etc.), and aldehydes (acetaldehyde, propanal, etc.). Several databases are currently available as saliva metabolome database which is integrated to HMDB database.

The secreted microbial VOCs involve predominantly volatile sulphur compounds (VSCs), indole, phenol and aliphatic amines such as putrescine and cadaverine (exogenous source). Futhermore, saliva derived VOCs could also be found in exhaled breath such as hydrogen sulfide, methyl mercaptan, and dimethyl sulphide, coumpound responsible of bad breath. In case of BC saliva analysis, VOCs were highlight to be discriminative such as acetophenone; 1-hexanol-2-ethyl-; 2,4-dimethyl-1-heptene and hexadecane (Table 2).

III. Skin and sweat

VOCs from the skin originate either from gland secretion metabolism of skin microbiota on the surface or from exposure to pollutant. The distribution of the glands at the skin surface partially reflects the difference in VOCs emitted by distinct parts of the human body. VOCs emitted from the skin surface are mainly derived from sweat, secreted by the sweat glands and sebum. In addition, an oily substance is secreted by the sebaceous glands located in the axilla, the perinal region and the areola of the breasts. The abundance of VOCs can be attributed to the presence of sebum, a unique continuous layer of lipids (mainly squalene, wax esters, and fatty acids) continuously exposed to microbiota activity, oxidative stress from UV radiation, or air pollution. Upon exposure to ROS, sebum degrades and produces a wide range of semiVOC and VOCs that are more localized on the skin. However some of these VOCs result from internal hormonal or metabolic changes .From human skin[64] (Figure 7) 532 VOCs have been identified including aldehydes, ketones, hydrocarbons, alcohols, and esters. A sweat

metabolome database is available and contains detailed information about many small metabolites found in human sweat with the associated concentration values. Each metabolite entry contains more than 110 data fields and many of them are hyperlinked to other databases including KEGG, PubChem, ChEBI, Chemspider, DrugBank, PDB and Uniprot.

IV. Urine

The exogenous and endogenous VOCs in urine are mostly derived from three renal processes: glomerular filtration, tubular reabsorption, and tubular secretion. This relationship assumes that the VOC is freely filtered and not bound to plasma proteins, particularly the end products of metabolism (urea, creatinine, uric acid, and urates) which are poorly reabsorbed and thus excreted in large amounts. The potential of urine as a diagnostic tool, was firstly evidenced by Hippocrates and Galen, who related its odour with diabetes and kidney failure. The urine based diagnosis is non-invasive and is reliable though sample collections, handling and preservation. To date, a total of 279 VOCs (Figure 7, B) have been identified and reported in available databases such as UMDB: (http://www.urinemetabolome.ca) and the urine metabolome database .These databases contained detailed information about ~3100 small molecule metabolites found in human urine. This aqueous urinary matrix (95% water) explains the small percentage of VOCs. Urine derived VOCs cover a large range of chemical families as acids, alcohols, ketones, aldehydes, amines, N-heterocycles, O-heterocycles, sulphur compounds, and hydrocarbons. Different VOCs (particularly terpenes) are considered to be the outcome of digested food. Endogenous VOCs comprise ketones, alcohols, heterocyclic compounds, different hydrocarbons, amines, aldehydes, and organic acids. The diagnosis of VOC urinary biomarkers (Table 2) from urinary sample is technically complex as the aqueous urinary matrix contains a small percentage of VOCs. Nonetheless, urine BC analysis have shown a decrease of butanal-3-methyl-, butanal-2-methyl-, benzaldehyde, benzophenone, dodecane, tetradecane in cancer patient.

V. Other sources

Other common sources of VOCs are found in feces, breast millk, tears and to date, 381, 256, 123 VOCs have been respectively reported. Databases are also available as HMDB and the fecal metabolome database.

Tears are body fluid exposed to both internal and external environments and contain a large amount of molecular information, which is useful for the diagnosis, prognosis, and treatment of ocular surface diseases[65,66].

Chapter II: Volatilome analytical methods

Due to the tremendous application of VOCs analysis, this field has gained increasing interest in recent years. In this context, numerous VOCs analytical methods were developed such as gas sensor technologies and mass spectrometry (MS) based strategies.

Gas sensor arrays are based on the recognition of specific VOCs (compound, pattern or class) and used for diagnosis and monitoring.

While MS based studies allow the detection of known and unknown ions according their mass to charge ratio (m/z) in the gas phase. These strategies are powerful tool for biomarker discovery.

Basically there are two different approaches to detect VOCs from body fluids and breath, the separation and non-separation based techniques. The separation technique includes LC-MS and GC-MS and non-separation includes SIFT-MS, PRT-MS, MIMS-MS, gas sensor, DART-MS, LTP-MS. Their advantages and drawbacks are reported in the Table 3**Erreur ! Source du renvoi introuvable.**.

Table 3: Recapitulative table of all VOC method analysis with their advantages and limitations.

	advantages	disavantage
GC-MS	offline	High purchase and maintenance costs
	Low LOD (ppt-ppb)	Long analysis times
	High sensitivity	
	High specificity	
	High selectivity	
	Accuracy	
	Qualitative & semi quantitative	
	Commercial libraries/ reliable identification	
	available Software	
SIFT-MS	Real-time analysis	
	direct injection	Uncertain identification of analyte ion
	Low LOD (sub-ppb)	Limit of quantification
	High sensitivity	Lack of commercial libraries
	High specificity	
	absolute quantification	
	tentative identification compound	
	Self-calibration	
PTR-MS	Real-time analysis	Maximum measurable concentration
	direct injection	Lack of commercial libraries
	Low LOD (low ppt)	
	High sensitivity	
	High specificity	
	absolute quantification	
	tentative identification compound	
	Soft ionisation	
MIMS	Real-time analysis	
	direct injection	
	Low LOD (ppt-ppb)	
	High sensitivity	
	absolute quantification	
IMS	Real-time analysis	
	direct injection/ low technical expenditure	
	Low LOD (ppt-ppb)	
	sensitive and inexpensiv	
	transportable	
DART-MS	Real-time analysis	Lack of commercial libraries
	ambient source/ No injection sample	lack of software
	gas, liqui, solid ionisation	
	simultaneous desorbtion and soft ionisation	
	High sensitivity	
	High specificity	
	tentative identification compound	
LTP-MS	Real-time analysis	Lack of commercial libraries
	ambient source/ No injection sample	lack of software
	LOD ppb	ozonolyse phenome/ lot of adduct
	simultaneous desorbtion and soft ionisation	coumpond identification
	high range of polarity	
	High sensitivity	
	High specificity	
	tentative identification compound	
	Cheap / home made construction	
sensor	Real-time analysis	No discovery
	low ppb	only targeted analysis
	High sensitivity	
	High specificity	
	semi quantative quantification	
	Identification	

Separation based analytical techniques

I. Gas chromatography-mass spectrometry

The global identification and quantification of trace level biomarkers in metabolomics and metabonomics is required to measure the concentration of metabolites involved in pathologies and to detect variation in response to treatment. Many metabolites which are extracted from complex samples, present similar physical and chemical properties in terms of molecular weight and polarity. In this context, a separating dimension prior to their analysis is necessary to improve their detection and to reduce the ion suppression effect. GC analysis (Figure 8) starts with the injection of the sample in liquid or gaseous state into a GC column at a temperature comprises between 100 and 300°C meaning that the molecules have to be volatile and thermostable. The compounds are propelled by an inert carrier gas such as argon, helium or nitrogen and gradually heated between 5-400°C. Molecules are separated according their physical/chemical properties and the nature of the stationary phase. The detection of VOCs can be achieved by GC[67] coupled with various detectors including mass spectrometer (MS), flame ionization detector (FID), photo ionization detector (PID) and electron capture detector. GC-MS (Figure 8) was first introduced in 1950 by Roland Gohlke and Fred McLafferty and was used to separate and analyze complex organic and biochemical mixtures in gaseous state Moreover, the strategy is the only one allowing the detection of known and unknown compounds. To date GC coupled to MS (GC-MS) is the gold standard technique for VOCs analysis and prove its efficiency in different application as environmental, quality control, fundamental analysis and diagnosis [67](e.g. asthma, cancer, diabetes and microbiome).

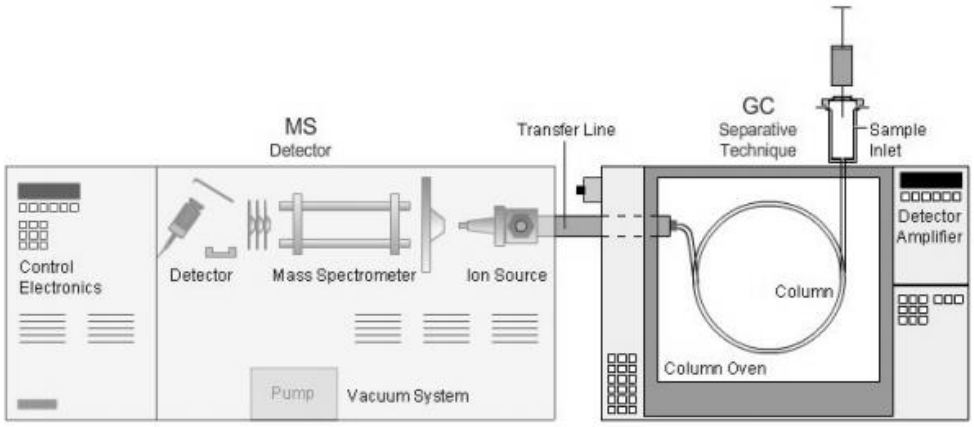

Figure 8: Schematic diagram of GC-MS.

In the case of GC-MS analysis, the separated molecules are ionized in the source of the mass spectrometer using electron or chemical ionization sources. The generated gas phase ions are then analyzed according their m/z in the mass analyzer (e.g. quadrupole).

GC-MS is known for its reproducibility, repeatability, accuracy, specificity and able the separation and quantification of analytes from a complex mixture. GC-MS has however some drawbacks including the preferential addition of reactive functional groups for molecular derivatization during sample preparation and a long chromatographic runs (30–60 min). Nevertheless, the advantage of using GC-MS in VOC research is the concentration and separation of molecule as enantiomer and isomers shuch α - and β -pinene[68]. Furthermore sample may be taken stored in tubes and analysed months later. As the selectivity is conditioning by the stationary phase of GC column, the only way to overcome this limitation and overlapping peaks experienced in one dimensional chromatograms GC columns are set in succession. Additional GC dimension (2D-GC-MS) could be also used.

All in all GC-MS analysis provide quantitative data but require a separative step which increasing the time analysis (40 min for GC separation); quality not research for rapid diagnosis. To respond to this demand, separative step are then discard for real -time instrumental approach non separative analysis method.

Non-separation based analytical techniques

Due to the envy of overcome the long separative step, numerous non separative methods were developed for direct analysis and became attractive. One of the most unusual/interesting developed techniques is the use of trained animals to detect cancer using nematode[69] and canine as dogs[70]. For instance, the KDOg project[71,72], the diagnosis of BC cancer by training dogs shows a sensitivity of 90.3% and specificity of 82%. These analysis have proven that methods without separative step could diagnoses cancer by VOCs, reinforcing that VOCs reflecting a physio pathologic state. It is then possible to establish analysis method only based on molecular pattern or classes of molecule. However, this kind of detection does not provide any information on the stage or type of cancer; crucial information for appropriate treatment. Furthermore, it is very time consuming to train a dog, 2 years is required and sensitivity begins to decrease in the fourth year. The increasing interest of direct analysis have led to the development of numerous gas sensors and MS techniques.

I. Gas Sensor (e-nose)

Over last decade, extensive research has been successful in developing gas sensors[73]. Sensor development benefits from the advances made in microelectronics and in micro- and nano-fabrication technology, in order to expand the analytical capabilities of high-performance gas sensor toward costless and ubiquitous system. Gas sensor enables the detection of VOCs released from the human body with high sensitivity and selectivity. Sensor analysis focus on the selective and accurate detection of predetermined metabolites as biomarker or pattern recognition (targeted analysis). In contrast to MS based techniques, gas sensor is cheap, requiring less operation skills, less cost maintenance, low power consumption and have the possibility to be miniaturize. Furthermore, high throughput analysis, cost-effeteness, long lifetime, and potential integration in a wireless network have led gas sensors to be used in various medical applications. Gas sensor is majority used for breath analysis in clinical diagnosis thanks to its non invasiness, application for point care and real time clinical management.

Gas sensors comprise a receptor, transducer and an active layer, which converts the desired chemical reaction into a measurable electronic signal such as a variation of

resistance, frequency, current or voltage. They are commonly categorized as chemical detectors and be can be separated into (i) electrochemical sensors: including metal oxide semiconductor (MOS), carbon nano-tube sensors (CNT); (ii) acoustic gas sensors including quartz crystal micro-balance(QCM) and surface acoustic wave(SAW); (iii) optical sensors including fiber-optic sensors and photonic crystal gas sensors and (iv) photoionization device gas sensor .

a. Electrochemical Sensors

Electrochemical sensors offer several advantages for low-concentration VOC detection such as low manufacturing costs and simple designs. An electrochemical based on sweat VOcs analysis measured the ethanol with a detection of limit of 52 ppm with

i. MOS Gas Sensors

Metal oxide semiconductor gas sensors (Figure 9) are based on the change in conductivity of material when gaseous molecules are adsorbed or desorbed on the surface of a MOS. MOS gas sensors employ specific sensing materials deposited on a set of electrodes along with a micro-heater; electrically separated from the sensing element by an insulating layer. An advanced micro-electro-mechanical system (MEMS) can be achieved to an optimal thermally isolated structure as MOS sensors commonly operate at a high temperature, ranging from 150°C to 400°C. At high temperatures, oxygen is adsorbed on the surface of MOS and then captures electrons from the conduction band, which leads to a change in the charge carrier concentration affecting the resistance of the MOS sensing. The sensitivity of MOS sensor relies on the thickness of the receptor layer, the catalytic metal particles placed in it and the temperature of the receptor layer.

MOS gas sensors are among the preferred candidates for applications that require detection of low-concentration VOCs because this type of sensor is durable easy to miniaturize and cheap to manufacture.

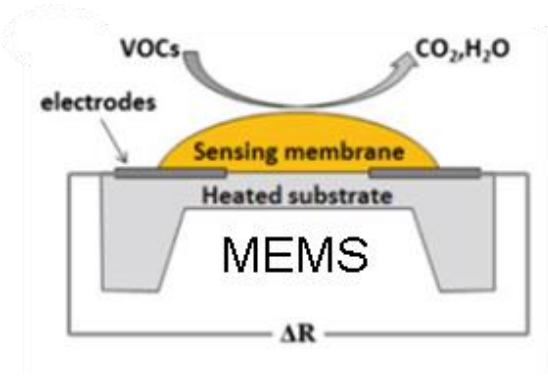

Figure 9: Schematic representation of MOS sensor.

The numerous MOS sensor was developed on VOCs detection mainly focused on the use of formaldehyde (HCHO)[74], methanol (CH_3OH), ethanol (CH_3CH_2OH)[75], xylene ($CH_3C_6H_4CH_3$)[76].

ii. CNT Gas Sensors

Carbon nanotubes (CNTs) sensors[77] (Figure 10) can be divided into two categories: single-walled carbon nanotubes (SWCNT) and multi-walled carbon nanotubes (MWCNT). SWCNTs consist in one layer of CNTs while MWCNTs have different layers of CNTs inside each other. The unique properties of CNTs come from the high aspect ratio with very strong intermolecular bonds and low density, resulting in an enhanced sensitivity, low detection limit, and fast response time. Based on their principle of operation these sensors can be divided into categories of gas sorption, gas ionization, capacitive and resonant frequency gas sensor. One advantage of CNT sensors is the flexibility of CNT functionalization with different chemical groups which allow caption of various compound.

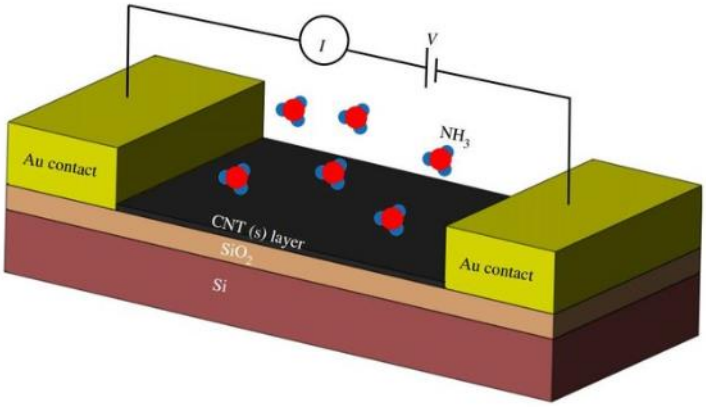

Figure 10: Schematic representation of a CNT gas sensor. The CNT layer is used between, two electrodes and the current response to constant applied voltage is measured. Change in resistance of the CNT layer, which causes in change in current, shows gas absorption.

b. Acoustic gas sensors

Acoustic gas sensors respond to the adsorption of analytes in the sensing film and can detect gas molecules immobilized on the surface of the device. Several acoustic gas sensors based on piezoelectric device have been proposed and investigated such as quartz crystal micro-balance (QCM) and surface acoustic waves (SAW). Piezoelectric sensors have a radio frequency resonance under such electric potential and are highly sensitive to the mass change applied at the surface of the piezoelectric sensors. These devices are able to generate and transmit acoustic waves in a frequency-dependent manner. Bulk acoustic wave (BAW) devices operate by transmitting a wave from one side of the crystal to the other, while surface acoustic wave (SAW) device transmit waves along a single crystal face.

i. QCM gas sensors

QCM sensors (Figure 11) use a piezoelectric quartz crystal which is coated with the sensing material and sandwiched between two electrodes. The sensing material is coated at the center of the top sensing electrode which is exposed to the analytes. QCM sensors detect the mass change of the sensing layer by measuring the resonance frequency shift of the quartz. BAW is an advanced type of microbalance mass sensor, made of a polymer-coated resonating quartz disk, vibrating at a

frequency (10–30 MHz). The analyte adsorption depends on the sweep gas properties and concentration.

The adsorption of gas molecules onto the polymer surface (sensing films) results in a shift in the resonant frequency of the quartz crystal (QC). Its oscillation frequency proportionally decreases, while the bounding-mass increases on the crystal surface.

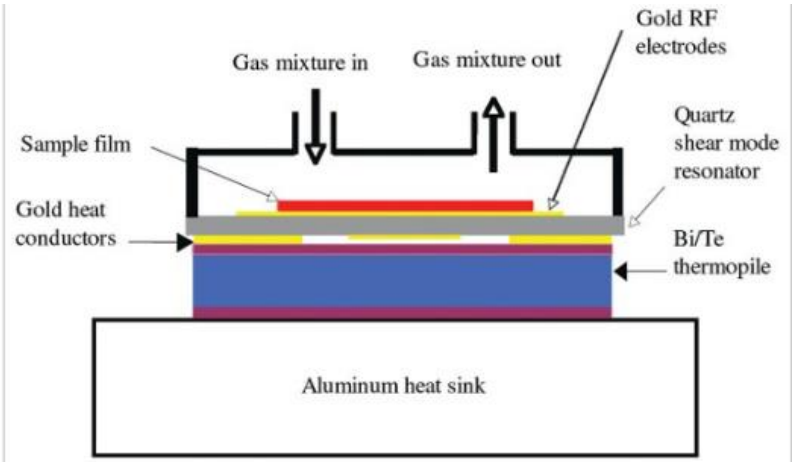

Figure 11: Cross sectional view of the QCM gas sensor.

ii. SAW gas sensors

SAW gas sensors (Figure 12)[78] include two SAW reflector arrays on the crystal substrate separated by a cavity where a pair of electrodes is located. SAW sensors operate at higher frequencies (100–1,000 MHz) than BAW and thus generate a larger changing in frequency. SAW sensors can be electrically excited and detected in a piezoelectric substrate using a transducer. In this configuration and unlike bulk quartz resonators, the frequency of SAW sensors does not depend on the wafer thickness.

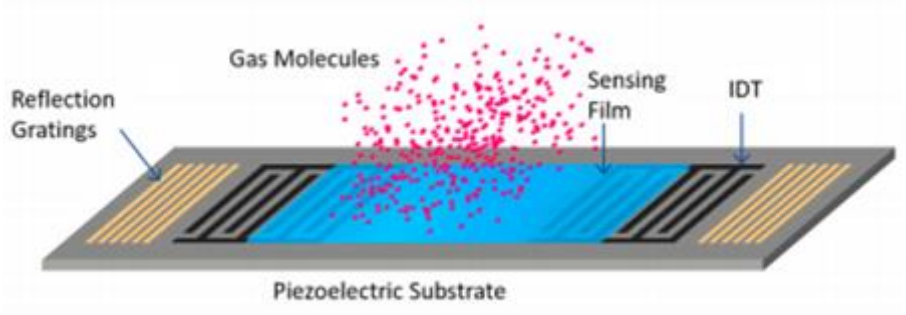

Figure 12: Schematic representation of SAW gas sensor.

The output and input transducers are both interdigital transducers (IDTs) which are core components of SAW. When the environment of the transducer changes due the

adsorption of gas molecules adsorbed, the frequency vibration changes. Hence, the weight information of gas molecules can be obtained by comparing signals of output IDTs with input IDTs.

In general, SAW sensors are reported as being highly sensitive with short response time and reversible and also applicable in wireless technologies.

For example, gas saw sensor coated with poly-N-vinylpyrrolidone (PNVP) film is used for monitoring low concentration ammonia below10ppm[79].

c. Optical sensors

Optical sensors have been widely used in many applications due to their selective response which can be measured precisely and their fast multiplexing feature. These sensors are based on a light source that excites the VOCs, and the signal can be measured in the resulting absorbance, reflectance, fluorescence, or chemiluminescence. The detection mechanism of optical sensors relies on the following properties of the electromagnetic waves: wavelength, phase, amplitude, intensity, and state of the polarization. Optical sensors are excessively sensitive and are able to identify individual compounds in mixtures. However, their connected electronics and software are complex and expensive. These sensors have a relatively short lifetime, which also results in increasing the cost of detection. Optical sensing tools have concentrated on their surface, optical fibers, gas sensors and photonic crystal gas sensors.

i. Fiber-Optic gas sensors

Fiber-optic sensors (Figure13) are composed of a sensing layer, an optical fiber and the substrate. The polished optical fiber is held on the substrate to partially expose the sensing layer to light. The sensing membrane is placed above the polished fiber where the interaction between the analyte and the sensing layer occurs which produces

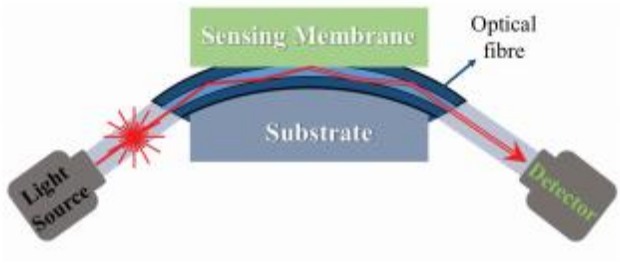

Figure13: Schematic representation of fiber optic gas sensor

physical and chemical changes such as in the refractive index. Therefore, optical fiber sensors can detect analytes that create a measurable optical changes in the sensing layer. The working mechanism of optical fiber sensors can be explained by the pulse width modulation (PWM) and also the interaction between the analytes and the sensing layer. When the sensing layer is exposed to the desired analytes, the pulse width changes. This technique enables the detection of small changes in light associated with the light pulse amplitude and fall time. Althought this method is used for the meausurment of carbnon dioxide and amonia in healtcare[80,81].

ii. Photonic crystal gas sensors

Photonic crystal (PhC) sensors (Figure 14) are refractive index-based sensors that employ periodic arrangements of dielectric materials with a different refractive index for detection. These sensors have been proposed as potential candidates to achieve high sensitivity with the ability of detecting nano-meter size chemical compounds. They can also detect environmental parameters such as temperature, pressure and humidity, enable design flexibility, provide greater security by averting electromagnetic interference from electrical signals and by reducing the device dimension by integrated an optical circuit platform. High-performance PhC gas sensors have been developed, such asthose with a LOD in the ppm range or for accurate detection of hydrogen sulphide bond H_2S[82].

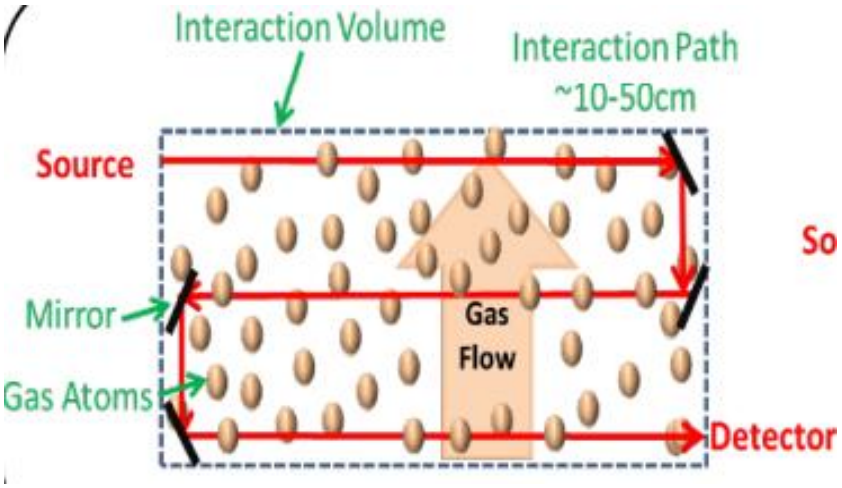

Figure 14: Schematic representation of photonic crystal gas sensor.

d. Photoionization device gas sensor (PID)

PID sensors are still relatively low cost and are highly sensitive chemical sensors that are used extensively for the detection of a broad range of VOC. They can provide a linear output to a single chemical or mix of chemicals, in real-time, and have a sensitivity in the ppb (parts per billion) range. The PID uses ionization of gaseous compounds by light as working principle to quantify chemical in gas samples. In these device a gas sample containing species the species to be detected flows through the ionization chamber, where proton emitted reach the sample molecules. The electrodes established an electric field in the ionization chamber where the ionized molecule generate an ionization current proportional to their concentration. Improvements have been made to low carrier gas consumption and to decrease the ionization volume (µPID)[83] resulting to in a higher surface volume ratio, which translate into more sensitive signal.

VOC sensors respond to a need for continuous real time and selective monitoring of various physiological and pathophysiological conditions. Intensive development in miniaturization, micro-electronic, sensitive material, nanotechnology is leading to real time non-invasive monitoring device with wearable application. Consequently sensor are widely used for breathomics as monitoring and diagnosis system[84]. The FDA are already approved monitoring and diagnosis system, among them (i) the EC50 ToxC+ analyser wich is an electrochemical sensor baser breath CO monitor,(ii) the NOBreath® which is a fractional exhaled Nitric Oxide (FENO) breath monitor design to help improve asthma management,(iii) Heartsbreath™ a non-invasive breath test for breath biomarkers that predict the probability of grade 3 rejection in heart transplant recipients who received their transplants in the preceding year (iv) OneBreath breath sample (one normal breath into a 1 L non-reactive bag) is promptly evacuated across a silicon microreactor chip that selectively and irreversibly captures exhaled carbonyl compounds produced as a result of cancer metabolism.

Nevertheless, even if gas sensors are able to accurately diagnose and monitor with high sensitivity, these techniques are not designed for biomarkers discovery; key component for the establishment of model discrimination. This lack of biomarkers hunting can be overcome by MS techniques and moreover can elucidate structures of unknown compounds in combination with NMR.

II. MS based strategies

Numerous real time approaches are available for VOC analysis including methods based on direct injection mass spectrometry (DIMS) as selected ion flow tube-MS (SIFT-MS), proton transfer reaction mass spectrometry (PTR-MS) and ambient ionization MS techniques such as Direct Ambient in Real Time (DART) and Low Temperature Plasma (LTP). MS is a powerfully fast, sensitive and robust analytical technique used to separate and detect specific gas-phase ions from a complex matrix according to their m/z. MS is recognized as the most sensitive general purpose analytical methods. MS studies provide high dimensional information of data set and consequently require extensive processing in order to handle data set. Different workflow is possible for metabolomics analysis including, targeted and untargeted analysis.

a. Direct injection mass spectrometry (DIMS)

DIMS technique has been characterized by the direct introduction of the sample gas (breath, balloon, and headspace) is into the device. The technique is applied to rapid monitoring and quantification of VOCs. PTR-MS and SIFT-MS have already been used for this type of analysis and proved their potential for the real-time monitoring of VOCs[85].

i. SIFT-MS

Created at the University of Birmingham, UK in the mid-1970s, SIFT-MS (Figure 15) is an analytical technique for real-time, on-line analysis of VOCs in a large range of applications[86,87]. It was developed to satisfy the need for kinetic data on gas-phase ion-neutral reactions that required to describe the production of molecules. Absolute quantification is achieved by knowing the rate coefficients and ion products of the selected precursor ion with the analyte trace gas molecules in the air sample. In this way, several trace compounds can be accurately and simultaneously quantified in an air mixture.

The essence of the SIFT-MS relies in the selection of positive precursor ions such as H_3O^+, NO^+ or $O_2^+\bullet$, to ionize the trace gas molecules in a sample that is introduced

directly into an inert carrier gas (usual helium) in a flow tube. First, the chosen precursor ion H_3O^+, NO^+ or O_2+• is selected by a quadrupole mass filter from a mixture of ions generated in a microwave discharge. They are injected into the drift region and operate under fast-flowing He carrier gas (pure He at 100 Pa) through a Venturi-type inlet. The selected ion is used to ionize the trace gases in a sample that is introduced via carrier gas previously heated at a known flow rate. The reactions between the precursor ions and compounds traces within the sample resulting in characteristic productions that identify compounds and allow quantification. This swarm gas travels along the flow tube and the ions are sampled downstream via a pinhole orifice and focused into a differentially pumped quadrupole MS. After m/z analysis they are detected and counted by an electron multiplier/pulse counting system.

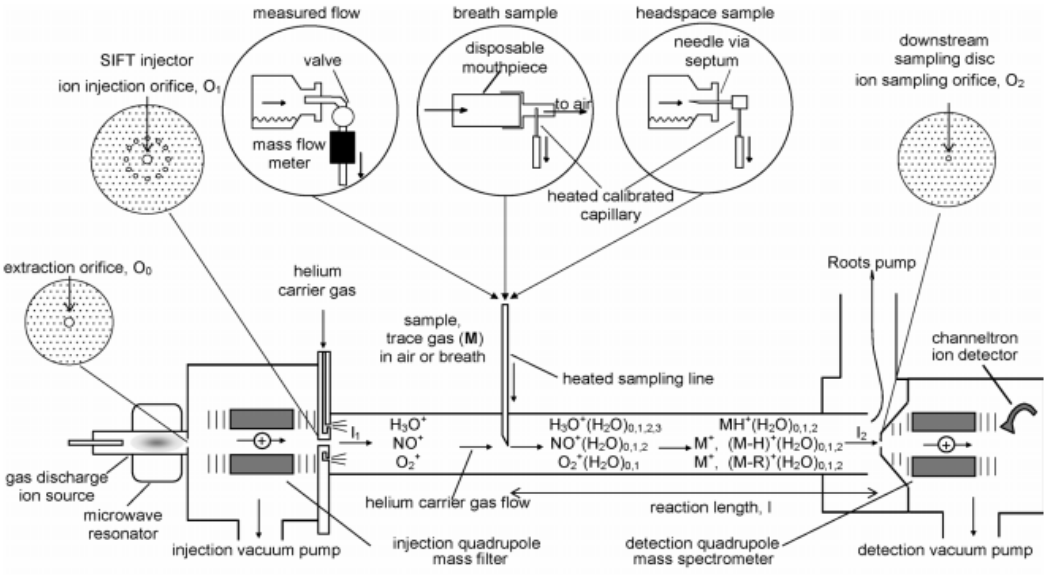

Figure 15: Schematic representation of SIFT-MS instrument extracted from Spanel et al. Reagent ions generated in the microwave discharge are extracted via the ion source orifice and then selected by the injection mass filter. Selected ion pass into the flow tube and react with the trace gas analytes in the sample bag, desorbtion tube, or exhaled breath. Reagent and product ion are then analysed by MS.

ii. PTR-MS

PTR-MS (Figure 16)[85] was first introduced in the mid-1990 and stemmed from selected the ion flow-drift tube mass spectrometry (SIFDT-MS), which combined the SIFT with the flow-drift tube (FDT) developed in the NOAA Aeronomy Laboratory in Boulder, Colorado, USA in the early 1970s. It is currently used in breath and food analysis.

Unlike conventional MS technology, often based on electron ionization (EI); PTR-MS relies on chemical ionization (CI), a soft ionization based on proton transfer from a

protonated reagent which is mainly H_3O^+. The fundamental ionization process can be expressed as $H_3O^+ + R \rightarrow RH^+ + H_2O$. Protonated water ($H_3O^+$) interacts with the trace gas molecule (R). During this interaction, a proton transfer from the hydronium to the gas molecule occurs leading to a protonated form and therefore an ionized molecule (RH^+) and a neutral water molecule (H_2O). This proton transfer reaction is energetically favourable for all VOCs with a proton affinity higher than that of water (691 kJ/ mol).
The main constituents of a PTR-MS apparatus are the ion source, the reaction region (drift tube), the mass analyzer, and the ion detector. In the ion source, the hollow cathode ion source produces a H_3O^+ primary ion beam. High intensity and high purity of the primary H_3O^+ ion allow the injection of the primary-ion beam directly into the reaction chamber without prior mass selection as SIFT. Once created, the ion is driven by an electric field (600V) under temperature (50-100 C°) and pressure (200Pa) through a short drift tube (9cm) and then interacts with the gas sample. Linear quadrupoles (mass analyzer) were used in most instruments for robustness. Time resolution (order of seconds) and mass resolution is overcome by the coupling of PTR with a time-of-flight (ToF) mass analyzer.

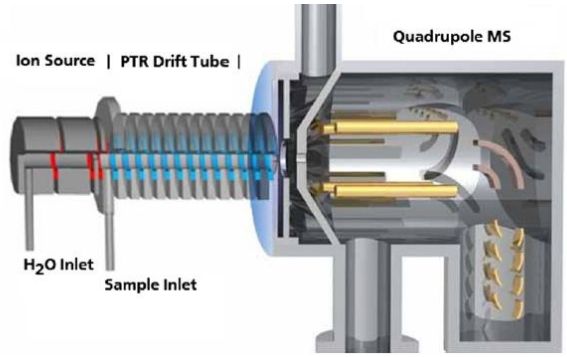

Figure 16: schematic representation of a PTR-Q-MS instrument. The entrance of H_2O in the hollow cathode ion source produce precursor ion. The sample gas entrance is through the drift tube reaction chamber. The quadrupole mass filter are coupled to a secondary electron multiplier detector. Reagent and product ion are then analysed by MS (IONICON analytic GmbH).

b. Membrane introduction mass spectrometry (MIMS)

Membrane introduction mass spectrometry (MIMS) (Figure 17) has been introduced in 1963 and utilizes a semi-permeable membrane as an interface between a sample to be measured and a mass spectrometer[88,89]. The membrane pre-concentrates analyte from the sample based on their physicochemical properties and transfers them (as a mixture) to the mass spectrometer. MIMS systems can be classified into two groups by the nature of the acceptor phase on the downstream side of the membrane.

Gaseous phase MIMS (GP-MIMS) refers to the strip of analyte from the membrane and they are pneumatically transferred to the mass spectrometer in the gas phase (e.g. helium carrier gas or vacuum). If the analyte volatility limits or prevents efficient pervaporation of analyte from the membrane into the gas phase, an additional condensed liquid acceptor phase (CP-MIMS) is used, mostly methanol. The direct coupling of semi-permeable membranes to mass spectrometers enables rapid and direct analysis with minimal sample handling. MIMS reduces the use of solvents and provide real-time data. Furthermore, it can be used as a continuous, sensitive (ppt-ppb level) on-line monitoring approach over long periods and employed to follow dynamic changes in trace analyte[90]. MIMS has greatly benefitted from developments in material science (e.g.membrane interface), ionization techniques (e.g. EI, CI, ESI, APCI, APPI) and mass anlysers (e.g. Quadrupole, Time of flight, Fourier transformation MS allowing a degree of versatility for specific analyte/sample combination) for optimal sensitivity and selectivity. These extensions of MIMS enable the characterization of previously inaccessible groups of compounds, including semi-volatile compounds, trace organic compounds in the atmosphere, free radicals and organometallic compounds.

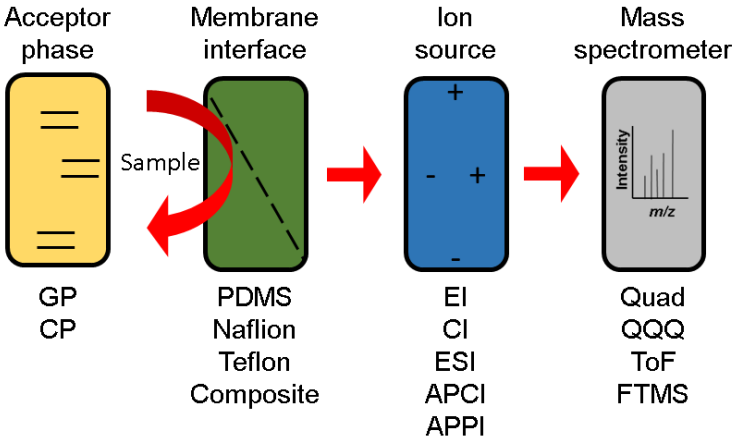

Figure 17: Schematic representation of the various set up of MIMS. The pre-concentration of analytes from a sample into a semi permeable membrane followed by their ionization and measurement.

c. Ion mobility spectrometry (IMS)

Developed in the early 1970s, ion mobility spectrometry (IMS)[91] (Figure 18) consists in two main parts: ionisation and reaction region (formation of gas phase ions) and a drift tube (drift region). The ionization in analytical IMS is commonly realized at ambient pressure. Between the ionization chamber and drift tube a shutter grid is located which passes a batch of ions into the drift tube. In the few centimetre length drift region, ions

moves through purified air at ambient pressure in short impulses (10- 100ms) of a voltage gradient or electric field (E in V/cm). Additional gas chromatographic columns can be supplemented to IMS to guarantees the pre-concentration and separation of gaseous metabolites before entering into the drift tube[92]. Combined with high-speed data acquisition, IMS is transportable, sensitive and inexpensive. IMS has many application including food processing and quality[93], microbial control[94], health care[95] and diagnosis[96].

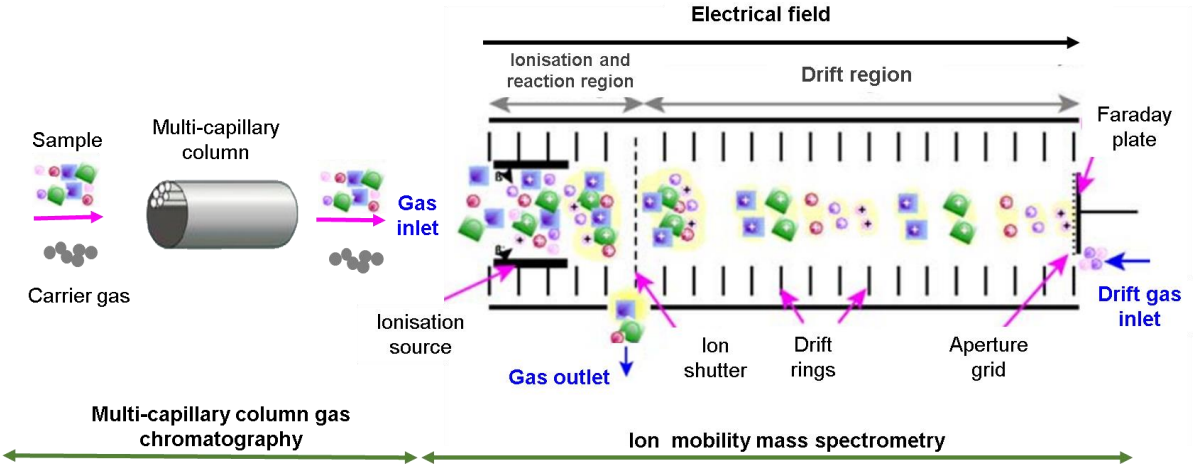

Figure 18: Schematic representation of MCC-IMS. Overview of multi-capillary column separation technique coupled with an ion mobility mass spectrometer. An ion mobility spectrometer is composed of. Left: ionisation and reaction region to form ions of the analytes. Right: drift chamber to separate the ions formed. The gas inlet is the entrance point of the carrier gas air with all molecules including the metabolites; the drift gas is a pure gas flowing towards the ions drifting to avoid entrance of ion at the ion shutter; the gas outlet is the outlet of the carrier and the drift gas; the aperture grid protects the Faraday plate; the drift rings stabilise the electric field within the drift region.

d. Ambient mass spectrometry

Ambient ionization mass spectrometry (AIMS) describes all mass spectrometry ionization methods, which are able to ionize constituents of natural samples under ambient conditions[97]. Ambient desorption ionization techniques for mass spectrometry have been developed, for samples in solid, liquid or gaseous states which can be directly ionized under ambient conditions with or without sample preparation[98]. Since the introduction of the desorption electrospray ionization mass spectrometry (DESI-MS)[99,100], thirty other methods have been developed and classified in three groups according to the desorption process corresponding to (i) solid-liquid extraction using droplets, (ii) thermally desorbed and chemical ionized and (iii) laser ablation ionization Among the thermally desorbed and chemical ionized or the electrical discharge or

plasma based ambient ionization methods, the direct analysis real time (DART)[101], the desorption atmospheric pressure chemical ionization (DAPCI)[102], the plasma-assisted desorption ionization (PADI)[103], the dielectric barrier discharge ionization (DBDI)[104] and the Low-temperature plasma (LTP)[105] are the most used and described methods. The advantages of plasma based ambient ionization include excellent ionization efficiency (polar and nonpolar compounds), no solvents or waste generated, little dependence on sample placement and many are capable of portability. However the largest disadvantages of ambient ionization plasma source is their inability to desorb/ionize large, non-volatile analytes as it is heavy relying on thermal desorption.

i. DART-MS

DART was developed in 2003 (Figure 19) by Cody and Laramee as a new atmospheric pressure ionization process well suited for the analysis of small molecules (below m/z 1000). The operation of DART involves the application of an electrical potential to a gas with a high ionization potential to form a plasma of excited-state atoms and ions, in order to desorb low–molecular weight molecules from the surface of a sample. Within the DART ionization source, electrical discharge is applied to He gas producing an electrical glow discharge and generating ions, electrons, and excited-state neutral species as metastable. Cations, anions and electrons are removed with intermediate lenses electrodes leaving electrically excited neutral metastable species at the exit of the source. These exiting gaseous species pass through a gas heater which adjusts the gas temperature (thermal analyte desorption) between 50°C to 550°C.The sample is placed under ambient conditions in the zone between the ion source and the inlet of the mass spectrometer (5-25 mm). Ionization occurs when direct interaction of the analyte with the metastable He or with the ions formed by a secondary reaction of He with water clusters surrounding air. DART source is generally coupled to a TOF or and an Orbitrap. DART-MS is used for the analysis of plant, animals, food[106], microbes and metabolites from living tissue and biological fluid[107] .

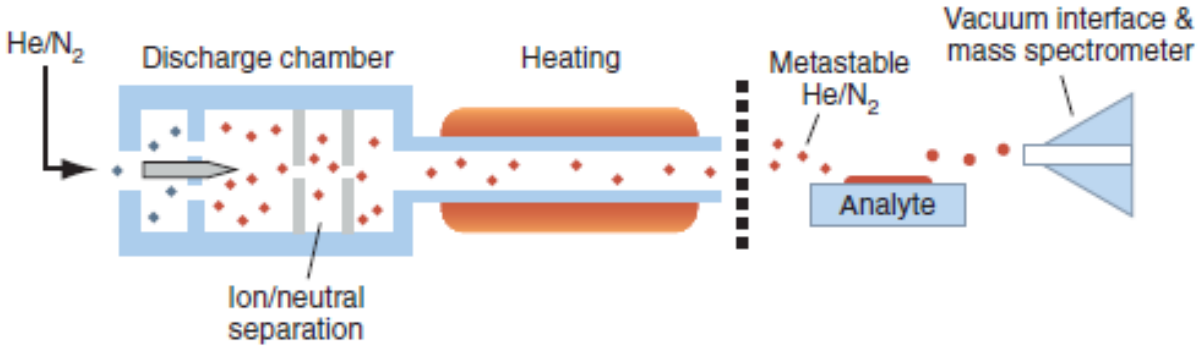

Figure 19: Representation of DART for ambient high throughput mass spectrometry analysis (skin, urine, tissues and drugs).

ii. LTP-MS

First introduced in 2008 by Harper et al[108], the LTP (Figure 20, a) is an atmospheric ionization source based on a dielectric barrier discharge (DBD)[109] process. However, it differs from DBDI (Dielectric Barrier Discharge Ionization) in the way that the counter electrodes are placed within the probe allowing the analysis of any type of object without placing the sample between two counter electrodes. In the case of LTP analysis[110], the sample is exposed to non-thermal plasma (NTP) (23°C) in contrast to DART (50-550°C). LTP uses a high AC electric field to induce a DBD in a buffer gas (generally He).Thus, the LTP operates through numerous micro-discharges which generate such chemically active species such as high-energy electrons (20eV), metastable neutrals, and radical ions. LTP has been shown to be efficient to analyze molecules of high volatility and various polarities, covering applications outside the field of other AIMS techniques including Electrospray Ionization (ESI) and Atmospheric Pressure Chemical Ionization (APCI). An advantage of this method is that the cascade of reactions in the plasma leads to the formation of both positive and negative ion species without modifying the LTP probe parameters. This enables of a large variety of molecules to be analyzed in a single experiment by changing the polarity of the MS instrument.

In addition, LTP sources are easy to set up, cost-effective and low power consumption. Number of diverse types of applications have been developed (Figure 20, b), including food safety[111,112], plant biosynthesis[113], pesticide detection[114,115,116]. Besides analytical applications, LTP devices have also been designed for wound healing[117], skin decontamination[118], treatment[119] and imaging[120]. Additionally, a LTP source could be coupled to numerous types of mass spectrometers such as ion trap, orbitrap, Q-TOF

and even coupled to a GC system for on line separation[121]. Furthermore low power and He consumption and miniaturization system lead to portable ionization source coupled to MS has been already described and applied for the detection of melamine into the milk, detection of explosives[122] from surfaces and the determination of organic vs. non-organic apples in supermarkets[123]. Thus, LTP is definitively an interesting technology for the analysis of the volatilome.

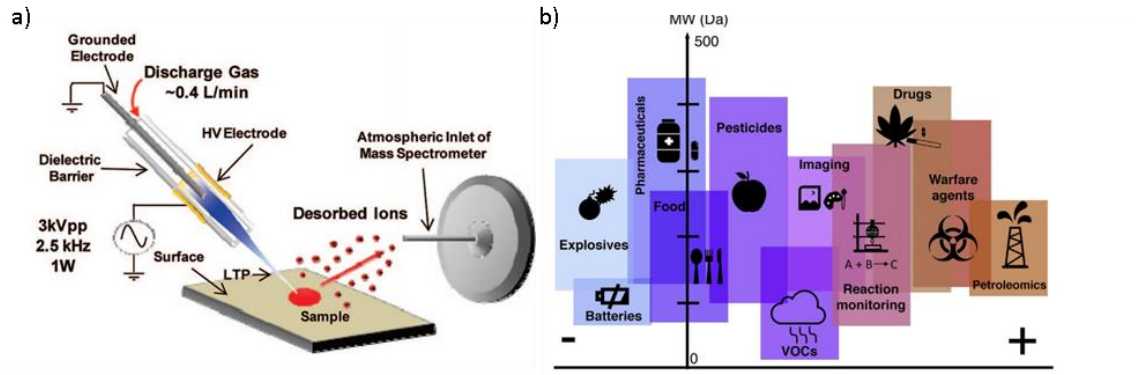

Figure 20: Low temperature plasma system. a) Low temperature representation b) Domain application of LTP.

LTP Configuration:

Even if the LTP probe[124] is not commercially available, it's easy to construct and present a low cost and power consumption. The LTP probe setup consists of a glass tube with an internal grounded electrode made of stainless steel and centered axially. The wall of the glass tube serves as the dielectric barrier and a piece of copper tape is wrapped around the exterior as the high voltage electrode. An AC, between 1 and 30kV at a frequency between 1 and 30 kHz, is applied to the outer electrode with the center electrode grounded to generate the DBD. A discharge gas either He, Ar, N_2 or air, is fed through the glass tube to facilitate the discharge and to transport the analyte ions to the mass spectrometer. The flow rate of the discharged gas can be ranged from 1 to 1000 ml/min. The generated plasma is thus formed and directed toward a sample. Excited species from LTP are pushed out of the glass tube to interact with the sample and are then sucked into the MS inlet capillary.

For a constructed LTP source of any dimension/geometry, the major adjustable parameters that have an impact on desorption/ionization capabilities include the choice and the flow of the discharge gas, the positioning of the two electrodes and the correct current/voltage. Discharge gas composition also plays a large role in

desorption/ionization capabilities. He is typically chosen as it yields the best sensitivity, related to the fact that He has much higher excited states than each of the other gases and can form the necessary reagent ions more efficiently. The performance of the LTP probe has been found to be minimally sensitive to the distances and angles of the probe-sample-MS inlet geometry whereas the width of the copper tape electrode has an effect on the power. The electric field is another important parameter that can have an effect on the analyte signal. Harper et al[108]. have showed that increasing the gap between the ground and high voltage electrodes resulted in increased analyte fragmentation. Furthermore increasing the applied power results in an increase in the plasma temperature via joule effect and leads to an increased thermal desorption capabilities.

LTP reactions:

The properties of an LTP ion source[22] depend on the probe design, electrical power input (frequency, voltage, and power), and the discharge gas. There are three main types of reaction that occur during LTP ionization, which are the electron transfer, the proton transfer and the adduct formation.

The main ionization mechanism (Figure 21) is the electron ionization by free electrons accelerated in the applied electric field. In particular, at low pressure the positive ions created in the ionization process drift to the cathode and lead to secondary emission of electrons. This subsequent delivery of free electrons seeds new avalanches; the main aspect of the Townsend-breakdown mechanism that leads to the generation of a self-sustained gas discharge. He is usually used as the discharge gas because most molecules (M) can be ionized by the excited helium metastable He_m (22.7 eV) through a Penning mechanism (electron transfer):

$$He_m^* + M \rightarrow He + M^+ + e^-$$

Note that He_m^* is an exited metastable He and is the species that result from a loss of a photon from the 3^3S_1 triplet state (i.e. emission of photon at 706.5nm).

Charge transfer by proton transfer is also a major reaction occurring during LTP ionization. Ion-forming reactions occur with molecules from the atmosphere surrounding the plasma in the afterglow region, especially with nitrogen and water. Protonated water clusters are often observed and the humidity of ambient air affect the LTP ionization. Same formation of APCI water cluster process from He*(Equation 2) is commonly accepted for LTP. In LTP-MS analysis, water cluster formation are the major

reageant ions responsible for analyte protonation and thus proton transfer ionization (Equation 2). This protonation is largely plays by H_3O^+ due to its low proton affinity (PA) at 690 kJ/mol which enables it to transfer a proton to many different compound; much more than two protons bonded water $[H_2O+2H]^+$ which has a PA greater than 900kJ/mol.

$He_m^* + N_2 \rightarrow He + N_2^+ + e^-$

$He_m^* + H_2O \rightarrow He + H_2O^+ + e^-$

$N_2^+ + 2N_2 \rightarrow N_4^+ + N_2$

$N_4^+ + H_2O \rightarrow H_2O^+ + 2N_2$

$H_2O^+ + H_2O \rightarrow H_3O^+ + OH$

$H_3O^+ + (n-1)\ H_2O + N2 \rightarrow (H_2O)n\ H^+ + N_2$

Equation 2: Water cluster formation with He in APCI mechanism.*

The analyte in gaseous state with high proton affinity is ionisated by proton exchange (soft ionisation): $(H2O)n\ H+ + M \rightarrow (H2O)n+MH^+$

Proton transfer is more effective when the sample is placed in a more energetic afterglow region of the plasma. In positive ion mode, protonated water clusters are responsible for the majority of analyte ionization through proton transfer. Spike like N_2^+ O_2^+ and NO^+ are capable of ionizing analyte via eletron transfert while NH_4^+ is capable of forming analyte ions through the formation of adducts. The following reaction cascade are responsible of the formation of water adducts, ionization and fragmentation.(Kambara & Kanomata 1977) (Equation 3).

$N_2^+ + e \rightarrow N_2^{+\bullet}$

$N_2^{+\bullet} + 2N_2 \rightarrow N_4^{+\bullet} + N_2$

$N_4^{+\bullet} + H_2O \rightarrow H_2O^{+\bullet} + 2N_2$

$H_2O^+ + H_2O \rightarrow H_3O^+ + OH$

$H_3O^{+\bullet} + (n-1)\ H_2O + N_2 \rightarrow (H_2O)n\ H^+ + N_2$

$H_2O^+ + H_2O \rightarrow H_3O^{+\bullet} + OH^\bullet$

Equation 3: Mechanism of ionization and fragmentation.

In negative ion mode, the various reagent ion include OH^-, O_2^-, NO_2^- and NO_3^- which combine to form ions through each of three mechanism mentioned.

Ozonolysis reactions can be observe due to the interaction of ozone plasma poduced with atmospheric oxygen (Equation 4).

$O_2 + e^- \rightarrow 2<O> + e-$

$<O>+O_2 +M \rightarrow O_3+M$

Equation 4: Mechanism of ozonolysis

Ion formation with LTP

Ions reported in LTP-MS[125] studies include $[M]^{\cdot+}$, $[M]^-$, $[M+H]^+$, and $[M-H]^-$, adducts and reaction products, such as [M+H2O]+, $[M+NH_4]+$, [M+O]+, $[M+2H]^{2+}$, $[M+NO_3]^-$, $[M+NO_2]^-$. Often, clusters products are also identified such as $[2M+H]^+$ and $[3M+H]^+$.

Ionization of liquid and solid samples can be proceeded by several mechanisms (Figure 21) momentum transfer by the plasma flow and b) thermal desorption (TD) for ambient desorption ionization MS. The interaction of plasma with surfaces leading to the generation of charged particles on these surfaces might be the result of secondary electron emission, photoemission, thermal electron emission, or field electron emission. However, charges may be lost by direct electron absorption. Desorption of molecules by LTP is known to be related mainly to the thermal desorption (TD) processes of molecules prior to their ionization by LTP.

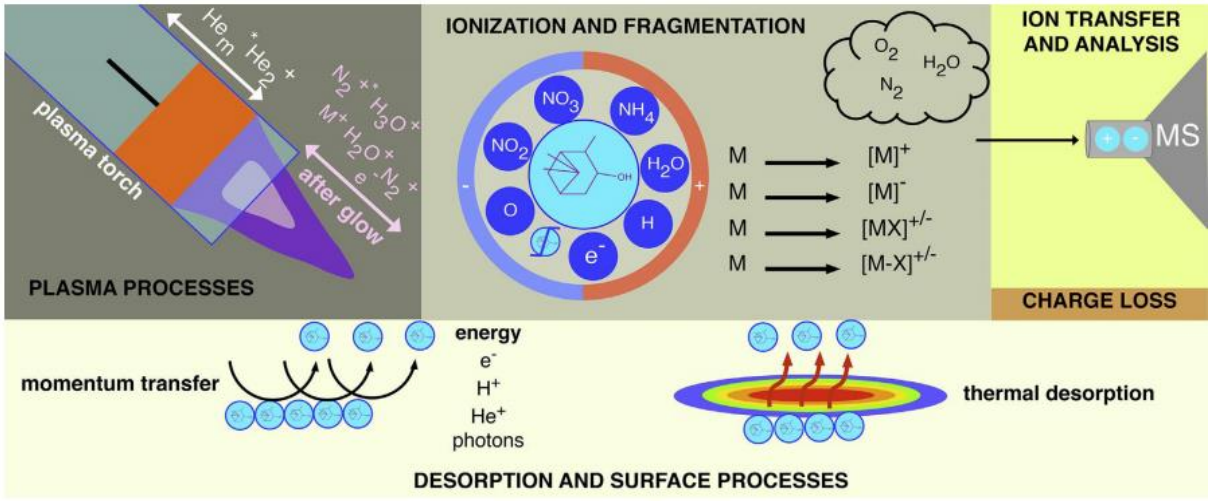

Figure 21: Schematic representation of ion process occurring in the plasma probe with surrounding molecule (M) and on surfaces. Ionization and fragmentation events are possible. Molecules and ions are lifts from surfaces by thermal desorption and transferred to the mass spectrometer (MS).

This last MS based method was described as the most versatile ambient ionization source for the simultaneous detection of different class of small molecule at liquid, solid or gas state without any separation step The LTP application cover explosives, drugs, warfare agent, petrol omics and pesticides detection and quality

control of air environment or food. In addition by VOCs analysis, imaging is first realised on pepper. It is furthermore a costless, easy to set up method and requiring less maintenance than other sources. This source able the VOCs ionization from membrane solid and liquid and could be couple with multiple mass analysers.

Chapter III: Volatolome sampling method

An adequate volatolome sampling is a paramount component for a successful VOCs analysis. To select the optimal sampling method several parameters need to be consider including (i) the nature of the sample (e.g. gas, liquid and solid), (ii) the presence of targeted analyte into the sample (coefficient partition, concentration), (iii) the type of sampling (e.g. direct and indirect) and (iv) the coupling of sampling method and the analytical instrument (**Erreur ! Source du renvoi introuvable.**). As previously mentioned, the bio distribution of VOCs in the body fluids are governed by the partition coefficient leading to a difference of VOCs concentration. For instance hydrocarbons are highly apolar and few soluble in urine. Consequently, in breath >3000 (913 link to diseases) VOCs were reported with an over representation of hydrocarbons (40% of total OVC in breath) and only 200 VOCs were reported in urine with an under representation of hydrocarbons (12% of total VOCs in urine). The concentration of VOCs will then govern the choice of the sampling (e.g. direct and indirect). VOCs present in high concentration within the sample, could be detected by both sampling; whereas the less representative ones should be pre-concentrate to facilitate and enables their detection. (iii) The direct sampling consist of the online analysis of the sample without any sample preparation and the indirect sampling consist of the preparation and pre-concentration of the sample. Beyond the huge difference of time process, indirect sampling provide a better limit of detection (ppb) of VOCs than direct sampling. It includes cryogenic pre-concentration, solid sorbents (thermal desorption tube), membrane devices, solvent extraction, solid-phase micro-extraction (SPME) and needle trap (NT). For instance breath analysis could be proceed online by SIFT-MS analysis or could be pre-concentrated onto thermal desorption tubes and then subsequently analysed by GC-MS. In this context, the sampling method has to be chosen according to the nature of the sample (e.g. breath, liquid and solid) and the class of the VOC (polar, apolar) while considering the associated partition coefficient when available. The Figure 22 present the different combination between sample type and sampling type. Each strategy is specific of the sample to be analysed.

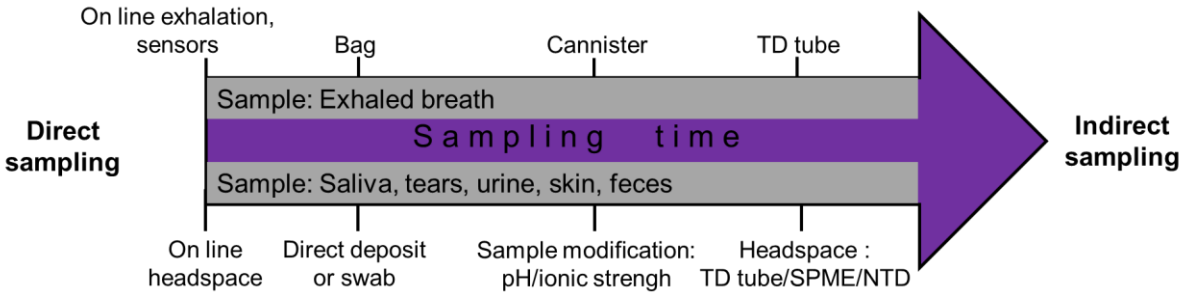

Figure 22: Schematic representation of sampling method according to the sample type (e.g. exhaled breath, saliva, tears, urine, skin and feces). The arrow represent the sampling time difference between direct and indirect sampling. TD tube: thermal desorption tube, SPME: solid phase microextraction, NTD: needle trap device.

Exhaled Breath.

The rising interest of exhaled breath sampling in clinical, medical monitoring and diagnosis is attributed to its non-invasive nature, the fast sample collection and the accessibility to an unlimited sample supply (e.g. breath). Moreover, breathomics is very well suitable for the diagnosis of children or even in baby considering that the collect do not require cooperation (e.g. full face mask and tidal breathing). Even more, breathomics is orientated toward personalized medicine since the final clinical goal of studies is to optimize treatment for patients by taking into account individual patients' breath characteristics. However, progress from laboratory setting to routine clinical practice has been slow. The lack of standardization though reliable breath collection, sample storage and analysis techniques leading to a poor repeatability and the difficulty in comparing and combine data.

The collection of breath sample represents a crucial issue in breathomics due to the sample dilution effect, contamination and the loss of analytes during the sampling procedure. Numerous sampling methods have been developed as so the number of sampling and analysis workflow. Sampling method can be classified by (i) the type of collected breath (e.g. mixed expiratory or end-tidal), (ii) the sampling duration (e.g.- single breath vs fixed time or fixed volume), the number of exhalation (e.g. single or multiple exhalations) the expiratory flow and (iii) the type of sampling (e.g. direct and indirect).

(i) During breath sampling different portions of the breath can be collected and divided into late expiratory, end-tidal, and mixed expiratory samples (Figure 23). In principle there are two basic approaches for breath collection, the mixed and the end-tidal collection.

Mixed expiratory sampling: the total breath is taken including dead space air (air not involved in gaseous exchange) and end tidal air. This breath sample does not provide the best quality of sample due to a large abundance of environmental, mouth, and nose contaminants. However, this simple sampling method does not require additional equipment.

Alveolar sampling (end-tidal): means that pure alveolar gas is collected from the beginning to the end of phase III of the breath cycle. This breath contains high concentrations of endogenous VOCs and minimal contaminants. With this type of sampling, the discrimination model has higher sensitivity and specificity than mixed breath. It's explained by the concentration of endogenous VOCs which are two or three times higher than in mixed expiratory air because there is no dilution by dead space gas and contamination is lower. However this sampling method is much more restrictive. It involves the discarding of the initial portion of the exhaled breath (estimated dead space, phase I and II) and the capture phase III breath cycle.

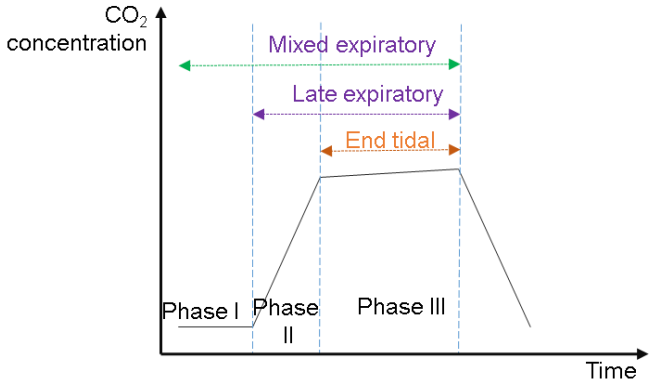

Figure 23: Schematic representation of a single exhaled breath phase by capnography. Phase I: dead space, phase II: transition, Phase III alveolar. Adapted from (Meikisch and al.2008)[126].

The choice to include or not this part of the breath depends on the consider disease. In order to identify the origin of the detected VOCs, comparison of both bronchial and alveolar part is advised. Selective sampling of the alveolar compartment can reduce oral contaminant concentrations, but the techniques remains challenging

(ii) The concentration of VOCs is impacted by the number of exhalation, the flow and the collected volume of exhaled breath. It was reported in single breath analysis that breath sampling during a fixed time can reduce variations in breath-to-breath volatile concentrations. Breath sampling from a predefined fixed volume is also used. New method of integrating real-time breath sampling with spirometry was technically and

medically validated. The spirometer allow the measured of volume exhaled air to selectively let through the end tidal breath.

(iii) VOC concentrations in exhaled breath are generally in the parts per billion (ppb) to parts per trillion (ppt) range (nM to pM). For this reason different breath sampling methods are currently used.

I. The direct sampling methods

The strategy is based on the online analysis of the exhaled breath without any-pre-concentration by an analytical detector. Additional sampler could be used to selectively extract the end tidal breath and discard the bulk of contaminant (spirometer). The exhaled breath is then guided to analytical detector such as mass spectrometers (e.g. IMS, SIFT-MS, PTR-MS, LTP-MS) and sensor devices. Sensors being particularly attractive for personalized and routine monitoring of health parameters due to the ease to use and rapid diagnosis. Despite exhaustive study and no sensor has emerged as a clinically accepted standard for monitoring respiratory rate.

II. The indirect sampling methods

This is the offline analysis of exhaled breath by MS techniques (e.g. GC-MS, SIFT-MS, PTR-MS and LTP-MS) and sensors.
VOC concentrations in exhaled breath are generally in the parts per billion to parts per trillion ($\mu g/m^3$ to pg/m^3) range. For this reason, exhaled breath is collected in inert container (e.g. Mylar, Tedlar bags) and possibly condensed in a canister and / or submit to pre-concentrations methods. Thorough handling sample is require; especially in case of bag sampling in order to ensure sample authenticity, short storage times as compounds may be degraded and lost (e.g. by diffusion through Tedlar bags). Several devices and pre-concentration techniques based on adsorption onto sorbent traps or coated fibres have been developed to overcome degradation during storage and dilution effect. These methods include solid-phase micro extraction (SPME), sorbent-tubes (TD tubes) and needle trap devices (NTDs). Nowadays, some sampler has been developed to assure sampling standardization as it can be found with the RECIVA system (owlstone medical) and BioVOC-2, (MARKES international).All the pre-concentration methods are design to be directly connected to sampler, bags or canister to enhance the VOCs stability and concentration.

Ideally, breath sampling method should be compact, fast, reliable, and easy to use in clinical care allowing targeted selection of airway and/or alveolar air to be collected and eliminating sampling from the dead space and environment.

Liquid and solid.

As previously described, two types of sampling are available the (i) direct and (ii) the indirect sampling depending the concentration level of VOCs within the liquid and solid sample.

I. The direct sampling methods

They can be directly analyzed without any sample preparation and pre-concentration. Examples were presented by means of MS based instrument including LTP-MS and DART-MS analysis. These two technics are able to desorb and ionize volatile molecule from surfaces or liquid which can be subjected to MS analysis. It has been showed that pesticide were directly detected from apple by LTP-MS and aspirin was also directly detected by DART-MS. LTP-MS was also used as control quality of tequila. Nevertheless, samples continuously produced and emanated VOCs. To accumulate the release VOCs in the above gas phase called headspace, the sample is place in glass vial or suitable container. The glass vial or a sweep gas could be heated in order to increase the transfer of semi volatiles in gas phase and therefore this heating improve the compounds detection (Figure 24). Though a sweep gas, the VOCs headspace are then transferred through a line heated or directly to the analyser. Such device are used with PTR-MS and SIFT.

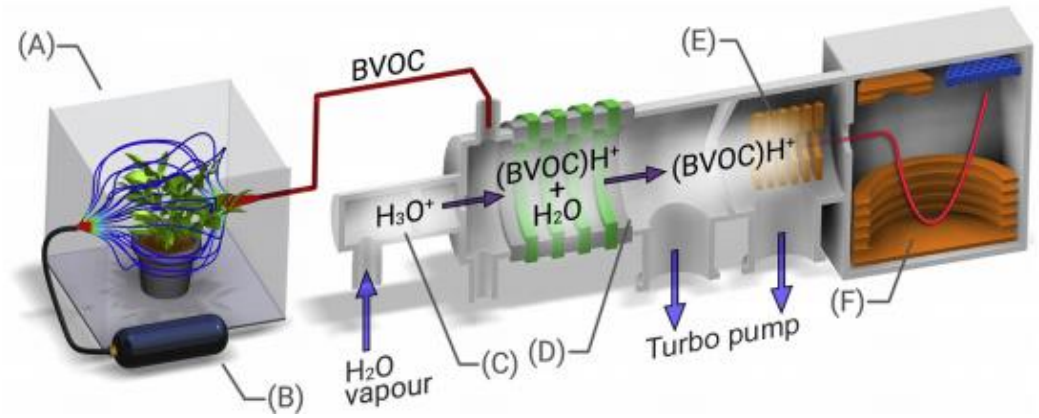

Figure 24: Principle of Proton Transfer Mass Spectrometry (PTR-MS) for real time analysis of VOCs plant emanation. The element of the diagram are: (A) the sampling enclosure, (B) ambient air VOC filter, (C) hollow cathode, (D) dirft chamber,(E) transfer lenses and (F) TOF mass analyser.

II. The indirect sampling

The gold standard of indirect sampling of VOCs from liquid and solid sample is the headspace sampling (HS) which is the fastest and non-destructive method for the VOCs investigation. This green sample preparation (GSP) allows the amount of organic solvents used to be decreased with a lower power consumption

This indirect sampling is commonly based on released of VOCs into the gas phase (headspace, above the liquid phase) by means of Headspace sampling (HS) (Figure 24). In HS the sample is place in a sealed glass vial and incubated at a constant temperature. In this system, analytes are distributed between two phases – the sample phase (either liquid or solid) and the gas phase above it (the headspace). Some sample preparation (e.g. pH, ionic strength, stirring, volume sample) influence the headspace formation. The VOCs will be then pre-concentrate onto sorbent (single or multiple bed) by different method (e.g. SPME, TD Tube and NTD) and then submit to analysis.

a. Sample preparation:

It has been demonstrated that many factor can influence the transfer of VOCs and semi volatile compound from solid/liquid phase to the gas phase and therefore the HS. In this context, sample preparation including the PH, ionic strength, the extraction time and temperature, stirring and sample volume size are fundamental parameters which have to be considered to greatly improve the extraction and the transfer of VOCs in the HS. To enhance transfer of some VOCs in the gas phase, the sample can be submit to multiple preparation step as follow (i) pH modification (ii) ionic strength modification (iii) addition of temperature during the sampling (iv) addition of stirring.

(i) Modification of pH: The pH of the medium affects the extraction efficiency of acidic and basic metabolites as they can only be extracted by sorbent in the protonated form.

(ii) Ionic strength: The salt addition influences the extraction efficiency by changing the properties of the boundary phase and decreasing the solubility of hydrophilic compounds in the aqueous phase. Sodium chloride, sodium hydrogen carbonate and potassium carbonate are generally used. Enhancing the salting-out effect during the extractive process and therefore facilitate the diffusion of metabolites to the vapor phase, called headspace. A gain in extraction efficiency is obtained generally with up to 15-20% NaCl (w/v). On the other hand, excess of salts in solution do not favour the extraction.

(iii) Temperature: enhancing the temperature facilitate the mass transfer of the compounds from the bulk sample to the headspace vapor phase. This increases the

diffusion coefficient and decreases the distribution constant, reaching faster the balance between the two phases; by increasing the temperature the extraction time is reduce.

(iv) Stirring: Constant and efficient sample stirring or agitation facilitates sample homogenization and VOCs diffusion from the liquid to the headspace phase, thus reaching equilibrium more quickly. A constant sample stirring at 800 rpm contributes to a considerable improvement in the extraction efficiency of the methodology, almost two times more efficient than with no stirring approach.

b. Headspace (HS) sampling:

However, even if direct detection of VOCs from solid or liquid samples remains attractive and straightforward, the strategy suffer from a lack of sensitivity, only the most abundant VOC can be detected. In this context, it is important to develop method allowing the accumulation of VOCs in a restricted gas phase volume prior their analysis. This is possible considering that sample continuously produce and emanated VOCs and therefore it has been widely demonstrated that HS strategy lead to the accumulation of VOCs in a restricted gas volume allowing detection of the less abundant one. (Figure 25).

To accumulate the release VOCs a restricted gas phase, the sample to be analyzed, is placed in a sealed glass vial or a suitable container. The glass vial could be heated and agitated in order to increase the transfer of semi volatile compounds in the gas phase and therefore improve their detection.

This indirect sampling is commonly based on the released VOCS into the gas phase (headspace, above the liquid/solid phase). In HS, the sample is placed in a sealed glass vial and incubated at constant temperature. In this system, analytes are distributed between two phases: the sample phase (liquid or solid) and the above gas phase (the headspace). The phase formation depends on two parameters: the partition coefficient (K value), and phase ratio. The partition coefficient equation is K = CM/CG (CM: Concentration in Matrix, CG: Concentration in headspace/gas phase). The lower the K value is, the higher the concentration of analytes in gas phase will be. The K value could be reduced by increasing sample temperature or by addition of inorganic salts to the sample matrix phase ratio (b value).The phase ratio correspond to the following equation $\beta=Vs/Vgs$ (Vs: volume of solid phase Vg:volume of gas phase).The

lower the b value is, the greater the yield response will be. The b value can be lowered by increasing the sample volume. Parameter as extraction time, PH matrix, temperature sampling, volume sample, volume vial and stirring affect the headspace sampling.

Headspace sampling is separated into two types, static and dynamic sampling.

i. Static headspace sampling (SHS):

In the SHS sampling method (Figure 25,a), a solid or liquid sample is placed in an air-tight glass vial and heated for a given period of time(30 minutes to 3 days) at a constant temperature(25°C to 70°C). The analytes are transferred into the headspace and the equilibrium is reached between the solid/liquid phase and the gas phase. The volatile compounds evaporate into the gas phase at the same rate as the volatile compounds condense into the liquid phase, producing a partial pressure. VOCs in the HS can be transferred through a heated line by means of a sweep gas directly to a sensor, MS instrument or in a GC-MS instrument.

The SHS can also be coupled with all pre-concentration techniques. The headspace VOCs will be then passively adsorbed onto pre-concentrate method or manually aspirated after sampling for adsorption onto pre-concentrate method. In SHS the equilibration time is comprise between 30 and 50 min and a plateau of concentration adsorbed onto the membrane is reach. Nonetheless this technique is more adapted for volitle with high volatility.

ii. Dynamic headspace Sampling (DHS):

To overcome the inability of SHS to detect substances at low concentrations and substance with a disadvantageous partition coefficient between the liquid and gaseous phase; sampling headspace dynamic DHS (Figure 25, a) was developed by Van Wijk. In contrast to SHS, a aspiration or sweep gas (usually nitrogen) is used to continuously purge the glass vial and therefore to continuously transfer VOCs released gas to pre-concentration device. This continuous process favour the transfer of semi-volatile to the headspace and thereby the less volatile compound are trapped and concentrate in a shorter time than SHS (20 min compare to 40 min), thereby the equilibration time is reach faster. On the opposite of SHS when this equilibration is attained, the

concentration trapped analytes tends to decrease along with the time. Limit of detection (LOD) of SHD is close to ppm to ppt levels.

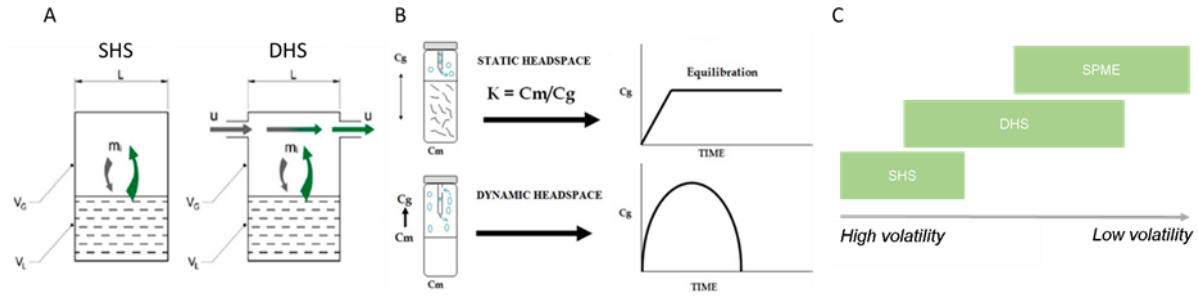

Figure 25: Headspace sampling. A.B. representation of static headspace and dynamic headspace.B. schematic comparison of adsorption efficiencny of SHS, DHS and SPME.

The HS method can be is then coupled with a pre concentration method based on sorbent materiel including, solid phase micro-extraction (SPME), thermal desorption tube (TD tube), and needle trap device (NTD) tube or sorbent disc for a subsequent analysis. This strategy has greatly improved the detection of low abundant VOCs considering that VOCs are first accumulated in the HS and then concentrated on sorbent prior to their detection

Sorbent based pre-concentration methods

Here a focused will be done on pre-concentrate method based on sorbent (e.g. SPME, TD tubes, NTD). With these methods, VOCs are trapped onto the sorbent by reaction (filter impregnate of reacting chemical) or by adsorption.

I. Sorbent

Sampling through sorbent materials serves to enrich the analytes in the sample, as they are generally found in trace and ultra-trace quantities. The selective characteristics of the sorbent chosen will determine which target compounds are removed from the matrix. Sorbent materials have a wide range of physical forms (tube, disc, tips and needle), surface and porous structures. The choice of sorbent will influence the type and concentration of target chemical, the sampling equipment and the extraction method (e.g. thermal desorption (TD) or solvent extraction) and analytical methods (e.g. direct and indirect).

The adsorption is influenced by the surface area, pore size, surface chemistry and the surface energy γ (mJ/m²). γ is probably the most appropriate feature of adsorbents to evaluate their adsorption properties since it has been found to be the most common intrinsic value to explain the adhesion force. It represents the physical interaction on surface considering that adsorption of compounds leads to the reduction of the surface energy.

γ is the combination of dispersive and specific component as described by the following equation :

$\gamma_s^t = \gamma_s^d + \gamma_s^s$. ($\gamma_s^t$: total energy of the sorbent, γ_s^d : dispersive component of the surface energy, γ_s^s : specific component of the surface energy).

The dispersive component is linked to London forces and describes unspecific interactions while the specific component reflects specific interactions including acid-base interaction, hydrogen bonding and polar interactions.

In the case of VOCs adsorption, the solid-gas partition coefficient K can reflect the interaction with an adsorbent since it describes the adsorption mechanism at low concentration.

The solid-gas partition coefficient is given by the following equation:

$$\ln K = -\frac{\Delta H_{ad}}{RT} + c$$

As shown in the equation, the ln K value of VOCs decreases with the increase of temperature and the adsorption enthalpy ΔHad (kJ/mol) of VOCs can be measured according to the Van't Hoff equation. Recently, Liu et al[127] have demonstrated that if ΔH_{ad} is negative, the adsorption of VOCs is an exothermic process indicating that the VOCs are not only adsorbed by condensation but also by specific interactions. They showed that γ is correlated with the solid-gas partition coefficient K and therefore, γ can be used to evaluate the adsorption properties of adsorbents for each VOC.

a. Sorbent characteristics

Three general types of solid sorbent (Table 4) are generally used for VOC trapping, (i) inorganic sorbent like silica and zeolites (ii) carbon-based porous materials such as activated charcoals and carboxen (CAR) and (iii) porous organic polymers including divinylbenzene (DVB), poly(dimethylsiloxane (PDMS) and Tenax (TX).

Table 4: Recapitulative table of the different sorbent according the type, structure, surface area, desorption, polarity, thermal stability and water stability.

type	structure	surface area (m^2/g)	Products	Desorption	polarity of coating	thermal stability	water stability
Inorganic	Silica gel	1-30	Volasphere	solvent	polar	400°C	high
	aluminium oxide	300	alumina F1	Solvent	polar	<400°C	high
carbon based	corbon moleculaur sieves	387–485	CAR	Thermal/ solvent	polar	>400°C	low
	graphitized carbon blacks	240–250	Carbopack	Thermal	apolar	>400°C	low
porous polymer	DVB	550	Porapak, chromosorb	Thermal/solvent	Polar	<250°C	low
	Phenylphenylen oxide polymers	20-35	Tenax	Thermaln/solvent	Bipolar	<350°C	low
	PDMS	280-350	PDMS	Therma /solvent	non-polar	<300°C	low

The amount of substance adsorbed by the medium is influenced by the surface area (m^2/g) of a sorbent, whereas the type of adsorbed compound is determined by the surface polarity of the sorbent (e.g. polar or apolar). Hydrocarbon is commonly trapped by the inorganic sorbent. Very low boiling point VOCs are trap by carbon sorbent with large surface area; whereas high boiling compounds (e.g. glycols, phthalates and aldehyde) are trapped by porous polymer for adsorption and desorption. Hence, the choice of sorbent trap is one of the paramount factors for VOC analysis in order to

obtain good recovery and high enrichment of a wide range of target compounds. A combination of several sorbents, preferably carbon-based materials and inorganic sorbent, may result in better performances for adsorption of a wide range of compound.

i. Carboxen (CAR)

The range of sorbents called Carboxen is manufractured from the partial to full carbonization of porous polymers. The most commonly encountered is Carboxen 564, which has a high porosity, and which is relatively hydrophobic.

ii. Tenax (TA, GR)

Tenax (2,6-diphenyl-p-phenylene oxide polymer) is the most widely used solid sorbent for pre-concentration of VOCs with specific surface areas (20–35 m^2/g) and potentially susceptible to chemical decomposition and degradation of reactive analytes during sampling. Tenax® is used particularly when target compounds are nonpolar, and high boiling points, typically from 100 C to 300°C. By contrast, TA has been determined not to be a suitable adsorbent for very volatile organic compounds (VVOCs, 0 < boiling point < 50–100°C). At lower temperatures, Tenax® (60°C) is able to isolate polar and nonpolar analytes although it is not as effective as other adsorbents[128]. In order to enhance the polar adsorption capacity Tenax GR (Tenax TA with 30% graphite) has been developed. Furthermore, this polymer is available in different shapes such as a tube, disc and mesh.

iii. PDMS

Poly(dimethylsiloxane) consists of a flexible (Si–O) backbone and a repeating (Si(CH3)2O) unit PDMS is a non-toxic, highly hydrophobic, translucent polymer that does not bio-accumulate. PDMS belongs to the group of silicones, which consist to mainly of silicon, carbon, hydrogen and oxygen. PDMS was first used in analytical techniques such as SPME, then in stir bar sorptive extraction (SBSE) and later was adapted as a receiving phase in sheet, rod or disk form for direct exposure as a passive sampler in environmental water. PDMS enables the enrichment of hydrophobic organic compounds with a broad range of polarities (log Kow > 3) from aqueous solutions including polycyclic aromatic hydrocarbons, polychlorinated biphenyls, organochlorine, and organophosphorus pesticides. PDMS is also insoluble in common solvents used

for analyte back-extraction (methanol and acetonitrile), and it allows thermal desorption at high temperatures (250–300°C).

b. Sorbent influence factors

An ideal sorbent for pre concentrating VOCs needs to have four main properties namely: infinite breakthrough volume; complete desorption of the target compounds at moderate temperatures; no generation of artefacts and no retention of water vapor. Only one single available sorbent material cannot meet all of these criteria for a wide range of VOCs thus there is a tendency to use multiple adsorbents. The parameter influencing the sorbent selection are as follow:

Sorbent strength: The sorbent or the selected sorbents must have high efficiency for the pre-concentration of the target species and weak enough to release the analytes during the desorption phase. Sorbent strength is usually measured in terms of retention or breakthrough volumes. Breakthrough volumes are susceptible to temperature. Strong sorbents, such as carbonized molecular sieves, are adversely affected by high relative humidity (RH). Possibility to use multi-sorbent beds can allow the pre-concentration of a wide range of volatilities.

Inertness: The sorbent material should not chemically react with the analytes. Some sorbents contain chemically active materials as carbon blacks, many of which derive originally from natural charcoals and contain trace metals. These sorbents are therefore generally unsuitable for labile (reactive) species – sulphur compounds, terpenes and amines.

Hydrophobicity: Most common weak- and medium strength sorbents are very hydrophobic, thus their sorbent strength is not compromised even when sampling at high (>80%) relative humidity. In case of GC combination, sorbents are very hydrophobic in order to avoid excess water on the capillary column which could change the adsorption properties of the stationary phase and cause unpredictable changes in the retention times

Artefact*:* Sorbents vary significantly concerning inherent artefact levels. The Chromosorb®, PoraPakTM among porous polymers have relatively high artefacts with several peaks at 5 - 10 ng levels. For well-conditioned materials Tenax® TA is better with minimum levels between 0.1 and 1 ng. Porous polymeric sorbents may form trace artefacts when sampling air containing significant concentrations of reactive gases such as ozone. This effect has been reported for Tenax® TA which generates trace

artefacts including benzaldehyde and acetophenone if ozone concentrations exceed 100 ppb. Both carbon blacks and carbonised molecular sieves, are excellent with respect to inherent artefacts between 0.01 and 0.1 ng if it iswell-conditioned.

II. Pre concentration methods

a. Solid-phase microextraction (SPME)

SPME developed by Pawliszyn in1989 was first applied to breath analysis[129,130] and then to liquid and solid samples. The SPME device consists in a fused silica fiber (1-2 cm) coated with a thin film of a suitable polymeric sorbent (stationary phase) or an immobilized liquid. SPME is based on a partition mechanism and on the equilibrium of the analyte and the extractant. The key component of detection sensitivity is the affinity between the target analyte and the stationary phase. SPME extraction could be followed by two main methods (Figure 26): (i) direct immersion of the fiber (DI-SPME); or (ii) headspace extraction (HS-SPME).

(i) In DI-SPME extraction, the coated fiber is directly immersed in the aqueous samples, and the analytes are transported directly from the sample matrix into the extracting phase. To decrease the equilibration time and improve the analyte transportation to the fiber, sample are often agitated. This method favour the adsorption of semiVOCs.

(ii) On the other hand, in case of HS-SPME method, the analytes are extracted directly from the headspace above the sample to avoid modifications caused by non-volatile and high molecular weight substances present in the sample matrix (e.g. enzymes and proteins). Furthermore, this technique allows the matrix to be modified, such as pH and ionic strength without modifying the fiber adsorption capacity. The amount of analytes onto the fiber is determined by sorption kinetics and the distribution coefficient of the compound between the coating fiber, headspace and the sample (HS-SPME). Regarding the sampling time, DI-SPME have a shorter sampling time as no equilibrium time is required, the optimal concentration is reached after 10 min extraction time whereas in the case of HS-SPME the extraction time required 45 min. Regarding the extraction efficiency , DI-SPME is at least ten fold more sensitive than HS extraction with a LOD 0.66 µg/ml and LOQ 2.25 µg/ml. Notes that in each case ,the temperature,

the ionic strength and the pH adjustment improve the transfer of analytes into the gaseous phase.

SPME fiber could be analysed directly after sampling by insertion of this one into the GC injector or submit to direct MS analysis by means of DART.

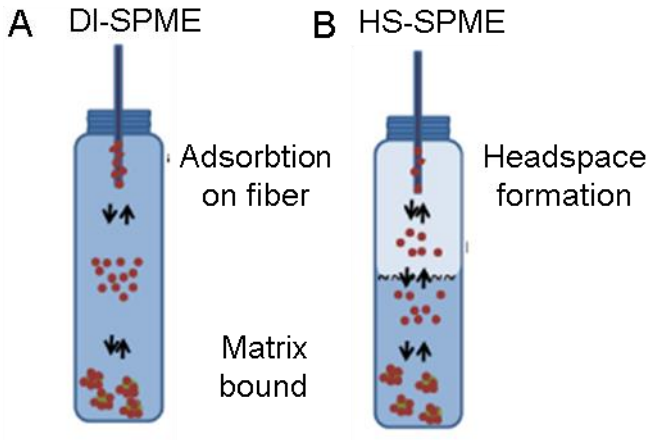

Figure 26: Schematic representation of SPME pre-concentration method. A. DI-SPME. The fiber is directly immersed onto the sample. B. HS-SPME: the fiber is placed in the headspace phase.

Numerous stationary phases are commercially available showing great selectivity for different analytes. SPME fiber coating include (i) poly(dimethylsiloxane) (PDMS) with different thicknesses (7, 30 and 100 µm), (ii) polyacrylate (PA) (85 µm), divinylbenzene (DVB) and (iv) Carboxen (CAR). No tenax fiber are commercially available and therefore to explore the possibility of utilizing Tenax TA film in SPME, silica fiber (125µm) need to be coated with liquid solution of Tenax TA (100 mg/mL) dissolve in dichloromethane. In order to capture molecules presenting different properties (polarity, volatility); mixed phases have been developed, including 75 µm carboxen/polydimethylsiloxane (CAR/PDMS) and 50/30 µm divinylbenzene/carboxen/polydimethylsiloxane (DVB/CAR/PDMS). See above for sorbent characteristic.

b. Thermal desorption tube (TD tube)

TD tubes (Figure 27) represent the most used VOCs pre-concentration methods thanks to its compatibility with GC-MS, SIFT-MS and PTR-MS (additional heater system). TD tubes are either use as pre-concentration method for breath and ambient air (e.g. RECIVA sampler; bags, canister) or directly connected to HS (static or dynamic). TD tube could be stored during several months without molecule

degradation. Even if the TD tube is the pre-concentration gold standard it is not compatible with miniaturization system.

Before using TD tube, the tube is conditioning with heating gas according the sorbent property. After this step molecule are adsorbed onto the sorbent during sampling.TD tube could be stored or directly submit to thermal-desorption of sorbent bed for the release of analyte. Furthermore when it's coupled to GC through the thermal desorption unit, automatically process allows conditioning and cleaning. Furthermore, these tubes are reusable after thermal desorption for most applications.

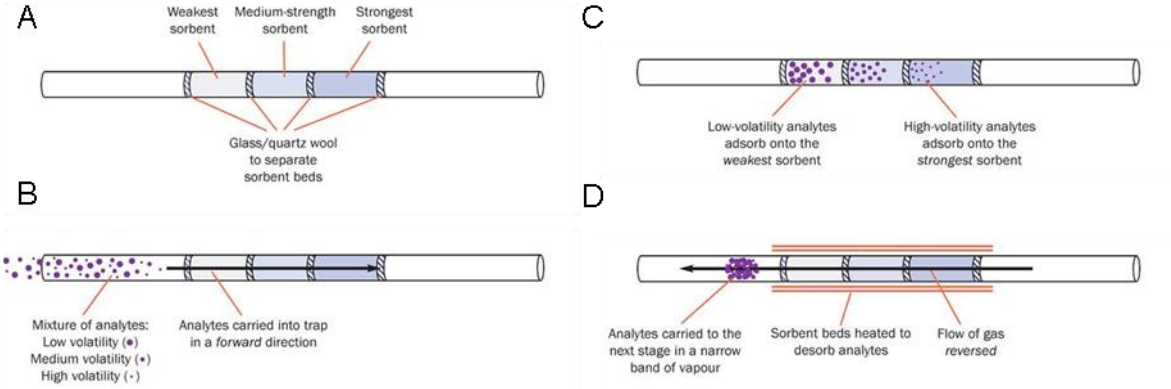

Figure 27: Schematic representation of TD tube pre-concentration method. A. Representation of typical sorbent multibed packed tube. B.C.D. Representation of the 3 steps for TD tube sampling and analysis. B. Step 1: sampling of the analytes onto the tube. C. Step 2: analytes are adsorbed onto the sorbent tube. D. Step 3: Thermal desorption of sorbent beds release analytes.

Commonly used sorbents include Tenax TA & GR (TX-TA, TX-GR), Carbograph 5TD, and Carboxen (CAR). Due to the distinct properties of these materials, there is a wide variability in the range of volatiles that can be trapped. The selection of the type of sorbent in the tube is dependent on the target VOCs, for example for vVOCs Carboxen® sorbent (~C2–C4 strong sorbent) are used and for VOCs breath a medium to weak sorbent Tenax® (~C7–C15) are used. Tenax® gave also great results for all the pesticides especially for pesticides with low volatility and/or poor thermal stability.

c. Needle trap devices (NTDs)

The NTD (Figure 28) is a new method, which combines the abilities of SPME and TD tube. It was first introduced in 2001 as a simple, rapid, inexpensive, solvent-free and single-step method. NTDs employ a specially designed stainless steel needle packed with a suitable sorbent material used as the extraction medium. Extraction is performed by passing the air thought the sample and drawing the sample inside the needle

through the sorbent bed. During this process, the analytes are trapped on the sorbent material and then they undergo thermal or solvent desorption[131,132]. The needle trap extraction is simple preparation automated technique due to the compatibility with the GC injector of analytical instruments and is a solvent-free technique combining the advantages of miniaturized exhaustive active sampling and passive diffusive sampling. Another advantage of NTD is its reusability, even up to ~5000 times, without loss of extraction efficiency. Sampling of gas analytes may be performed by active sampling (AS) or passive sampling (PS) methods. AS involves the collect of the gas sample through the needle trap device using a pump or gas-tight syringe. PS is based on passive diffusion extended in time. For liquid sampling the following methodologies have been proposed: (i) static headspace sampling (HS), (ii) purge and trap sampling (P&T) (dynamic headspace), and (iii) dynamic extraction.

(i) Static sampling are proceed as follow, the NTD is directly connected to the sample vial to the headspace for analyte concentration.

(ii) P&T system is used to transfer analytes from an aqueous matrix to the headspace via passing the purging air through the sample solution by another needle (purging needle) connected to a syringe pump. The analytes from the headspace are subsequently trapped on the sorbent particles inside the extraction needle. Helium, nitrogen or air can be used as a purging gas.

(iii) Dynamic extraction is performed by direct pumping the aqueous sample solution into the extraction needle at a constant flow rate using a syringe pump. The NT is then inserted to GC column for thermal desorption.

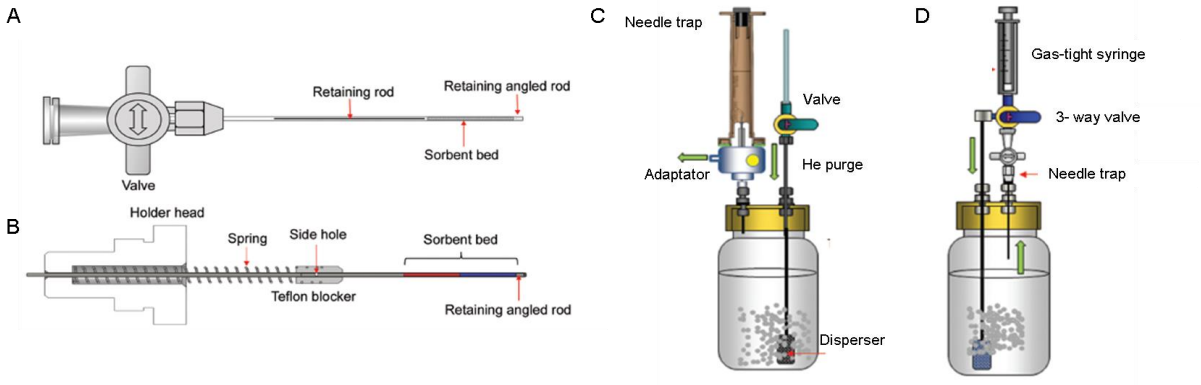

Figure 28: Needle trap device. A,B. Diagrams of needle trap (A) without and (B) with side hole. Needle o.d.=0.85mm, needle length 82mm. C.D. Diagrams of purge and trap systems used for sampling water with (A,B) gas purge and vacuum.

This first part was the presentation of the implantation of the volatilome as non-invasive source for diagnosis. The different steps of VOCs used as diagnosis tool were presented (Figure 29) (sampling, pre-concentration and VOC and data anaylisis) as the different possibilities of sampling, and coupling with analytical systems. In order to highlight the usefulness of developing a non-invasive method in real time which allow analysis of gas, liquid and solid.

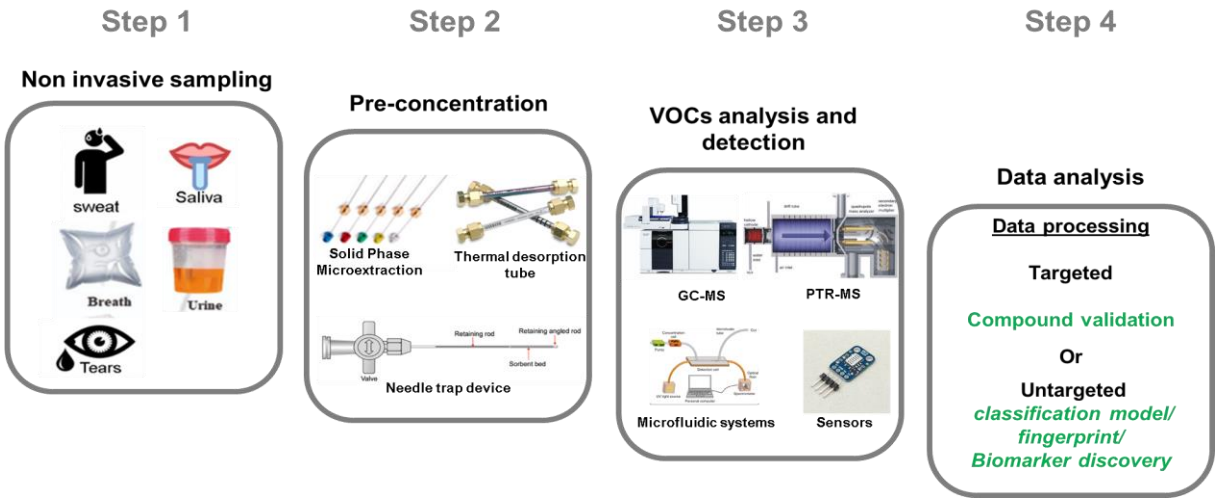

Figure 29: Steps of VOC analysis for biomarker discovery or compound validation. Step1: non invasive sampling, Step2:pre-concentration, Step3: VOCs analysis, Step4: Data analysis.

For this purpose an LTP-MS system will be developed to allow the real time analysis of VOCs. In this context VOCs will be concentrated on disc adsorbent membrane allowing the concentration of all types of biofluids (gas, liquid or solid) and the application of the membrane directly to the skin to get closer to the pathology BC.

In this context an LTP-MS system will be design for analysis of VOCs adsorbed onto an adsorbent membrane.

Part two: Development of LTP-MS system.

This part is dedicated to the development of an LTP-MS system for the analysis of VOCs adsorbed onto a disc membrane.

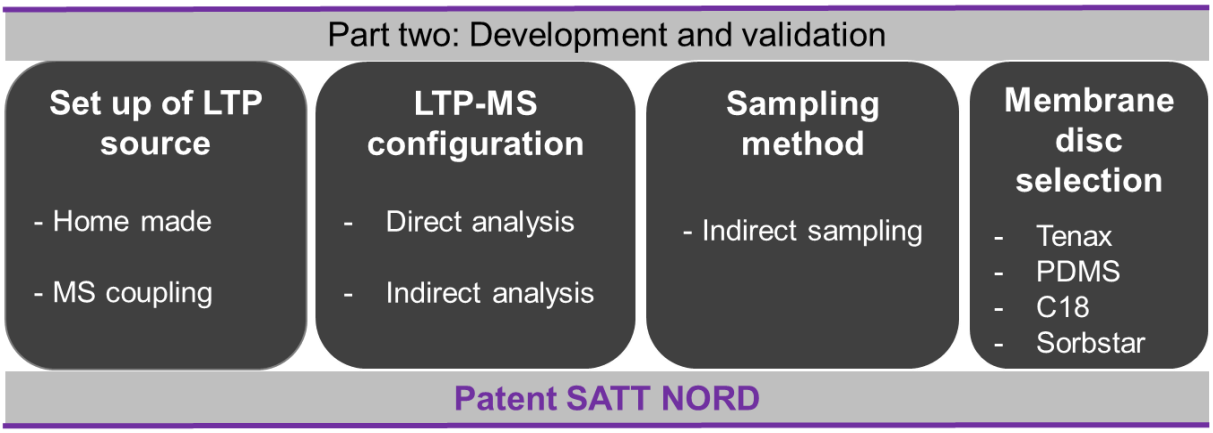

Figure 30: Main steps of dthe development and validation of the LTP-MS system. It compose by the set-up of the LTP source, LTP-MS configuration, sampling method and the selection of membrane disc.

First, ambient pressure plasma and their different configuration will be discussed to select and build the best suited plasma jet for VOCs analysis. The second chapter consists in the presentation of the extensive development of analytical system towards an optimal design for analysis of VOCs adsorbed onto a disc membrane. The enhancement of desorption process was the main development axis. The third chapter is focuses on the sampling method developments. Numerous investigations were required as no standardization is established for concentration of VOCs onto a membrane for subsequent LTP-MS analysis. Chapter four relates to the different sorbents available for such analyses. Four membranes were tested to select the most adapted disc membrane. All these developments were tested by analysing VOCs standards including two VOCs standard involved in breast cancer cyclohexanol and the 2-nonanone and a mix EPA containing different classes of VOCs (Table 5).

The last chapter develops on how all achieved development (e.g. sampling method, analytical method) were combine to lead to patent deposit. The 3 in 1 miniaturized deposit VOC system responds to the demand for versatile, inexpensive, (quasi)real-time, non-invasive, high-throughput system.

Table 5: Recapitulative table of VOC standard

	Molecule name	Molecular formula	Monoisotopic mass	m/z detected	Boiling point at 760 mmgH (Bp, °C)	Vapor pressure at 25°C (Vp mmgH)	molecule class	polarity
BC standard	Cyclohexanol	C6H12O	100.2	101.1	160.8	0.657	alcochol	non polar
	2-nonanone	C9H18O	142.1	143.1	195.3	0.62	Methyl ketone	non polar
Molecule detected from EPA mix	Tetrahydrofuran	C4H8O	72.11	73.09	65	132	Cyclic ether	non-polar
	Diethyl ether	C4H10O	74.07	75.11	34.6	538	Dialkyl ether	non polar
	Acetonitril	C2H3N	41.05	83.07	81.6	88.8	Nitril	polar
	Methyl acrylate	C4H6O2	86.036	87.08	80.2	86.6	Methyl ester	polar
	Methyl methacrylate	C5H8O2	100.05	101.2	100.5	38.5	Methyl ester	polar
	Ethyl methacrylate	C6H10O2	114.068	115.2	117	20.59	Ethyl ester	polar

Chapter I: Atmospheric Pressure Plasmas °

The term plasma was first used by Irving Langmuir in 1928 and describes quasi-neutral ionized or partially ionized gas in electric discharge. The plasma consists of a variety of particles, neutral atoms and molecules, charged particles (electrons and ions), metastable particles (excited atoms and molecules, radicals), and photons. By the end of the nineteen-eighties, huge efforts were made to transfer low-pressure plasma processes to atmospheric pressure conditions and thus overcome the expensive vacuum facilities. This was achieved through the use of pointed electrodes similar to corona discharges, with the use of dielectric materials to cover at least one electrode. Depending on the temperature of particles, plasma can be classified into two categories: equilibrium or thermal plasma and non-equilibrium or non-thermal plasma. The thermal plasma or local thermal equilibrium (LTE), is characterized by an almost completely ionized gas and high temperature of at least 14,000 °C. Furthermore, the electron temperature is equal to the temperature of heavy particles.

The non-LTE plasma or cold plasma is a partially ionized gas with temperature generally close to room temperature (maximum 40°C) and has a heavy particle temperature in the range of 27–727 °C. Also, the kinetic energy of electrons is larger than the gas temperature (Te >> Tg).

Atmospheric pressure non-equilibrium plasma jet (APNPj).

Various types of APNPj with different configurations have been reported (Figure 31), where most of the jets are working usually with noble gas. non-thermal plasma jets (NTP) operating with noble gases can be classified into three categories: dielectric-free electrode (DFE) jets, dielectric barrier discharge (DBD) jets, DBD-like jets.

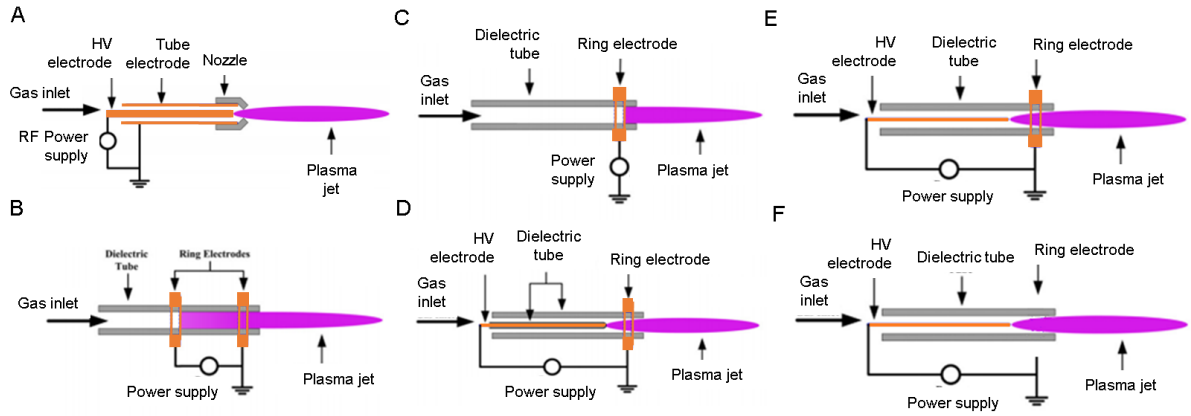

Figure 31: Schematic representation of atmospheric non equilibrium plasma jet: A. Dielectric free electrode jet. Schematic of a DBD plasma jet: D. DBD jet with two wrapped electrode. D. DBD with one inner electrode and a ring electrode and two dielectric tube. Schematic representation of DBD like plasma jet. E. DBD like with two electrode s (ring and inner) with one dielectric tube. F. DBD like plasma with one electrode and dielectric tube.

I. Dielectric free electrode

DFE (Figure 31, A) consists of an inner electrode, which is coupled to the power source, and a grounded outer electrode. A mixture of He with reactive gases is fed into the annular space between the two electrodes. To keep the jet from overheating, cooling water is supplemented. Nonetheless, the gas temperature of the plasma jet varies from 50 to 300 °C, depending on the RF power. The temperature of the plasma is then too high for biomedical applications. Furthermore, in DFE jet are, arcing is unavoidable when the stable operation conditions are not met.

II. Dielectric barrier discharge (DBD)

DBD (Figure 31, B, C, D) feature is defined by the presence of dielectric material between the electrodes, operate under frequency between 50 to 500 kHz and voltage amplitude in a 10 kV order. DBD jets display many different configurations such as planar and cylindrical electrode geometries and the presence of a single (SE) or double electrode (DE).

For cylinder electrode geometry, the first reported consists of a dielectric tube with two metal ring electrodes on the outer side of the tube (Figure 31, B). The gas temperature of the plasma is close to room temperature and the gas flow velocity is less than 20 m s−1. Even if the plasma looks homogenous, the plasma jet is a ‘bullet’-like with a propagation speed of more than 10 km s^{-1}. The applied electric field plays an important role in the propagation of the plasma bullet.

The HV electrode could also be replaced by a centred inner electrode covered by a dielectric tube with one end closed. This configuration enhances the electric field along the plasma. Finally, the ring electrode can be eliminated, which decreases and weakens the discharge inside the dielectric tube.

III. Dielectric barrier discharge like.

DBD-like (Figure 31, E, F) is based on the following facts. In case of one electrode configuration the inner electrode is favour and in case of double electrode, the inner electrode is not cover by a dielectric barrier. When the plasma plume is not in contact with an object, the discharge resemble standard a DBD. However, when the plasma plume contacts electrically conducting object (a non-dielectric material), especially a ground conductor, the discharge is running between the HV electrode and the object to be treated (ground conductor).

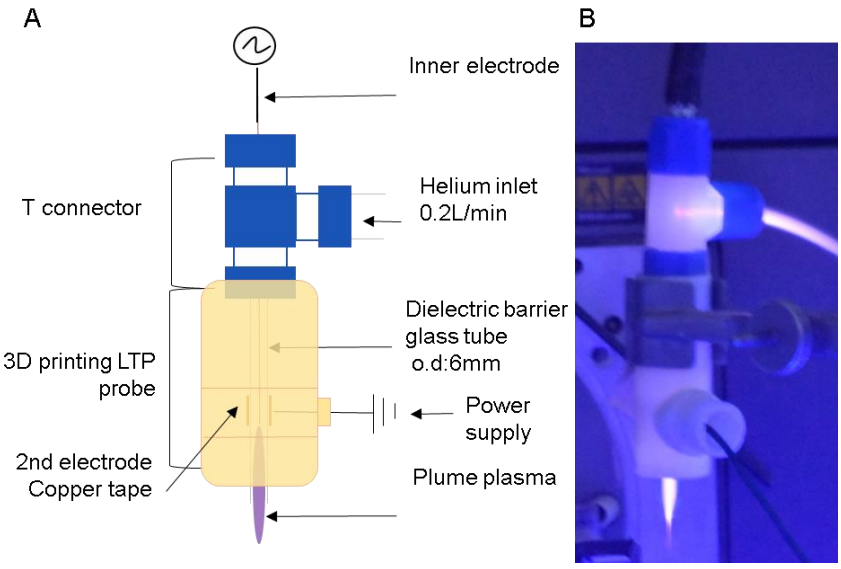

Figure 32: LTP probe. A schematic representation of the LTP probe. B. LTP probe in operation

LTP probe selection

DBD like jet was selected for LTP probe design due to the ease set up of plasma jet. DE was investigated since stronger discharge inside the discharge tube is formed and helps the generation of more reactive species compared to SE. In addition, this type of probe is currently used for LTP analysis.

LTP probe was designed based on the work of *Harper et al*[108]. The LTP probe setup (Figure 32) consist in a glass tube (6 mm o.d, 3.77 mm i.d, l: 7 cm length) with an internal electrode (stainless steel; diameter 2.03 mm) axially centred. The wall of the glass tube serves as the dielectric barrier. However, to enhance the mechanical resistance and insulation and to diminish the risk of arcing or electric discharges, the glass section of the probe is fully covered by 3D printed polymer (ABS acrylonitrile butadiene styrene).The 3D part was designed by LABIlab[133] and printed with a Zortrax M200 printer at the FABLAB makerspace. The grounded counter electrode (copper tape; width 6 mm) which serves as a dielectric barrier is placed 4 mm away from the inner electrode and 2 cm from the exit of glass on the 3D printed part and wrapped around the 3D part. The system is fitted into a 4/16'' Swagelok™ T connection. Compressed Helium (high purity grade 4.6, Air liquid) is fed through the T connection at a flow rate between 50 and 400 ml/min. Flow rates are controlled using a flow meter equipped with a carboloy floater (Dakota instruments, NY, USA). For safety purpose, the inner electrode is powered with the alternating current (AC) using a High Voltage generator (HVG) (PVM500/DIDRIVE1; amazing1.com) which enables the HV output to maintain tension between 1 and 40 kV and the frequency between 20Hz to 60 kHz.

.

Chapter II: LTP-MS analytical system:

Ambient sources such as the LTP can be coupled with any mass spectrometer equipped with an atmospheric pressure ionization (API) source. It has been coupled to various type of mass spectrometers such as linear ion trap[105] (LIT), a 3D ion trap[134], an orbitrap[135] ,a Fourier transform ion cyclotron resonance (FT-ICR)[136] and an ion mobility spectrometry (IMS)[137,138]. In order to assay the versatility of the LTP probe, the source was coupled with the following mass spectrometers available in the laboratory including a 3D Ion trap (HCT Ultra, Bruker), a Synapt G2s (Waters) and a Q-TOF premier (Micromass) (Figure 33).

LTP probe coupling

To measure the efficiency of the LTP-MS coupling VOCs standards were directly deposit or spotted onto an adsorbent membrane. Here, the cyclohexanol ($C_6H_{12}O$, Mw=100.16 g/mol) was used as standard and loaded onto filter paper (FP, thickness: 0.3 mm) type membrane which was then put on a glass slide. The membrane was positioned in front of the MS inlet entrance at a distance of 1 cm. The LTP was oriented toward the membrane to induce the desorption and the ionization of the adsorbed VOCs which are then sucked in the MS inlet. Due to the differences from one to another analyser including the ion entrance and the length of ion trajectory, the recorded spectra can differ between these three mass spectrometers.

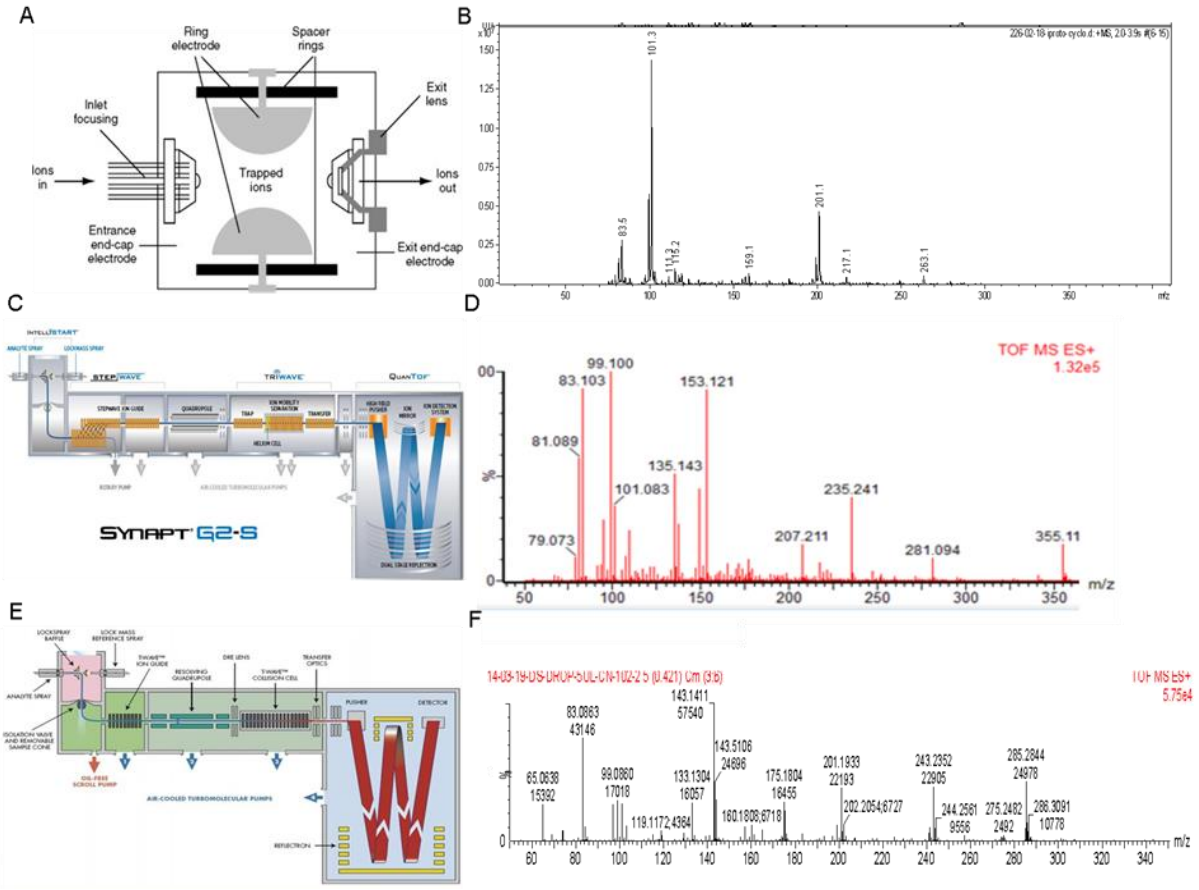

Figure 33: LTP coupled with different MS. A. Representation of IT configuration. B. MS Spectrum of cyclohexanol acquired by LTP-IT. C. Representation of Synapt G2-S. D. MS spectrum of cyclohexanol acquired by LTP-G2-S. E. Representation of QTOF-premier. F. Spectrum of cyclohexanol by LTP-QTOF analysis.

3D Ion trap (IT) (Figure 33, A and B): Considering the instrumental configuration, this instrument has a shorter length trajectory and has the capability of ion accumulation within the IT. In the MS spectrum the molecular ion $[M+H]^+$ (m/z 101.1) and the dimer $[2M+H]^+$ (m/z 201.1) and a fragment ion (m/z 83.5) are observed. This fragment (C_6H_{11}) corresponds to the water loss $[M+H-H_2O]^+(C_6H_{11})$. The pseudo molecular ion $[M-H]^+$ is also observed at m/z 99.The base peak corresponds to the monomer followed by the dimer. The plasma interaction with the ambient air lead to the detection of background peaks, such as the m/z 263.1 and the m/z 217.1. This peak are commonly observed during LTP analysis and were observed in the MS spectra of the LTP system alone without any sample.

Synapt G2-S (Figure 33, C and D): Given the instrumental configuration, the Synapt display the longest ion trajectory and enables Ion mobility for further gas phase

separation. The MS spectrum allows the detection of the $[M+H]^+$ at m/z 101 and $[M-H]^+$ at m/z 99. Fragment ions are also observed. Indeed, the base peaks ion corresponds to pseudo molecular ion form $[M-H]^+$ followed by the water loss forms $[M+H-H_2O]^+$ (m/z 83) and $[M-H-H_2O]^+$ (m/z 81). This overwhelming presence of fragment ions and background ions (m/z 135, 153, 207, 235) could hampered the interpretation of the LTP-MS spectra. In IMS mode, the detection of ion of interest is impossible, due to the loss of sensitivity. Nonetheless, the rate of ion entrance could be another factor of this lack of detection. To circumvent this drawback, additional ambient pressure interface could be implanted such as discontinuous ambient pressure interface (DAPI) to enhance the rate of ion entrance by aspiration to balance this drawback.

QTOF-premier (Figure 33 E and F): The geometry of the Q-TOF premier and the Synapt are close, similar. According to the MS spectrum, the $[M+H]^+$ (m/z 101), the $[M-H]^+$(m/z 99), dimer $[2M+H]^+$(m/z 201) and fragment ions measured at m/z 83 and m/z 65 are observed with a good signal noise ratio (S/N).

Due to the high intensity of the detected ions corresponding to cyclohexanol and the very low abundance of fragments ions observed by means of the 3D IT, this mass spectrometer has been selected to be coupled to our home-made LTP probe for the evaluation of the ionization efficiency. Furthermore this mass spectrometer is robust and allows ion accumulation.

Evaluation of the LTP probe.

Here, standards used were the limonene ($C_{10}H_{16}$, Mw=136.24 g/mol) and the 2-nonanone ($C_9H_{18}O$, Mw=142.14 g/mol). 5µl of standard solutions were directly deposited on the FP and analysed by LTP-IT (Figure 34).

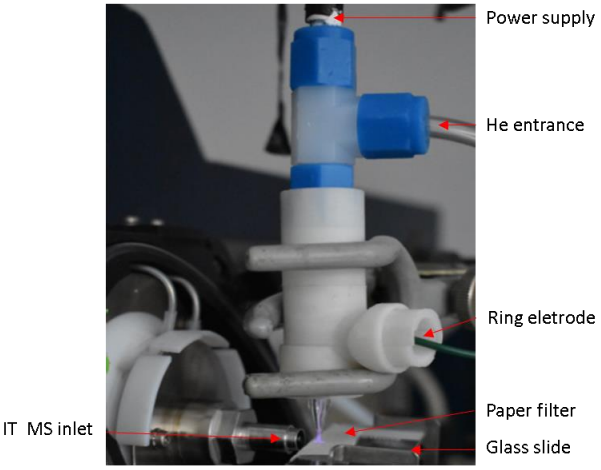

Figure 34: Picture of the LTP-MS coupling for the direct analysis of standard adsorbed on FP membrane.

Limonene analysis

The limonene ($C_{10}H_{16}$) is an aliphatic liquid hydrocarbon classified as a cyclic monoterpene. The detection of hydrocarbons by API sources including ESI and APCI remains challenging considering that the ionization is mainly governed by a protonation or deprotonation processes. This suggests that the molecule of interest must contain a basic or acid group. Several groups have demonstrated that some non-polar compounds such as hydrocarbons were not ionized by ESI or ACPI although they were perfectly detected by atmospheric pressure photoionization (APPI) with a predominant M^+ form[139]. Recently, saturated, unsaturated and cyclic hydrocarbons including polyaromatic hydrocarbons (PAHs) were detected by APCI. It has been demonstrated the use of small hydrocarbons (pentane, hexane, cyclohexane, heptane and isooctane) as APCI reagent leads to the detection of different types of ions such as $[M+H]^{\bullet}$, M^+, $[M-H]^{\bullet}$ and $[M-2H]^{\bullet}$ with almost no fragmentation.

Furthermore, the limonene is a fragrance of alkenes which rapidly undergo ozonolysis to produce a host of oxygenated products. Ozonolysis is the process by which ozone (O_3) reacts with alkenes to break the double bond and form two carbonyl groups. If the double bond of the alkene is substituted with hydrogen or carbon atoms, the carbonyl groups that are formed are either aldehydes or ketones. Limonene reacts with ozone (O_3) in the gas phase with a constant rate of 2.1×1020 cm^3 $molecule^{-1}$ s^{-1}. The initial phase of this product formation is dominated by the formation of a primary ozonide and

carbonyl compound. The intermediate can either decompose or react further to form the first generation of products including acids, carbonyls, secondary ozonides, and alkyloxy and hydroxyl radicals, as shown in Figure 35, B. O_3 plasma product of oxygen is formed in the atmosphere according the following reaction.

$$O_2 + e^- \rightarrow 2\langle O \rangle + e^-$$

$$\langle O \rangle + O_2 \rightarrow O_3$$

Noorgaard et al[140] have demonstrated that O_3 can react with the limonene leading to the observation of oxidation products.

The positive mass spectrum corresponding to the limonene (Figure 35) in the mass range of m/z 50 to 200 is characterized by the presence of peaks which could correspond to the molecular ion, ozonolysis product and many putative fragment ions. The ions measured at m/z 135 and m/z 137 could correspond respectively to the $[M-H]^+$ and the $[M+H]^+$ form. The ionization processes involved in the LTP include photoionization, electron capture, electron ionization, charge transfer, ions and metastable excited neutrals, associative ionization and charge transfer reaction. In this context, the detection of the [M-H] , $M^{\bullet}$ and [M+H] forms of unsaturated hydrocarbons is therefore highly expected.

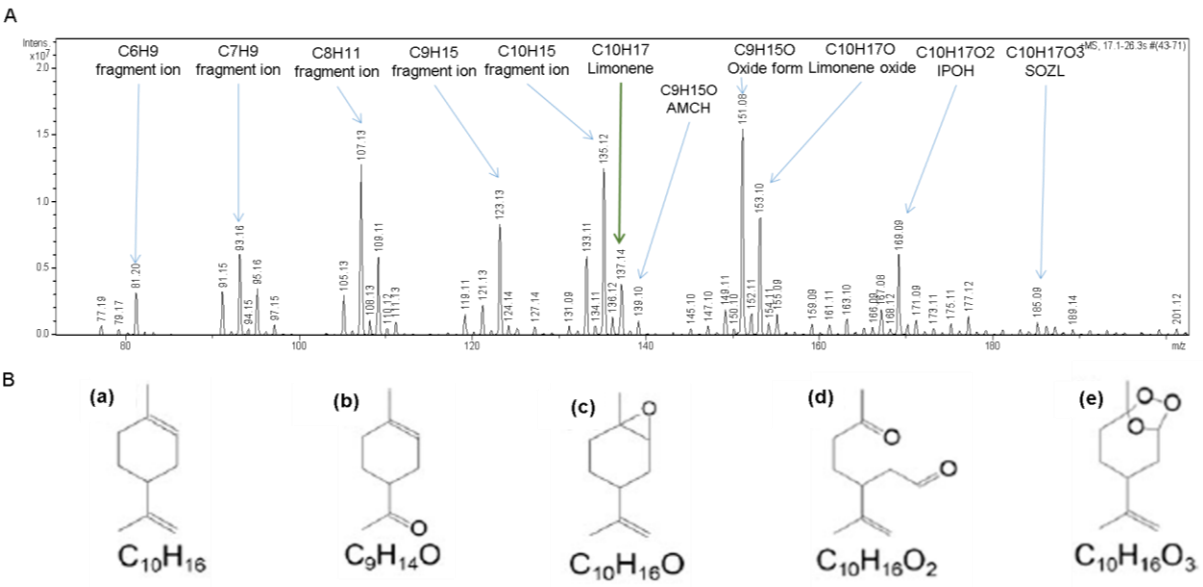

Figure 35: Limonene LTP-MS analysis. A. Positiv LTP-MS spectrum B. Structure of d- limonene (a) and selected ozone-iniated reaction product: (b) 4-acetyl-1-methylcyclohexene (AMCH), (c) limonene oxide, (d) 3-iosopropenyl-6-oxo-heptanal(IPOH), (e) secondary ozonide of limonene (SOZL).

The ions measured at m/z 139, m/z 151, m/z 153, m/z 169, and m/z 185 are assigned as primary products from the ozone-initiated limonene reactions which could correspond respectively to the 4-acetyl-1- methylcylohexene (4-AMCH, $C_9H_{15}O$), the oxide form $[M+O-H]^+$ ($C_{10}H_{15}O$), the limonene oxide [M+O+H]+ ($C_{10}H_{17}O$), the 3-isopropenyl-6-oxo-heptanal (IPOH, $C_{10}H_{17}O_2$) and the secondary ozonide of limonene (SOZL, $C_{10}H_{17}O_3$) as shown in Figure 35, B. The mass range below t m/z 160 is dominated by fragment ions such as the m/z 81, m/z 93, m/z 107 and m/z 123. This can be explained by the non-thermal LTP from which the electron temperature (T_{e^-}) is much higher than ion temperature (Tion) and gas temperature (TGas). It has been measured that T_{e^-} ≈ 104 °K and Tion ≈ Tgas ≈ 300K. In this partial thermodynamic equilibrium, electrons are in the glow beam with almost no electric field and they lose their kinetic energy in elastic and non-elastic collisions and by gas atoms ionization. Therefore, the kinetic energy is transferred from the electrons to the large particles at low pressure without affecting the temperature of the large particle which is very close to the room temperature and leading to the formation of cold plasma. In this non-equilibrium plasma, electrons are the particles bearing the mean kinetic energy of a few eV can induce the dissociation of molecules as shown in Figure 35, A with the limonene. However, the fragmentation rate is low in comparison to EI ionization (70eV) and therefore the use of EI-MS databases cannot be used to identify compounds and considering that LTP fragmentation is more comparable to CID (collision induced dissociation).

2-nonanone analysis:

2- nonanone is a metyl ketone deriving from nonane metabolism by the enzymatic activity of cytochrome P450. It's well established that an increase of 2-nonanone could be associated with the high activity of the different isoforms of this enzyme observed in breast-derived cancer cells.

The obtained LTP-MS spectrum of the 2-nonanone was compared with MS spectra obtained through electron ionization (EI) at 70eV and electrospray ionization (ESI). As shown in the Figure 36**Erreur ! Source du renvoi introuvable.**, A and B, the MS spectrum obtained from the 2-nonanone by EI at 70eV is mainly governed by the presence of fragment ions in contrast to the ESI spectrum from which the molecular ion (m/z 143) and the water loss form (m/z 125) $[M+H-H_2O]^+$ were observed. Recently, the 2-nonanone[141] has been analysed by an APCI-IMS-MS instrument. The molecule

has been ionized by a corona discharge (CD) in the presence or absence of ammonia dopant.

The obtained IMS-MS spectrum clearly shows the presence of the $[M+H]^+$ and the $[2M+H]^+$ without ammonia as observed with the LTP probe (Figure 36 C and D).

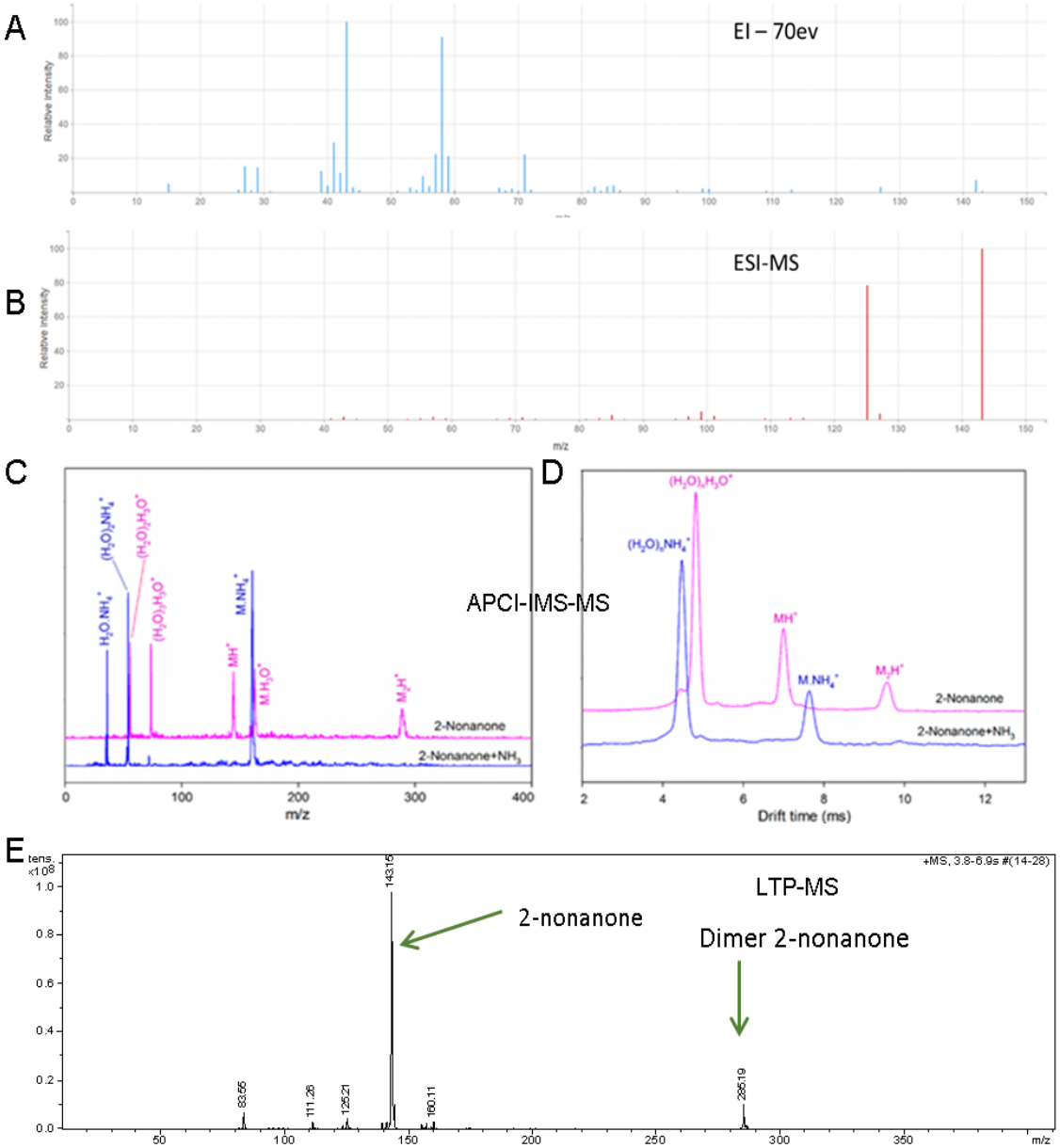

Figure 36: Positive MS spectra of 2-nonanone. A. Spectrum acquired by electron ionization (EI) at 70 eV. B. Spectrum acquired by electrospray ionization (ESI). C, D. Spectrum acquired by APCI-IMS-MS. E. Spectrum acquired by LTP-MS

The LTP-MS spectra (Figure 36, E) corresponding to the 2- nonanone, the molecular ion $[M+H]^+$ and dimer ion $[2M+H]^+$ measured respectively at m/z 143 and m/z 285 are observed. Additionally, we can notice the presence of a fragment ion measured at m/z 83 and m/z 125 which could correspond to the water loss form $[M+H-H_2O]^+$. The

observation of the proton adduct products is more likely in the case of molecule presenting a heteroatom as the oxygen in the carbonyl group of the 2-nonanone. The proton affinity (PA) of the 2-nonanone has been measured at 829kJ.mol^{-1}.

The obtained results by the designed LTP probe are in line with the previous studies demonstrating that the ionization process occurring in LTP is very close to what it can be observed with the APCI source. Recently, it has been shown that LTP is also very close to the DART source in terms of generated ions. Nonetheless, fragment ions are more frequently detected with DART source rather than LTP due to plasma highest temperature. However, fragment ions are better observed in the case of LTP than with APCI due to the non-thermal equilibrium occurring in the LTP source.
It has been demonstrated that the designed LTP probe is able to ionize polar and less polar compounds including hydrocarbons. Therefore the homemade LTP probe is very well suitable to simultaneously detect different classes of VOCs in a single experiment. This is a noticeable advantage for the diagnosis implementation perspective where molecular signature of different physio-pathological states consist of VOCs from different classes. Indeed, polar or less-polar VOCs were already detected in the same pathology such as acetone and styrene as demonstrated by Silva et *al*[142]*.* The detection of different classes of VOCs in a single analysis is without doubt a great benefit to obtain VOCs signature based accurate diagnosis.

LTP-MS analytical system

It has been demonstrated that the probe design, the operating parameters and the MS interface greatly influence the ionization, the desorption, the fragmentation and the ion transfer[143],[22]. Albert and Engelhard have proposed a chemometric approach to optimize the LTP probe geometry and the position relative to the MS inlet[144] . This work served as a basis to optimize our LTP probe. The authors showed that the ionization yield is directly correlated to the reaction time between the plasma jet and the targeted molecules. Additionally, they demonstrated that the distance between the LTP probe and the MS inlet also play a role on the ionization yield, since a too long-distance lead to the neutralization and loss of ions. Moreover, the input voltage, the frequency and the gas flow are additional factors reported to influence ionization efficiency. In this

context, each and every of these parameters were taken into account and optimized in tested configurations.

A total of 5 different configurations (Figure 37, Figure 47) were developed for the analysis of VOCs spotted onto a disc membrane. The development was directed towards the enhancement of the desorption of VOCs from the adsorbent membrane. These configurations can be separate onto 2 groups:

- Direct analytical system (DS): (configuration 1 and 2).
- Indirect analytical system (IS): (configuration 3, 4 and 5).

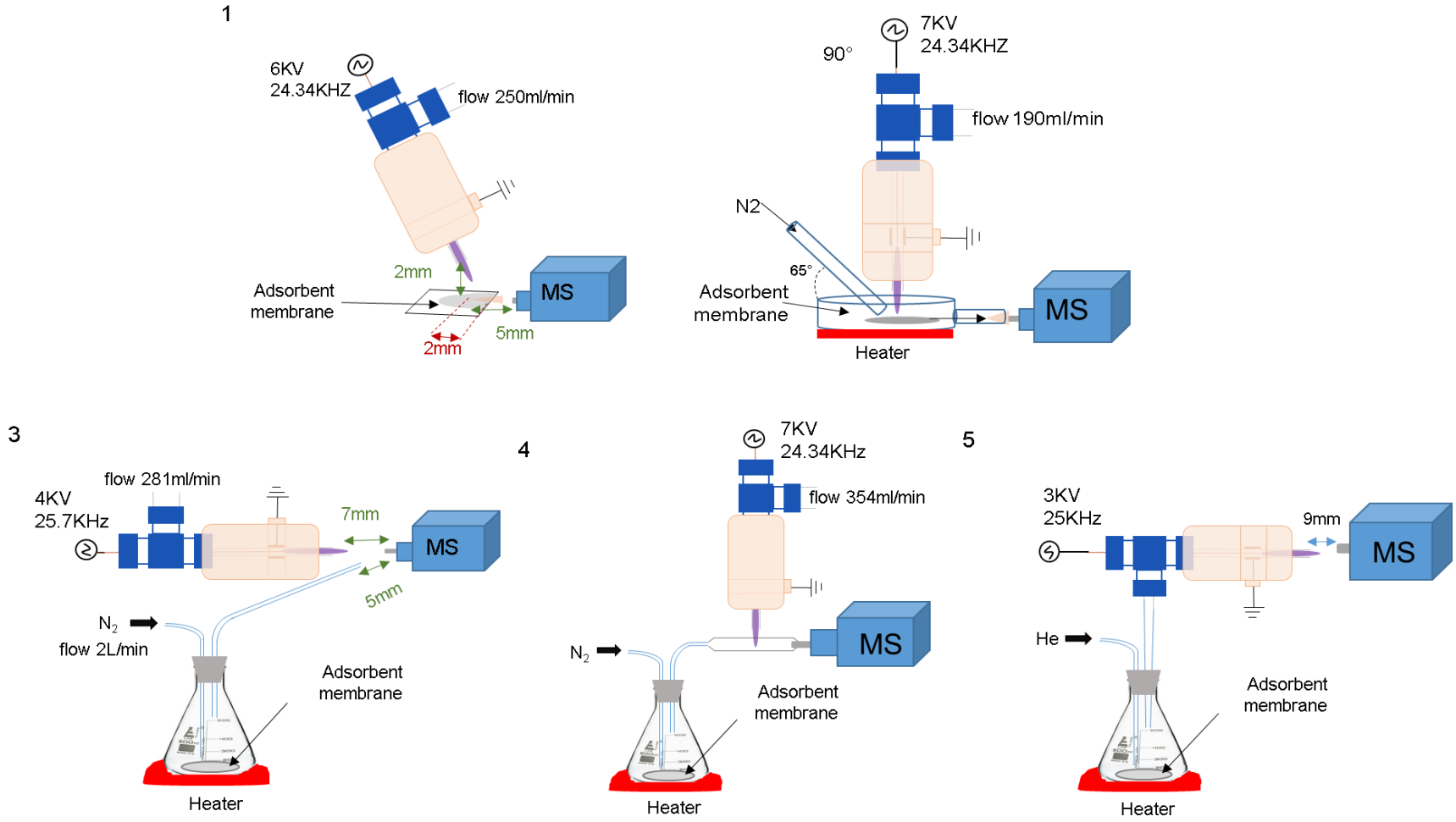

Figure 37: Developed LTP-MS analytical system set up. 1.B. Direct analytical system. C.D.E Headspace analytical system. F. Thermal desorption analytical system.

Different geometrical parameters of all LTP-MS configurations were investigated including the distance between the probe and the sample (PS), the distance between the edge of the slide (PE), the probe angle (PA), the distance between the probe to inlet of mass spectrometer (PM), the distance between the exit tube and the MS (TM), tube angle (TA). The input power (voltage, frequency) and gas flow (He and N) were also investigated to determine the optimal parameters for the VOCs detection. The same chemiometric method was used throughout all tested configurations with He as discharge gas with a deposit of 5µl of mix standard cyclohexanol: 2-nonanone (15:1) at different concentrations on Tenax TA (TX) membrane disc as adsorbent (d: 6mm, e:1.5mm). TX membrane was selected for its widely validated efficiency for VOCs adsorption. Additionally, each parameter was tested and measured in triplicate and each measurement was initiated by collecting a background MS spectrum corresponding to the ambient air and a blank TX membrane. The 3D Ion trap was used for all development due to its robustness and selectivity. The capillary voltage of the IT inlet was 1.5 kV and the transfer capillary heated at 150°C. The ion injection of the trap was set to 200,000 charges with a maximum ion-trap injection time of 200ms, using 5 µscans per spectrum. Full scan acquisition was performed over m/z range 50-1000 in positive ion mode. No dry gas was used to avoid the disruption of incoming ion projected by the plasma beam. External calibration was performed using ESI-T tuning mix (Agilent Technologies, USA).

I. Direct analytical system (DS)

a. Configuration 1

Configuration 1 is dedicated to the direct analysis of surfaces including VOCs adsorbed on disc membrane. For this DS, the LTP probe is oriented toward the membrane disc disposed on a glass slide front of the MS inlet. Different geometrical parameters of the LTP-MS configuration were investigated (Figure 38, A, B, C, D) optimized and are presented in the following table:

Parameters	Symbol	Range
Electronic parameters		
Voltage	HV	3- 30 kV
Frequency	Hz	20.3-35.3 kHz

Gas supply		
Gas flow	$Q_H e$	125 to 924 mL/min
Probe geometry		
Distance between the probe and the sample	PS	2, 5, 7 mm
Distance between the probe and the edge of the slide	PE	2, 5, 7 mm
Distance between the probe and the MS inlet	PM	5, 7, 9 mm
Probe angle	PA	45°, 60°, 90°

Optimization results:

In the positive mode, the PS distance (Figure 38, C) leads to a decrease in the signal intensity when increasing PS from 2 mm to 7 mm. PE (Figure, D) was found to differ significantly between 2 mm and 4 mm but no significant difference was found between PE 0 mm and 2 mm. The PA (Figure 38, E) lead to decrease in the signal by a factor 2 from 90° down to 45° although very good S/N ratio was still achieved at 45°. Angle under 45° was not tested. PM (Figure 38, F) distance was found as a key parameter with signal intensity decreasing from 5 to 9 mm with an important drop above 7 mm. HE flows (Figure 38, G) have no significant effect on S/N ratio between 125ml/min to 281/ml/min but the monomer intensity is much higher between 247 ml/min and 281ml/min. To avoid plasma arcing the 247ml/min flow was selected. Considering the input voltage/frequency, the highest S/N ratio (Figure 38, H) was at 6kV and 24.34 kHz. Very similar results were obtained for the dimer with the highest intensity and S/N ratio found for 7 kV and 20 kHz.

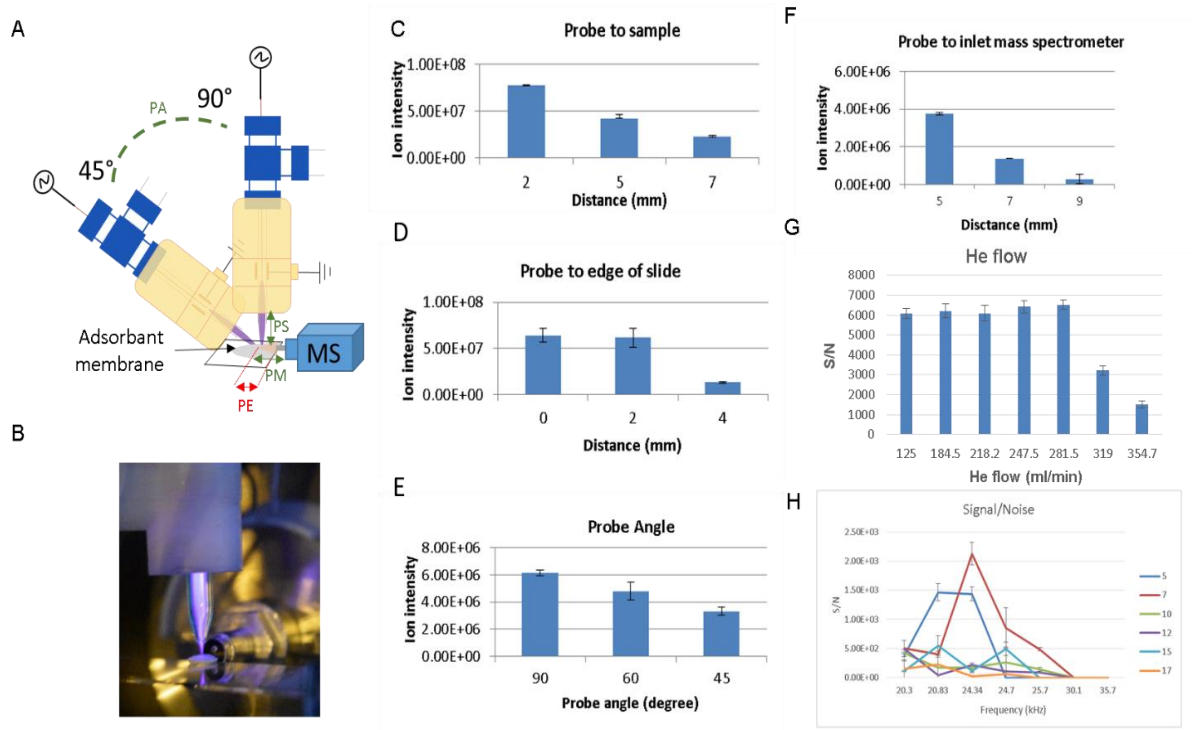

Figure 38: Optimization of LTP-MS configuration 1: the following parameter were optimized for the HE driven LTP probe based molecular ion m/z143.2 of 2-nonanone. A. schematic representation of Setup 1. B. Photo of setup 1. C. Distance between the probe and the sample. D. Distance between the probe and the edge of slide. E. probe angle. F. distance between the probe and the MS inlet, G. He flow H. Signal to noise ratio depending the relation frequency/voltage. All the experience was done in triplicate 3 times. PM 7mm, PS 2 mm, PE 2mm with 23KV,20 KHz .The intensity of molecular ion was extract from chronograms for each experiment

Finally, the geometrical parameters providing the highest analytical performances was observed for the following parameter: PS= 2mm, PM= 5mm, PE: 2mm, PA= 60°, PS: 2mm and He gas flow 250mL/min with a power input at 6kV 24.34kHz.

Estimated limit of detection (LOD):

To determine the LOD, standard was spotted on TX membrane disc as previously described. The membrane was analysed with the optimal DS-LTP-MS parameter. Each S/N ratio of monomer and dimer of standard were extracted for LOD determination. The configuration 1 enables the detection until 474.5 ng of cyclohexanol and 277.3 ng of 2-nanonone (Figure 39).

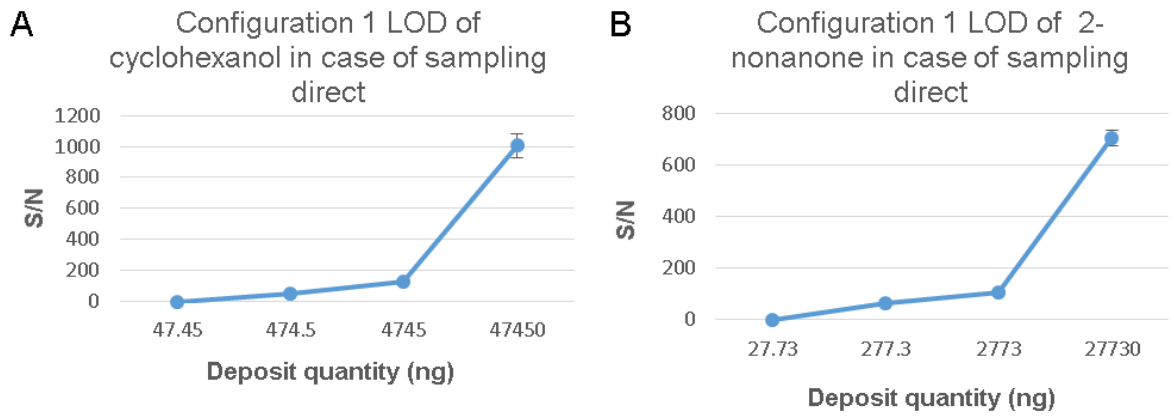

Figure 39: LOD of configuration 1 by direct deposit on Tenax membrane. A. LOD of cyclohexanol. B. LOD of 2-nanonone.

In order to improve the LOD, attempt of heating system implementation was proceed. Indeed, it's establish that the improvement of desorption process through heating favour the volatility of compounds and thereby the LOD of the configuration. First attempt was done by the electrical connection of the glass slide to a generator in order to induce a current and consequently temperature. The second was based on resistive wire placed under the slide in order to enhance the temperature. Due to a lack of robustness and too low temperature, the heating systems have been abandoned. However, other heating systems are available such as halogen heating or the Peltier system could be used to promote desorption of the analytes.

b. Configuration 2:

Configuration 2 *(Figure 40, A.B.C)* was also designed for DS of VOCs onto a membrane disc. Even if this analytical system allows the simultaneous VOCs desorption and ionization from a membrane, additional heat and sweep gas were added to the system. Indeed, heat favour molecule desorption from the membrane and the sweep gas allows the continuous arrival of desorbed VOCs to the MS inlet. In contrast to the first configuration, the second is closed (design glass enclosed system) and designed to desorbed and ionized VOCs which are transported to the MS inlet by means of sweep gas. In the center, the LTP probe is orthogonally positioned in front of the membrane to induce the simultaneous ionization and desorption of the VOCs. Finally, a heating system is added to enhance the thermal desorption (TD) of the molecules from the membrane.

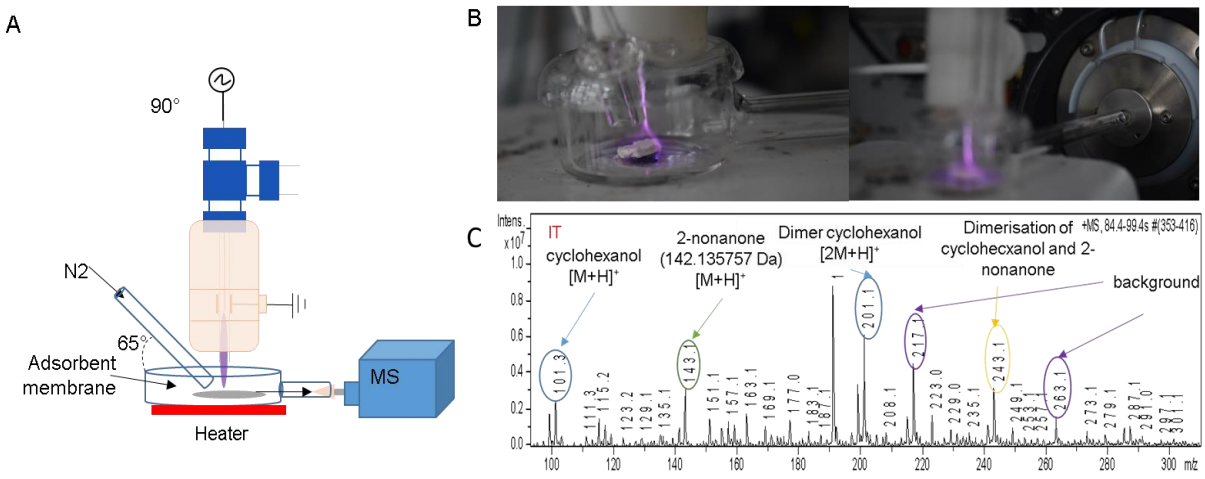

Figure 40: Configuration 2. A. Schematic representation of configuration 2. B. Photo of setup 2 in operation. C. Spectrum of mix standard acquired by setup 2 by sampling direct

Even if this system combines TD by additional heating system and simultaneous desorption and ionization by the LTP (Figure 40, C), this configuration presents some drawbacks. The sweep gas flow disturbs the plasma beam and displaces the membrane leading to non-reproducible analysis. The addition of strap to fix the membrane to the glass system is not compatible with heat due to the melting of glue. Furthermore, the configuration increases the concentration of He within the enclosed system and then to the MS, disturbing the He balance within the MS leading to the complete shutdown. Despite these important hurdles, few spectra were acquired as shown in Figure 40, C.

For cyclohexanol, molecular m/z 101.3 $[M+H]^+$ and dimer *m/z* 201.3 $[2M+H]^+$ ion were detected whereas for 2-nonanone only molecular ion *m/z* 143.1 $[M+H]^+$ was detected. Heterodimer of cyclohexanol and 2-nonanone was also detected at *m/z* 243.

In conclusion, the configuration 2 was rapidly abandoned due to several drawbacks mentioned here above, no further optimisation were tested and finally this analytical system configuration was finally discarded.

II. Indirect analytical system (IS)

a. Configuration 3

This configuration is the first developed for an indirect VOCs analysis onto a disc membrane based on the formation of VOCs into the headspace (HS) (Figure 41, A, B). The membrane is placed in glass design Erlenmeyer (l: 50mm, h: 4mm). An additional

heat (0 -250°C) has been implemented to induce the thermo-desorption of volatile species from the membrane, which are then accumulated in the headspace region. The custom erlenmeyer is sealed with a two holes cap; one for the entrance of gas buffer (nitrogen) supplied by the mass spectrometer; and a second to allow the transportation of the desorbed VOCs through a glass tube connected to the MS inlet. The VOCs are then ionized by the LTP probe which is axially positioned in front of the mass spectrometer. Parameter of the LTP probe are listed in the following table and were optimized to obtain the best signal intensity:

Parameters	**Symbol**	**Range**
Electronic parameters		
Voltage	HV	3-30 kV
Frequency	Hz	20-30 kHz
Gas supply		
He	Q_{He}	125 to 924 ml/min
N_2	Q_{N2}	0.5 to 4 L/min
System geometry		
Distance between the probe and the MS inlet	PM	7, 9 mm
Distance between exit glass tube and the MS inlet	TM	5 mm
Probe angle to the MS inlet	PA	0°
Exit tube angle to MS inlet	TA	-60°
Temperature		
Temperature system	°C	25 to 200°C

Due to the glass made prototype and the custom manufacturing prototypes, several geometrical parameters have not been investigated such as the PA: 0°, the angle of the exit tube glass (TA) is -65° and the distance between the glass tube and the MS (TM):5mm. Distance PM was not investigated under 7mm either to avoid arcing. All parameters investigated are presented in the following table:

Optimisation results:

Considering the HV and frequency effect on ion intensity (Figure 41, C, D), the best intensity was found at 25.7 kHz and 4.4 KV.The TM distance (exit glass tube to MS) was set at 5mm. The optimal He flow is 281 ml/min and for the nitrogen flow 2 L/min (Figure 41, E, F). Similar trends were observed for both standards. Considering the acquired spectrum, monomer (m/z 101.1 and 143.2), dimer (m/z 201.1 and 285.2) of both standards and heterodimer (m/z 243.1) are observed with good S/N ratio. Also, the fragment ion m/z 83 or 65 are not observed.

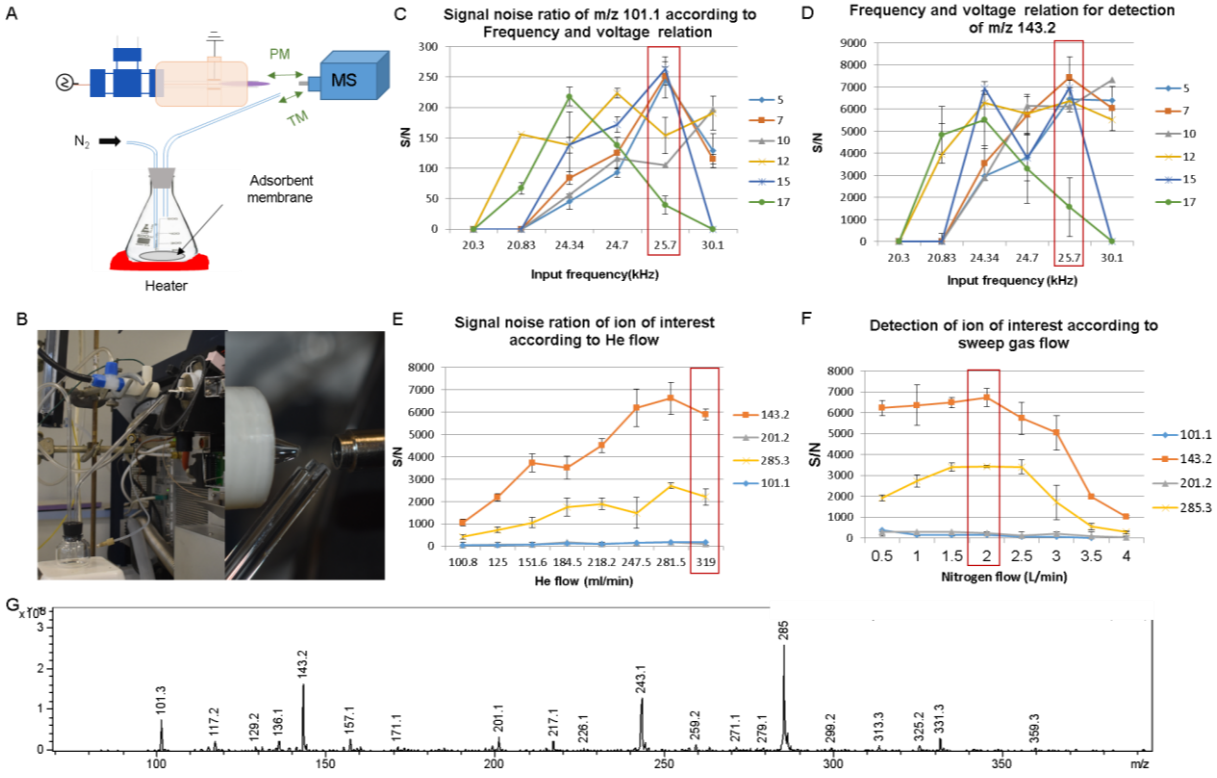

Figure 41: Optimization of LTP-MS configuration 3. A. schematic representation of configuration 3. B. Photo of setup 3. C. Detection of monomer cyclohexanol according the input power. D. Detection of monomer 2-nonanone according the input power E. Effect of. He flow on detection of mix standard. F. Effect of nitrogen flow on detection of mix standard.

After the optimization of the geometrical parameters, heat experiment (Figure 42, A) was tested in order to assess the efficiency of a heating system for the thermal desorption of VOCs from a disc membrane. Tested temperature were ambient temperature, 50, 100, 150 and 200°C. The enhancement of VOCs desorption was observed by the increasing of VOCs S/N ratio. Indeed for the same deposit quantity, the S/N ratio is multiplied by 1000 if the system is at 150°C compared to ambient temperature. The same effect was observed for both standards. Nonetheless, above 150°C due to the plastic composition of the two-hole cap, a compound is released and

observed at m/z 136. This contamination flattened the MS signal and made precluded to envision any experiment performed at this temperature (Figure 42, B).

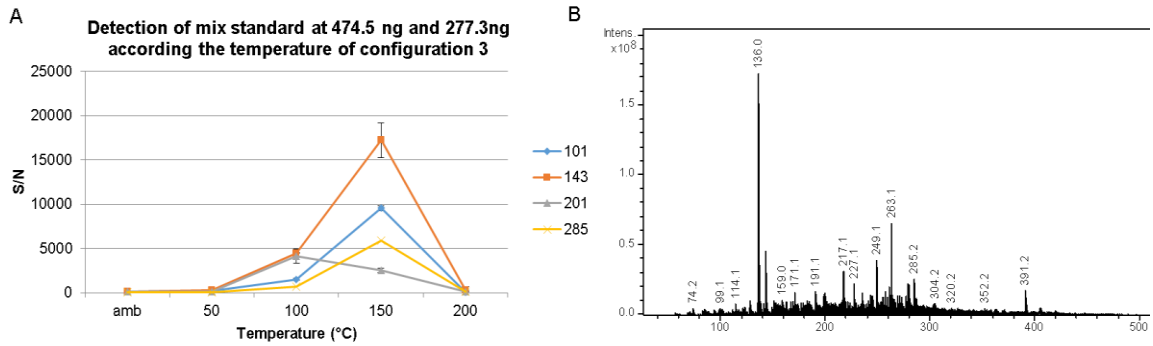

Figure 42: Detection of mix standard by configuration 3 according the temperature. A. Detection of mix standard at 474.5 ng and 277.3 ng of cyclohexnol and 2- nonanone according to the temperature of system. B. spectrum obtained at 200°C.

Finally, parameters which were providing the best analytical performances were observed for the following parameter: TM: 5mm, PM: 7.4mm, TA: 35°, PA: 0°C with a power input at 4.4kV and 25 kHz at 150°C.

Estimated limit of detection:

The LOD was investigated according the optimal parameter previously determined. The configuration was tested without heat and with heat at 150°C supplied by a hotplate. The temperature was monitored within the system with a probe. Without heating, the configuration 3 enables the detection until 474.5 ng of cyclohexanol and 277.3 ng of 2-nanonone (Figure 43, A, B). As previously explained, the increasing temperatures enhances the detection of analyte and leading to LOD is decrease as shown in the Figure 43, B and D with a detection at 47.45 ng of cyclohexanol and 27.73 ng of 2-nanonone.

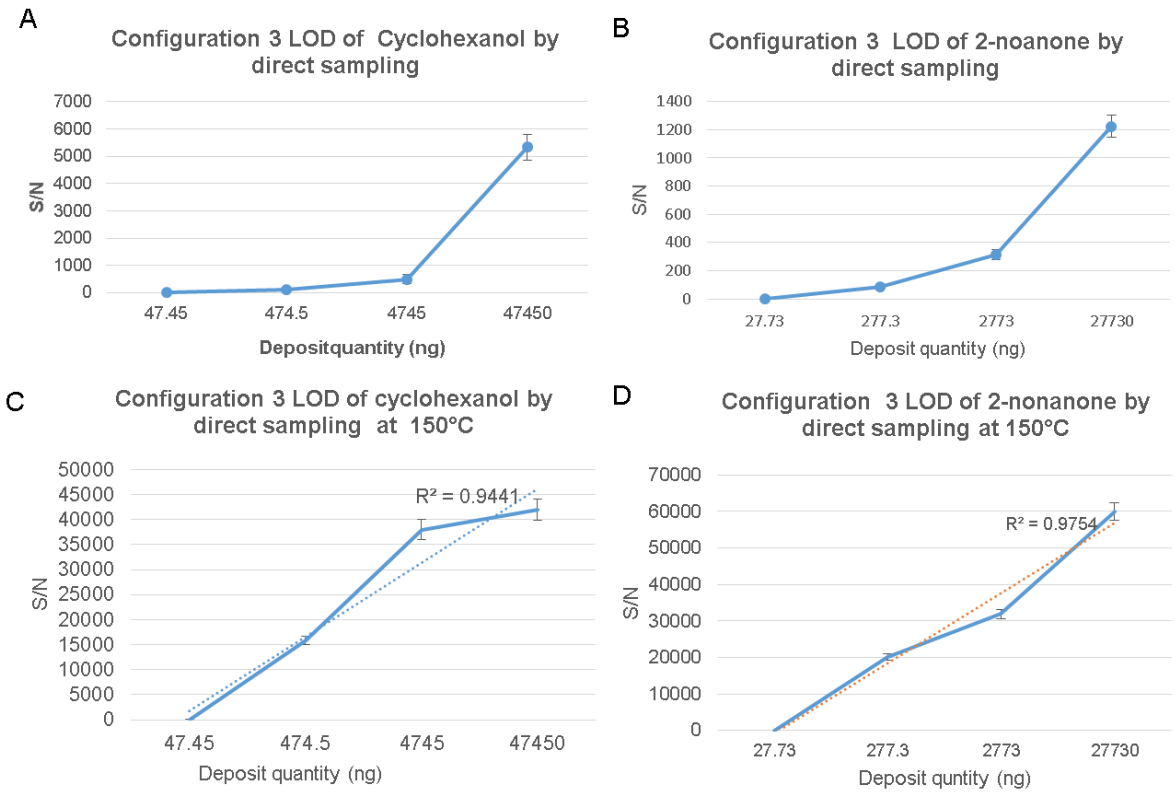

Figure 43: Detection of mix standard with the configuration 3. A, B. LOD of cyclohexanol and 2-nonanone at ambient temperature. C, D. LOD of cyclohexanol and 2-nonanone at 150°C.

Although this configuration allows the detection of VOCs with a reliable repeatability and sensitivity, many efforts must be deployed to optimize the desorption process. Indeed the glass directly in contact with the heater could easily reach its temperature resistance limit (300°C) and explode, and the phenomenon of heat loss has to be considered. Furthermore, the heating temperature set on the heating system is not the temperature actually reached within the enclosed glass system. A difference of more than 55 °C has been observed and a temperature above 220° C is often required for an optimal thermal desorption. Also the plastic cap prevents any experiment with an above temperature. For these different reasons, the configuration 3 wasn't considered for further analysis.

b. Configuration 4:

This configuration is based on the configuration 3. The main difference is the addition of T glass connector between the probe and the exit tube of the design erlenmeyer (Figure 44, A. B). The T glass connector was used to reduce the interaction with the ambient air and therefore to diminish the background noise observed in the MS spectra. The exit tube was directly connected to the inlet. No geometry probe was

investigated since no modulation is possible. All tested parameters are presented in the following table:

Parameters	Symbol	Range
Electronic parameters		
Voltage	HV	3-30 kV
Frequency	Hz	20-30kHz
Gas supply		
He		125 to 324ml/min
N_2		0.5 to 4L/min
Temperature		
Temperature enclosed glass system	°C	25-200°C

Optimisation result:

Unfortunately, the direct connection of the T connector exit to the MS inlet of mass spectrometer disturbed once again the He balance within the MS as previously described. This unbalance is recognized as an error and leads to the pump shutdown and consequently the mass spectrometer shutdown. Nonetheless few experiments were performed. This configuration allows the observation of monomer and dimer of both standard cyclohexanol and 2-nonanone (m/z 101, m/z 201, m/z143, m/z 285), the heterodimer (m/z 243) and also a fragment ion m/z 83 of 2-nonanone (Figure 44, E). Considering the He flow, the optimal setting was found at 354.7 ml/min with a decrease of S/N ration beyond this point (Figure 44, C). For the nitrogen flow a plateau is reached at 2.5L/min. By taking accounts all ions S/N ratio the optimal flow is found at 3.5L/min (Figure 44, D). The S/N ration was also found to be optimal considering an input power with the following values: 7kV, 24.34 kHz.

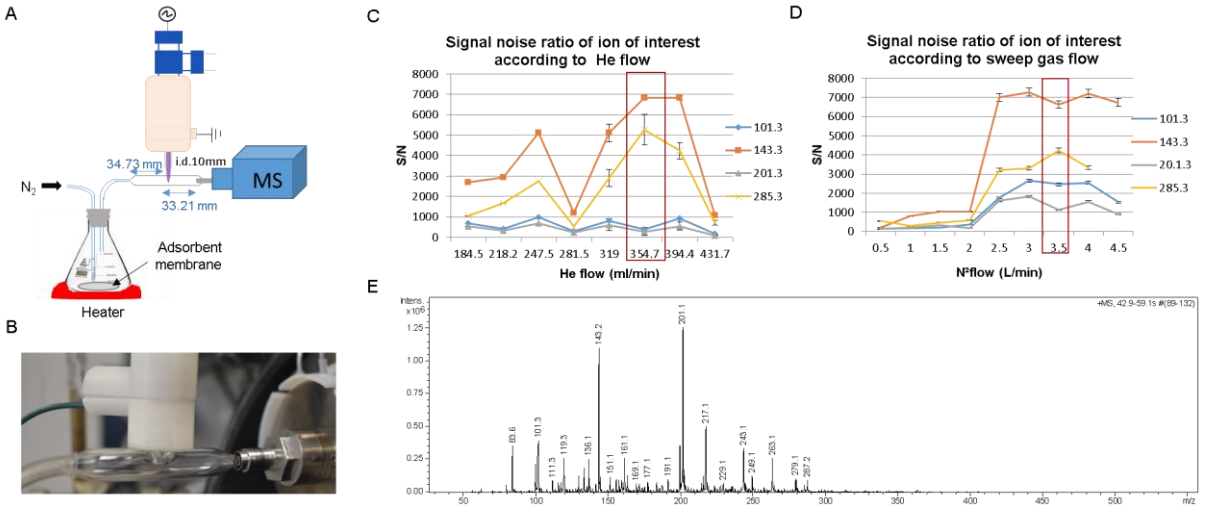

Figure 44: Optimization of LTP-MS configuration 4. A. Schematic representation of the configuration 4. B. Photo of the setup. C. Effect of He flow on the detection of mix standard. B. Effect of nitrogen flow on detection of mix standard. E. Example of spectrum of mix standard obtained buy this configuration.

Finally, the selected optimal parameters are: He flow 354.7 ml/min, N_2 flow 3.5L/min, input power 7kv 24.34kHz

Estimate limit of detection:

To determine the LOD, the standard mix was spotted on TX disc membrane. The experiment was done in triplicate with the optimized parameters.

Without heat, the configuration 4 enables the detection until 474.5 ng of cyclohexanol (Figure 45, A). As explained earlier, additional heat helped desorption of volatile from the membrane. Accordingly, the increasing heat enhances the detection of cyclohexanol (m/z 101.1) (Figure 45, B) multiplying by 5 the signal-noise ratio at 150°C compared to ambient temperature. Due to the plastic composition of the two-hole cap, at 200°C, some compound is released and detected at m/z 136 making any interpretation impossible.

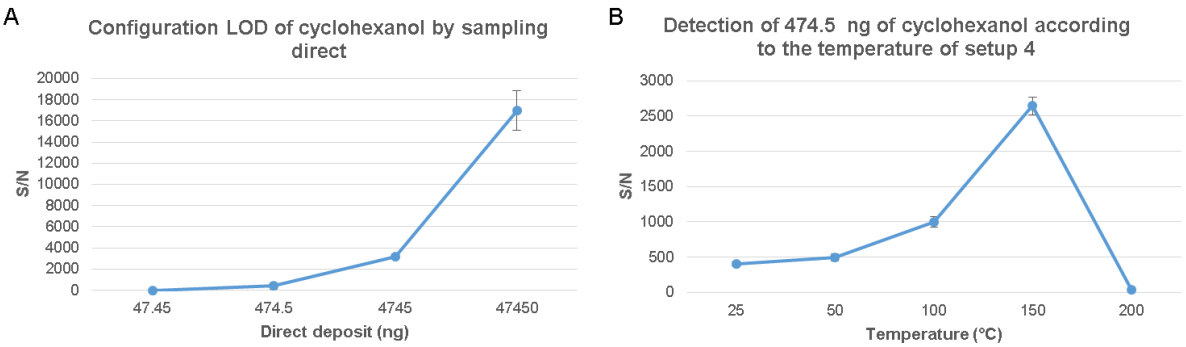

Figure 45: Detection of configuration 4. A. LOD of cyclohexanol by sampling direct. B. Effect of temperature on detection of cyclohexanol.

In conclusion, this configuration will not be further investigated with the coupling of IT due to the incompatibility of He arrival to MS inlet. Also, the glass made and plastic cap systems are not compatible with a heating above 150°C. The configuration 4 has been then discarded.

c. Configuration 5

Configuration 5 (Figure 46, A) is based on a previously developed headspace analytical system configuration (configuration 3 and 4). The main difference is the use of He as sweep gas and LTP gas. Indeed, He goes through the erlenmeyer inlet and conveys the desorbed VOCs to the exit outlet which is directly connected to the LTP probe. The LTP is coaxially positioned in front of the MS inlet. In this configuration, the desorbed VOCs are transferred by the He directly from the HS based erlenmeyer to the LTP probe in the discharge region where they are subjected to ionisation process. No geometry probe was investigated. The probe parameters used are listed presented in the following table.

Parameters	Symbol	Selected
Electronic parameters		
Voltage	HV	6 kV
Frequency	Hz	24.34kHz
Gas supply		
He	Q_{He}	2L/min
Probe geometrical		
Distance between the probe and the MS inlet	PM	9mm

Configuration results:

Several drawbacks appear with this system. Indeed, the time between the transfers of VOCs gas discharge to the probe for plasma formation takes more than 10 sec. This time gap leads to a loss of VOCs accumulated into the HS region. Also, this ionisation system increases the fragmentation and leads to a more complicated spectrum (Figure 46, C). Of note, it has been demonstrated that the ion residence time in the plasma can lead to many gas-phase reactions, therefore to a great increase of fragmentation rate (10.1002/rcm.4444). In configuration 5, the residence time of the desorbed VOCs is longer than in other configurations leading to the fragmentation. Compared to configuration 3, numerous fragmentation were present as the ions m/z 59, m/z 169, m/z 155, m/z 196, and m/z 234. In addition, more ion background is detected as m/z 217, m/z 263.

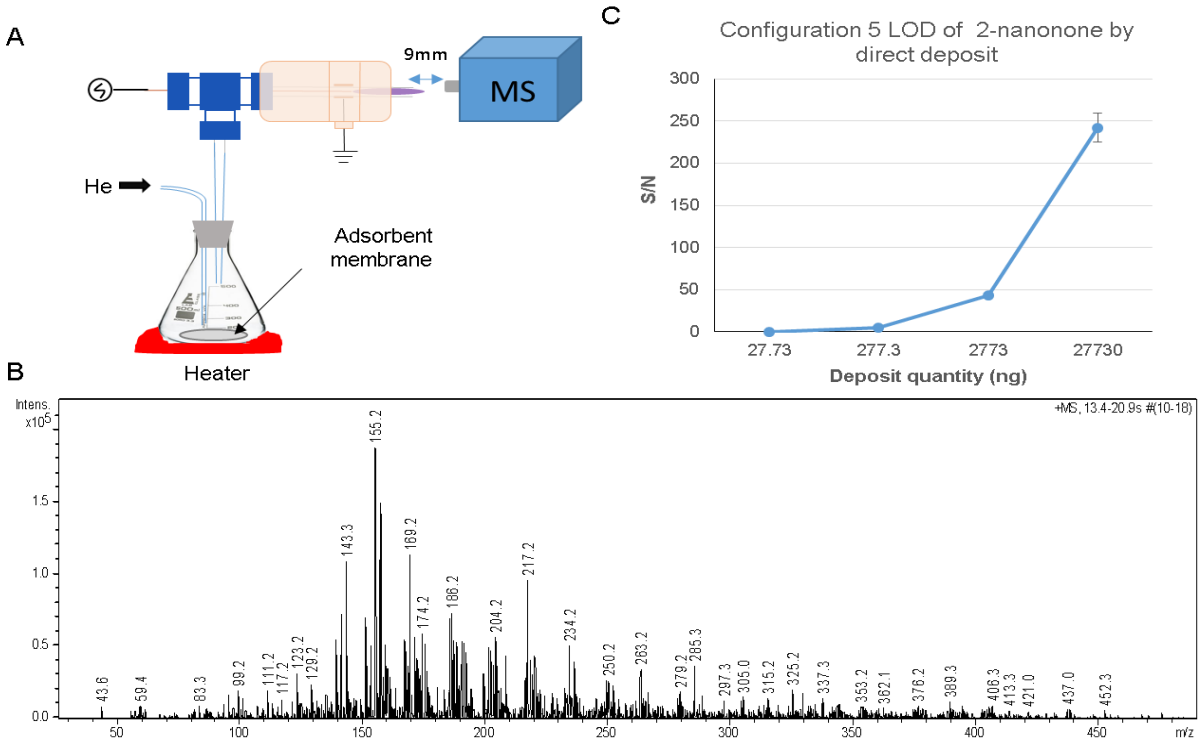

Figure 46: Configuration 5. A. Schematic representation of the configuration. B. spectra of mix standard. C. LOD of 2-nonaone with configuration 5.

In this context, the configuration of the LTP source is not soft enough to provide easily interpretable MS spectra. Moreover, it has to be considered that the fragment ion pattern obtained cannot be used for a direct identification using the available EI spectral libraries (70eV) and taking into account that no separation technique has been implemented in our system. This means that fragment ions coming from different VOCs are observed in the same MS spectrum. Nonetheless the ion selection could be done by MRM and then overcome this extensive fragmentation and complex spectra feature. By this method (Figure 46, B) the LOD of this configuration is established to 277.3 ng following the molecular ion of 2-nonanone.

For all these reasons, the optimal LTP parameters haven't been well established for this configuration considering that the effect of one parameter could not really be assessed in the MS spectra. Overall this configuration will not be further investigated

Selection of LTP-MS analytical system.

Among the five developed analytical systems, DS and IS, only one, the configuration 1 (DS) was selected for further experiments. A last and sixth configuration was developed for IS.

I. Direct analytical system

According to the LTP probe optimization, the configuration 1 has been selected for the direct membrane analysis. Indeed, the desorption/ionization is performed by the LTP beam and therefore, it can be used as a straightforward system for the detection of very and volatile VOCs considering that the configuration doesn't encompass a thermal desorption unit.

Regarding the second configuration, it didn't provide enough reproducible results mainly due to the instability of the disc membrane under the sweep gas and the beam plasma disruption. Moreover, the non-homogeneous heating and the He disruption within the MS make this configuration non-robust and therefore the analysis of the VOCs becomes tedious.

II. Indirect analytical system headspace based.

Concerning the indirect headspace analytical system (configurations 3 to 5), all three are excluded due to the incompatibility of the system with high temperature, mostly due to the glass parts, the plastic made cap and the dilution of analyte within the headspace even with a volume of the enclosed system reduced to 63cm^3. The volume of system could not be decrease to let the possibility of the placement of disc membrane into the glass system. Furthermore, the heat provide by the system is not homogenous, paramount for comparative analysis.

III. Indirect analytical system thermal desorption (TD) based:

Despite the efforts to set up a homogeneous heating system to induce the TD of adsorbed VOCs, none of the previous configurations is suitable. Thus, a direct membrane desorption system based on a heat sweep gas passing directly through the disc membrane was envisioned. This system should respond to an optimal membrane thermal desorption for an optimal VOCs ionisation in gaseous phase by the LTP probe.

To enhance VOCs detection, the configuration has been coupled to a more sensitive MS instruments presenting a higher resolving power (8000 FwH). In this context QTOF premier (Micromass) has been selected for further experiments. Furthermore, more software dedicated to the statistical data analysis are available and compatible with raw files generated by the MS instrument (Xomics, metabolomics.ca). The QTOF premier settings were then optimized for the detection of small molecule. The setting parameters were as follow: no capillary voltage was applied on the QTOF premier and the ion guide was set to 2.7. The quad settings was m/z 100, Dwell time 60, Ramp time 10. The mass range was set at m/z 50 to 500.

a. Configuration 6

This configuration is the last development of LTP-MS analytical system (Figure 47). It offers an optimal homogenous thermal desorption of the membrane providing by a dedicated heating device.

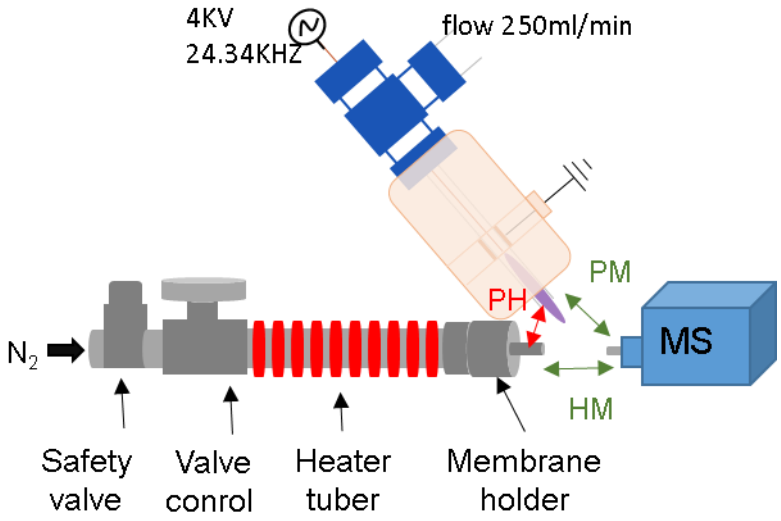

Figure 47: Schematic representation of TD-LTP-MS.

Multiple heating devices have been tested due to the numerous quality and electrical issues. Three heating device were tested including a heating tape (l: 1m, max temp: 450°C, 10210402 fisher scientific), a heating horse from Masterflex (Templine-A, l: 1m, temp max: 350°C, Masterflex SE) and a heating horse from Hillesheim GmbH (H 900 series, l: 5m; di: ¼" Tmax: 450°C) controlled by a digital temperature sensor. As the gas used for thermal desorption came from the mass spectrometer, upstream the heating horse (Figure 47), a safety valve was mounted to avoid the mass spectrometer overpressure and a valve control gas was installed to manage the nitrogen flow in order

to control the membrane thermal desorption analysis time. The membrane is placed downstream the heater into an inox holder (WHAT1980-001, d.i: 13mm, VWR, France). The exit of membrane holder faces the MS inlet and allow the LTP-driven ionization of the desorbed VOCs.

This TD-TP-MS system was tested with the following parameter:

Parameters	**Symbol**	**Selected**
Electronic parameters		
Voltage	HV	4kV
Frequency	Hz	26.34kHz
Gas supply		
He	Q_{He}	247 mL/min
N_2	Q_{N2}	2 L/min
Temperature		
Temperature gas supply by heating horse	TH	250°C
System Geometry		
Distance between the probe and the MS inlet	PM	5 mm
Probe angle	PA	45°
Distance between exit holder and the MS inlet	HM	4 mm
Distance between exit holder and the probe	PH	4 mm

Configuration results:

This configuration was assayed as previously by direct deposit of 5µl of mix standard (15:1) cyclohexanol and 2-nonanone on TX disc membrane. After analysis of TX disc and data analysis (Figure 48, A and B), the configuration enables the detection of standard (Figure 48, C) such as the molecular ion (m/z 101, 143), dimer (m/z 201 and 285) of each standard cyclohexanol and 2-nonanone and the heterodimer (m/z 243). For cyclohexanol, $[M-H]^+$ (m/z 99) form are observed.

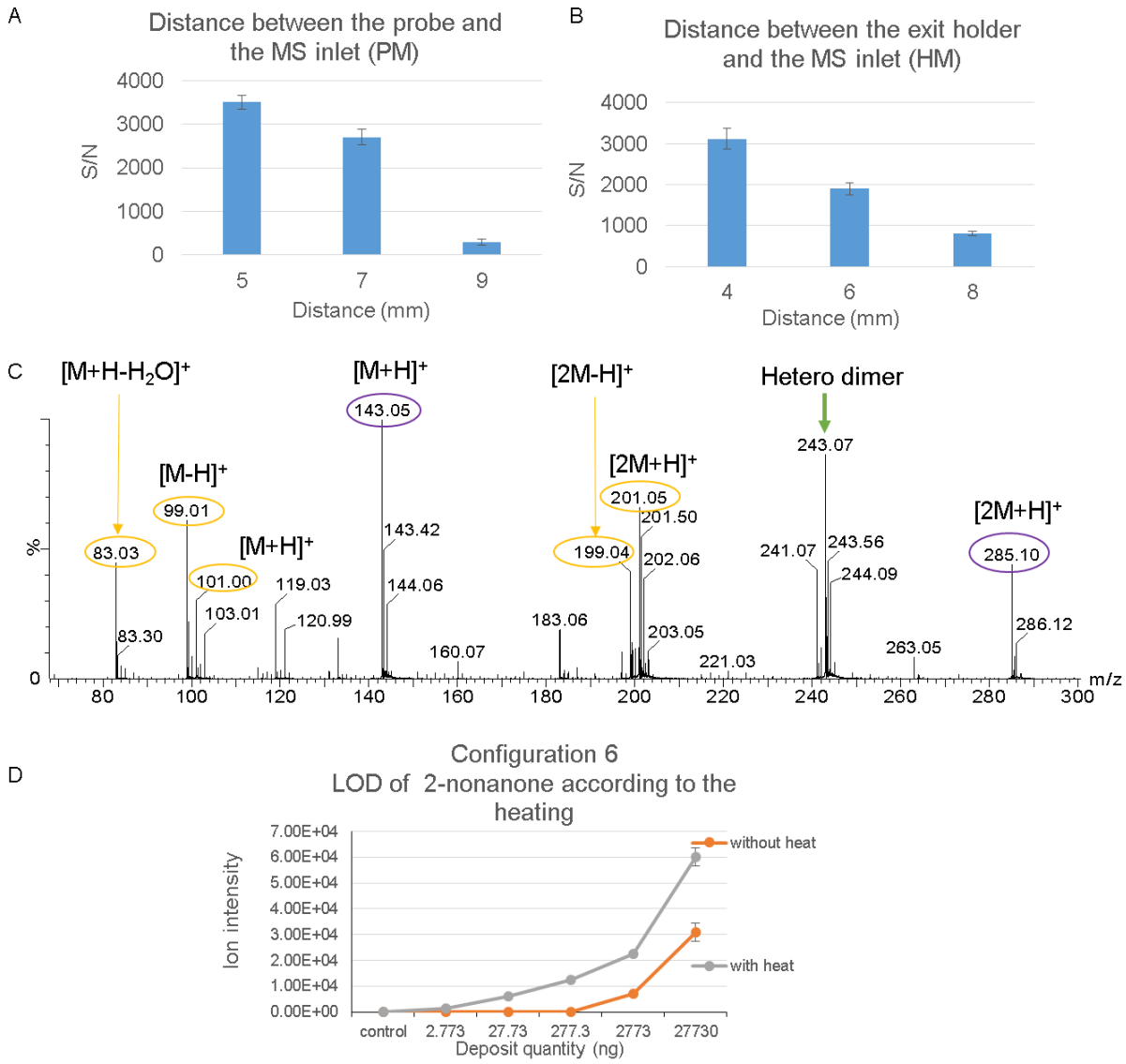

Figure 48: Configuration 6. A. Distance between the probe and the MS inlet B. Distance between the exit holder and the MS inlet C. LOD of 2-nanonone by sampling direct D.MS spectra obtained with the configuration 6

Estimated limit of detection:

As this configuration consist in a homogeneous TD unit, a better LOD is therefore expected. For each analysed quantity, the detection was substantially better with the addition of temperature. Furthermore, this is a steal and inox made system preventing any material based contaminations as previously observed.

To determine the LOD intensity of molecular and dimer ion of each standard were cumulated.

Without heat, the system allows the detection of 2-nanonone, and cyclohexanol with a minimum quantity of 277.3ng and 474.5 ng respectively (Figure 48, D). Expectedly, the addition of optimal heat helped VOCs desorption from the membrane, 250°C here.

With the appropriate temperature, the LOD increase to 2.773 ng and 4.745 ng for 2-nanonone and cyclohexanol respectively.

Even if this configuration showed the optimal results and appears as the most developed LTP-MS analytical system, several parameters can still be improved. Indeed, the system is heavy, bulky and extremely hot when it operating. The slightest movement induces a displacement of the whole system, especially the exit holder. Indeed the membrane is placed in stainless steel support which must be screwed and unscrewed between each analysis, which could results in shifting the focalisation exit. No extra geometrical optimisation has been realized given the numerous support necessary for a stabilized configuration. Futhemore the distance between the exit holder or tube, angle of LTP were already invistigated in the others configurations.

TD-LTP coupled to QTOF-premier mass spectrometer:

To enhance the robustness and experiment reproducibility, a source holder (Figure 49) was especially designed using Blender software and has been 3D printed. The holder consists of a milimemetric screw to control the probe high. The probe angle is also controlled by a screw. The holder can also move forward and background to perfectly align the system with the MS inlet. This LTP removable adjustable holder is designed for interface source of the QTOF premier but can easily be fitted on any other MS source interface. Considering the heating system size, a metal holder is fixed to the MS to support the weight of the heating system and ensure the proper alignment between the holder exit and the MS inlet.

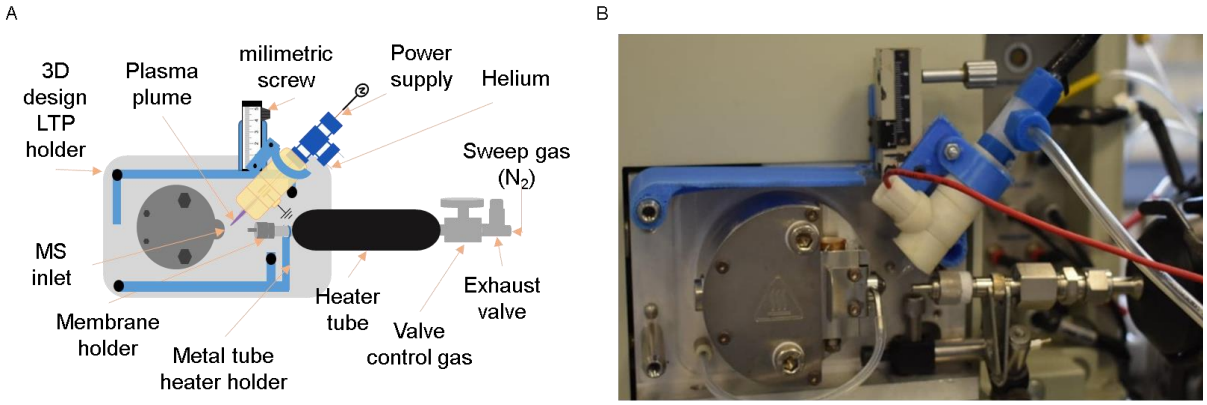

Figure 49: Optimal configuration of the TD-LTP-MS. A. Schematic representation of the TD-TLP source. B. Picture of the 3D printed TD-LTP holder.

The final configuration is the last development of homogenous thermal desorption without any dilution and exaggerated disruptions. The selected parameter for TD-LTP-MS analysis are present above and present in Figure 50 .

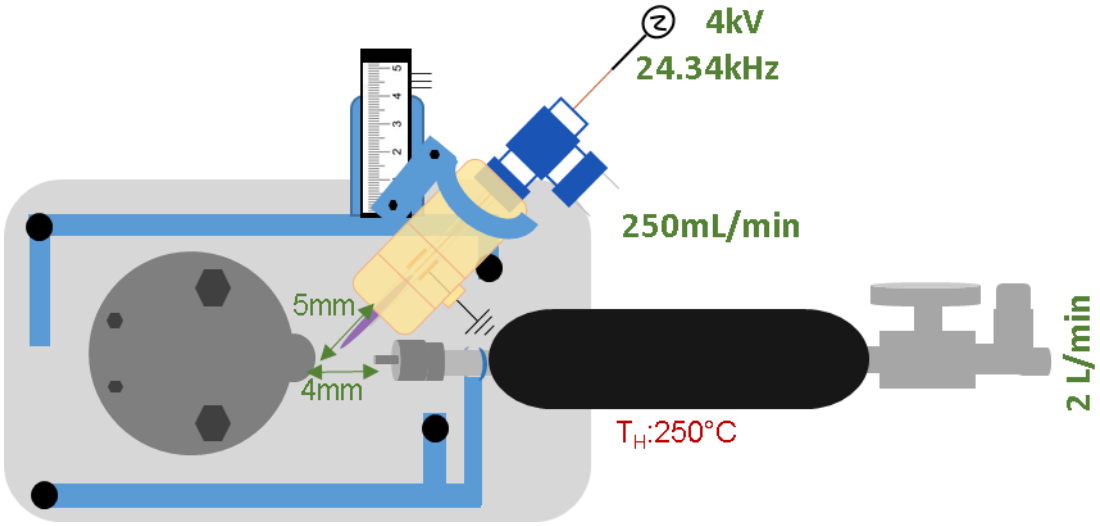

Figure 50: Schematic representation of optimal TD-LTP-MS system.

Chapter III: Sampling method for LTP-MS analysis

Sample collection is probably the major key in the entire analytical process. VOCs released in gas phase (e.g. exhaled breath or HS) are generally collected by means of SPME, TD tubes or needle trap devices. These systems were found to be very efficient for the detection of VOCs from body fluids including breath, blood, feces and urine. However, these procedures don't allow the *in situ* sampling of VOCs which can be released directly at the tumor site. In this context, we decided to use disc membranes as adsorbent to collect VOCs instead of the conventional SPME or TD tubes. Disc membranes can therefore be used to concentrate VOCs released in the HS from urine, blood, tears or present in the exhaled breath. Additionally, disc membranes can also be applied at the tumor site as a patch in order to adsorb the secreted metabolites containing volatiles metabolites. This strategy allows VOCs present in all body fluids or at the tumor region to be collected and subjected to LTP-MS analysis according a direct or a non-direct detection mode.

Direct sampling:

The direct sampling (DS) consists of the direct deposit of the analyte onto a surface, (common approach for all analytical developments) or consist of the direct contact of a membrane with the sample. Here, a focus has been made on the direct sampling of an adsorbent membrane maintained in contact with patient's skin, at tumor site during a controlled incubation. In line with the KDOG project principles (canine olfactory system), we conceived the SNOOP-I project.

I. Snoop I project

This project aims to diagnose breast cancer (BC) by LTP-MS analysis from a disc membrane incubated onto the patient's breast skin.

Unlike traditional VOCs analysis, the VOCs sample is not in gaseous state as for direct exhaled breath analysis or for VOCs headspace analysis. Here the VOC sample is the skin patient, therefore the sampling need to be adapted. In this context, VOCs skin patient are concentrate onto an adsorbent disc directly in contact with the skin, and

after adequate incubation the membrane will be analyse for VOCs fingerprint discrimination (Figure 51).

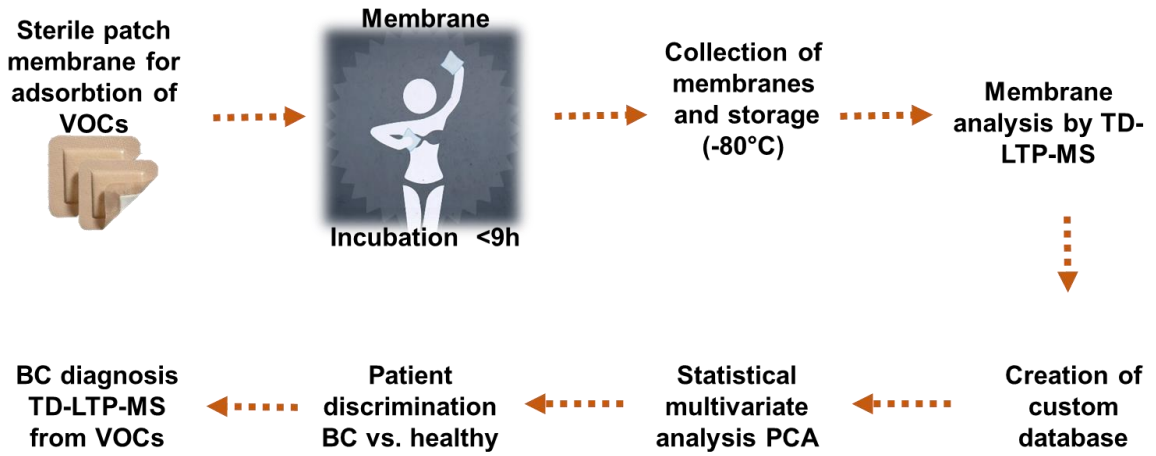

Figure 51: Workflow of SNOOPI project.

First, a sterile patch needs to be developed, to have a repeatable, reproducible, standardized and efficient VOCs sampling. TX disc membrane was used for all design patches. Three supports were tested and compared based on: (i) the fixation of the TX disc membrane to the band-aid, (ii) the patch fixation to the patient's skin breast and (iii) the band-aid and TX disc membrne background. The tested band-aids were sterile gas, Melipore and Mepilex (Figure 52, A, B). Sterile gas was put aside due to the impossibility of fixing the membrane on the gas and requires an additional step to fix the gas to the patient skin. Melipore is a combination of sterile gas and adhesive tape. However, the problem of TX disc membrane fixation remains. Mepilex is a silicone self-adhesive hydro cellular band-aid composed of a flexible silicone coating on the wound side, 2-layers absorbent polyurethane foam which permit the fixation of TX membrane to the band-aid and a vapor-permeable and waterproof outer film. This band-aid enables the easy fixation of TX disc membranes, the fixation of the band-aid onto the patient's skin and even avoid external contamination by permeability (Figure 52, C).
In order to appreciate the designed patch (Mepilex and Melipore), TX disc membrane was incubated during 9hours on patient skin and analysed by TD-LTP-MS (Figure 52, D) coupled to a QTOF premier.

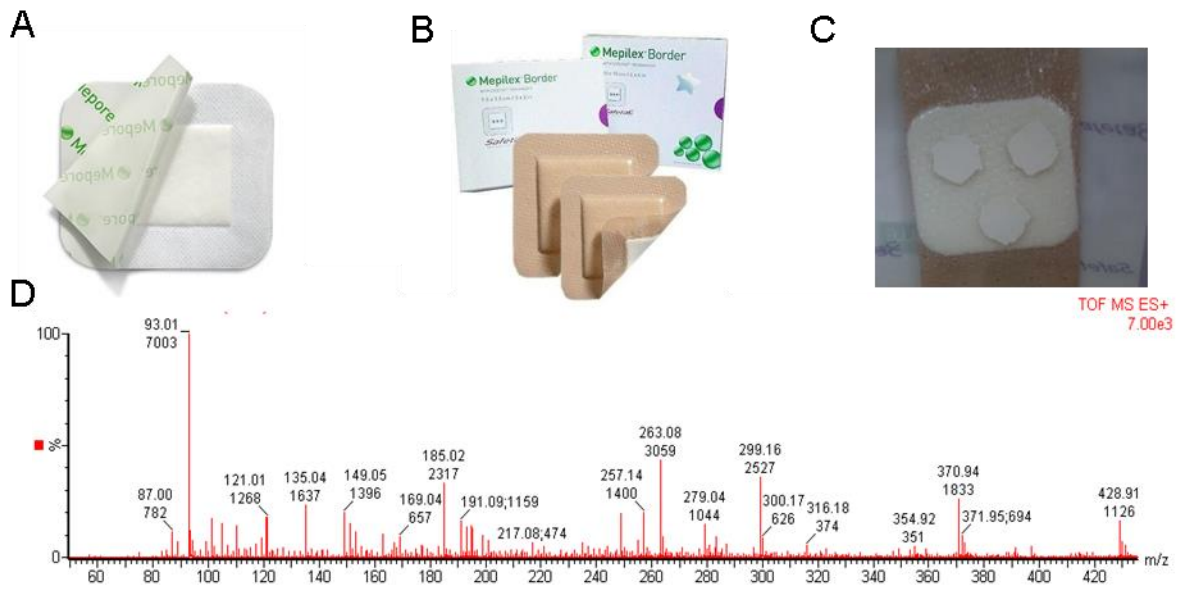

Figure 52: Snoop-I patch. A. Melipore band aid. B. Mepilex band aid. C. Final custom Snoop-I patch. Mepilex patch with 3 TX discs membranes. D. Spectrum of disc membrane after incubation with Mepilex band aid.

For Melipore patch, TX membranes were included in the first layer of gas, but as expected, TX membranes were not in direct contact with the skin but with the first layer of gas. Consequently, the VOCs were majority adsorbed onto the gas and not on the TX disc membrane. Not suitable for an efficient sampling.

For Mepilex patch, TX disc membrane were directly placed onto the adhesive band-aid (Figure 52, E). After analysis, no contamination from the adhesive band aid is observed between 50 and 500 Da (Figure 52, D).

Finally, the Mepilex band-aid was selected for the design of SNOOP-I patch as none of the others allowed easy fixation and ensured permeability, which reduced environmental contamination. Three discs membrane (d: 14mm) were disposed on the Mepilex band-aid for a triplicate of the experiment. This sterile custom patch was tested on volunteer with overnight incubation time. Before the placement of the band-aid, the area (cancerous mammary) was cleaned with chlorixidine. The Snoop I patch was then maintained in contact with the cleaned area and incubated for at least 9hours. The patch was collected and directly stored at -80°C in a glass dish until analysis to avoid sample degradation.

Indirect sampling: Headpace sampling (HS).

VOCs pre-concentration is mainly performed by means of HS coupled to SPME or TD tubes. Even if this method has been widely described, no HS sampling of trapped

VOCs onto a disc membrane was developed. Based on the existent method, HS sampling was investigated and separate into three approaches: static headspace sampling (SHS), sampling headspace dynamic (sDHS, vDHS) and static – dynamic headspace sampling (SvDHS).

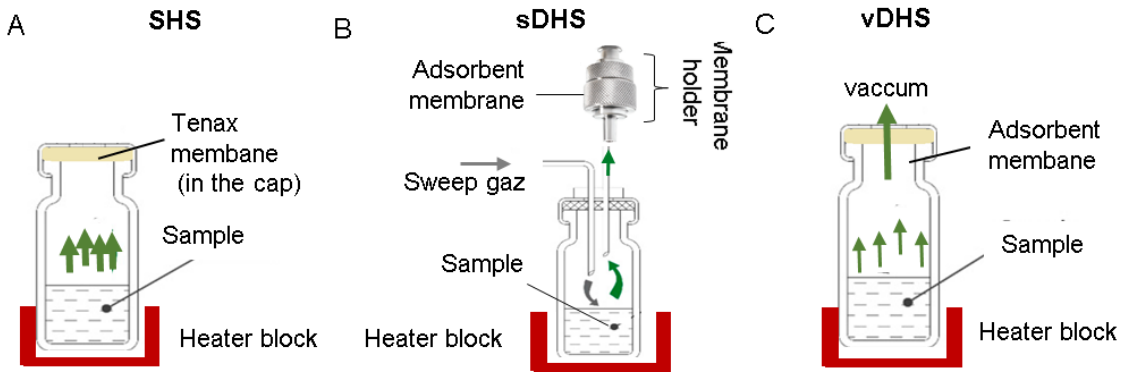

Figure 53 Schematic representation of headspace system sampling. A. Static headspace sampling. B. Sampling headspace dynamic sweep gas. C Sampling headspace dynamic under vacuum.

Static Headspace sampling (SHS): (Figure 53, A.) This sampling method depend on the formation of equilibrium conditions within a closed system. Here, a glass vial is used as a closed system and the membrane disc is placed into the cap. During the sampling, VOCs are captured and concentrated onto the membrane. Additional heat, stirring or shaking could be applied.

Dynamic headspace Sampling (DHS): (Figure 53, B. C.) Two DHS sampling process were developed:

Sweep gas-based dynamic headspace sampling (sDHS): During the sampling, the VOCs in the HS region are continually swept by a gas (nitrogen) and concentrated to an adsorbent TX disc membrane. Two syringes were used for the gas inlet and outlet. The syringes pass through the septum of the glass vial. The outlet conducted the VOC to the TX disc membrane which is placed into a membrane holder (WHAT1980, VWR) (Figure 53, B). The VOCs were trapped onto the membrane. During the sampling, stirring, and heat could be added. This technique requires significant installation and allows sampling of samples one at a time; which preclude any high throughput analysis here, as no holder was designed. Furthermore, the complicated sampling setup, renders this device no reliable for reproducible analyses. Thereby sDHS were not be further investigated.

Vacuum based dynamic headspace sampling (vDHS): To overcome the sampling of one by one sample, a multimodal sampling and sampler were designed (Figure 54).

As previously described, the sample is placed in an air-tight container and heated. A continuous aspiration (0.5bar) has been applied to generate a vacuum allowing VOCs to be transferred in the HS region and concentrated onto the TX disc membrane placed in the vial cap.

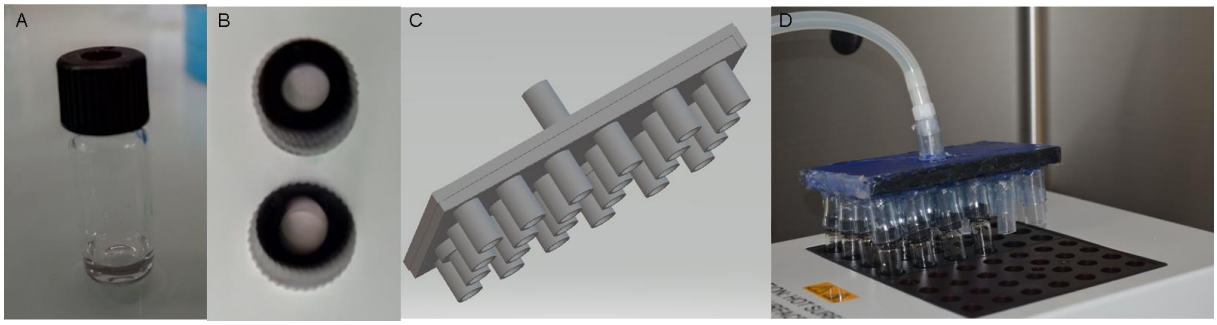

Figure 54. Vacuum based dynamic headspace sampling (vDHS). A. Picture of the glass vial. B. Picture of the membrane disc into the cap. C. Design 3D sampler. D. Picture of headspace sampling dynamic with the 3D design sampler.

The 3D sampler was designed on Blender software and printed by DAGOMA printer from Polytechnic. It was especially designed to sampling twenty-four samples at the same time, for high-throughput analysis and the sampler is compatible with heater system for a homogenous heat. The implementation of continuous aspiration at 0.5bar is the system novelty. Aspiration is another way to trap VOCs onto an adsorbent disc. This 3D holder allows the sampling of twenty four samples at the mean time for high-throughput analysis. After sampling the TX disc membrane are collected for direct analysis or stored at -80°C.

Static and vacuum based dynamic headspace sampling (SvDHS): This is a combination of a static and a vacuum based dynamic. The sampling began with a sampling headspace static followed by sampling headspace dynamic aspiration. As described previously, the disc membrane is place to the cap, and the vials were placed on the 3D sampler. This sampling permits high-throughput sampling and stirring, and heat could be added during the sampling. After preliminary result, SvDHS showed good efficiency sampling but did not give extra advantage to the vDHS and required and additional step of sampling. For this reason this sampling was not further investigated.

For each sampling optimisation 200 µL of standard at different concentrations were added in 2mL glass vials for incubation with. Incubation parameter such as time and temperature of incubation were investigated for the different sampling though mix

standard cyclohexanol: 2-nonanone (15:1) and EPA standard (30152, Restek). TX disc membrane was placed into the cap and each experiment was performed in triplicate.

I. Headspace sampling: time–temperature relation

Here optimisation sampling parameters were performed on SHS sampling as it is the easiest set up. Three sampling times (30 minutes, 1 hour and 2 hours) and temperatures (25°C, 50°C, and 82°C) were assayed with cyclohexanol and 2-nonanone (Figure 55). Each experiment was analysed by DS (configuration 1) coupled to IT-MS using the previously defined parameters. The ion intensity of monomer and dimer of each standard were cumulated to monitor the different sampling parameters.

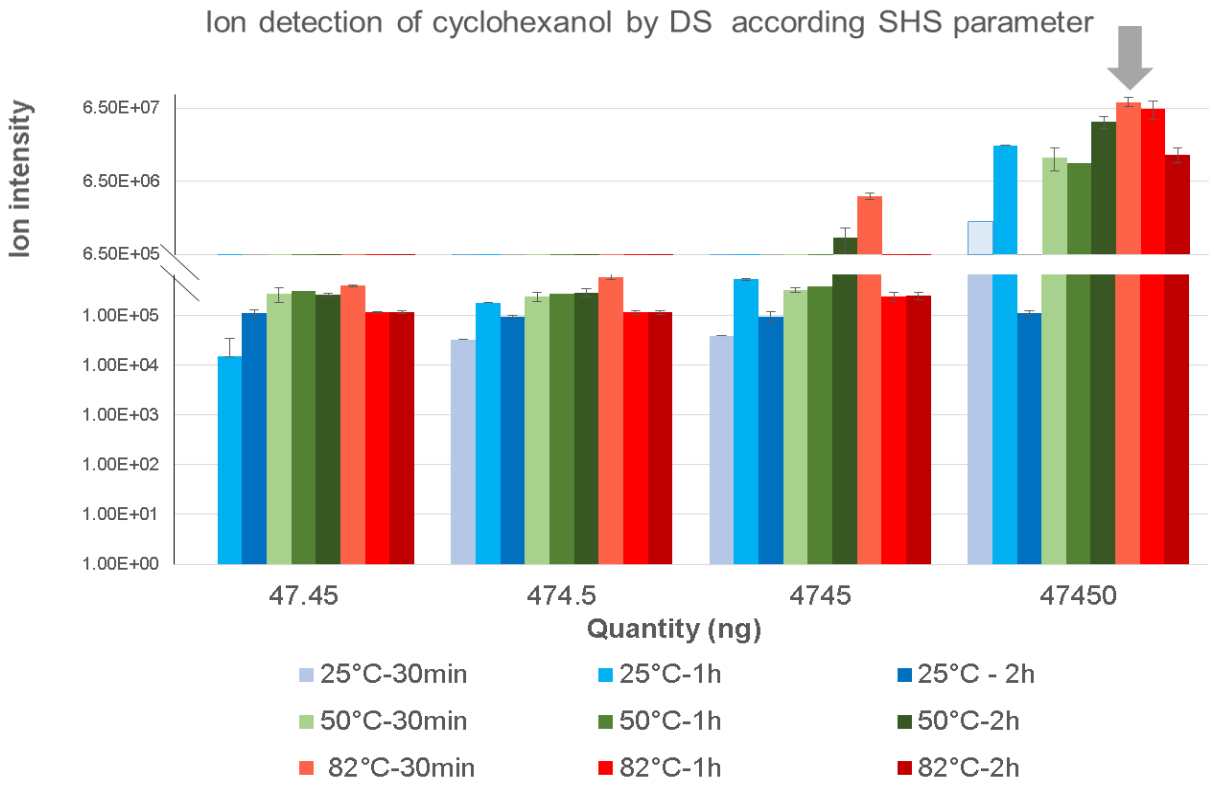

Figure 55: SHS sampling. The parameter investigated are the temperature and time sampling. . Ion detection of cyclohexanol according the temperature and time of SHS sampling.

Considering the sampling time at ambient temperature (30 minutes, 1 hour, 2 hours), the optimum was found at 30 minutes at 82°C (Figure 55). An increased in detection is observed between 30 min and 1 hour and a decrease between 1 and 2 hours at temperature. The sample incubated during 2 hours has provided the lowest signal.

Considering the sampling temperature, the addition of heat during the sampling enhanced the transfer of VOCs in the HS region and therefore the

adsorption/concentration of VOC onto the TX disc membrane. In case of cyclohexanol analysis at the same concentration and the same sampling time, the increase of temperature from25 °C to 82 °C multiplied by 3 the analyte detection (ion intensity). The addition of temperature during the sampling can also induce a decrease of sampling time as observe in Figure 55, A. For instance, best intensity has been observed at 30 min of sampling at 82°C. A similar trend was observed for 2-nonanone standard analysis, however the best intensity is found at 50°C during 2 hours of sampling. It can be explained by the higher boiling point of the 2-nonanone compare to the cyclohexanol. Taking into account the balance between temperature and sampling time the selected parameter for headspace sampling optimal parameters were 45 minutes with a temperature of 60°C.

II. Comparison of HS by TD-LTP-MS:

According to the previous experiment, the selected sampling time was 45 min with a sampling temperature of 60°C. The three sampling SHS, vDHS and sDHS were compared according to the detection of BC standard mix (cyclohexanol:2-nonanone, 15:1) (Figure 56). Cumuli of molecular ion, dimer and heterodimer of standard of cyclohexanol and 2-nonanone (101.1 and 2012; 143.1 and 2852; 243.3 m/z) ion were extracted to compare the HS.

Concerning the dynamic sampling, the vDHS sampling showed the best efficiency for standard adsorption. On the contrary, the other dynamic sampling sDHS, display poor repeatability and poor standard adsorption. The detection by this sampling is much lower than vDHS. In the other hand, SHS is repeatable with a satisfying ion detection, in a similar range than sDHS but with less variability.
vDHS a repeatable sampling method which allows the greatest concentration of the tested volatile onto the TX disc membrane.

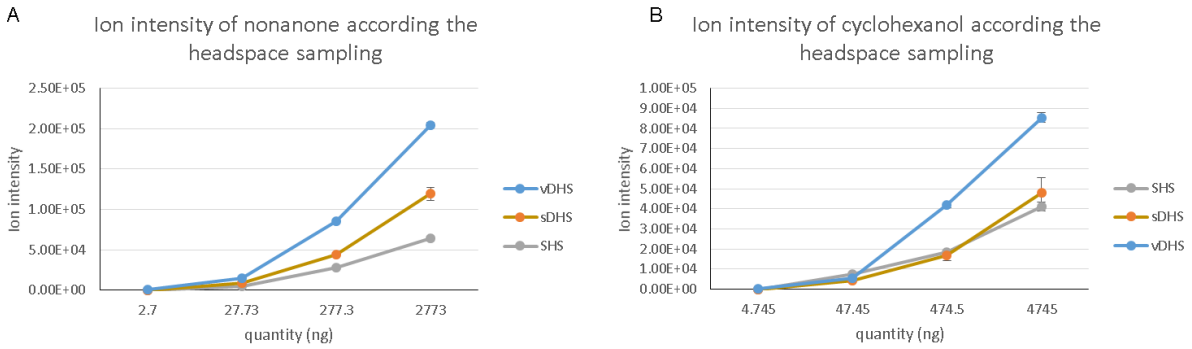

Figure 56: Comparison of headspace sampling. A. Ion intensity of 2-nonanone according the sampling SHS, sDHS and vDHS. B. Ion intensity of cyclohexanol according to the sampling SHS, sDHS and vDHS. All experiment were done in triplicate and analysed by TD-LTP-MS.

III. Comparison of selected HS by TD-LTP-MS

At last, headspace sampling method (SHS, vDHS, SvDHS) were compared by the detection of standard EPA (30152, Restek). It consist in a mix of 75 volatiles compounds at 2000µg/ml, and represent a more representative panel of volatile compound. Each experiment was done in triplicate and analysed by TD-LTP-MS at 250°C with the QTOF premier (Figure 57, A). S/N ratio were extracted for each detected compound, ion identification were validated by MS^2. Sampling were performed as explained earlier.

The detected and selected compound are listed in Figure 57, B. As expected the vDHS sampling showed the best efficiency for the concentration of a wide range of volatile species such as ether, ester, nitril, and hydrocarbon. Indeed for each selected ion, vDHS sampling system achieved the best detection. The SHS strategy showed also a good efficiency of VOCs adsorption/concentration. All the three sampling methods shows good a repeatability.

A

	Molecule name	Molecular formula	Monoisotopic mass	m/z detected	Boiling point at 760 mmgH (Bp, °C)	Vapor pressure at 25°C (Vp mmgH)	molecule class	polarity
Molecule detected from EPA mix	Tetrahydrofuran	C_4H_8O	72.11	73.09	65	132	Cyclic ether	Non-polar
	Diethyl ether	$C_4H_{10}O$	74.07	75.11	34.6	538	Dialkyl ether	Non polar
	allyl chloride	C_3H_5Cl	76,53	77.029	46	368	organochlorine	Polar
	Dimer Acetonitril	C_2H_3N	41.05	83.07	81.6	88.8	Nitril	Polar
	Methyl acrylate	$C_4H_6O_2$	86.036	87.08	80.2	86.6	Methyl ester	Polar
	Methyl methacrylate	$C_5H_8O_2$	100.05	101.2	100.5	38.5	Methyl ester	Polar
	Ethyl methacrylate	$C_6H_{10}O_2$	114.068	115.2	117	20.59	Ethyl Ester	Polar
	Trimer acetonitril	C_2H_3N	41.05	124.03			Nitril	Polar
	Uknown fragment		125.03	126.03				
	Iodomethane	CH_3I	141,94	143.09	42	405.04	Methyl halides	Polar
	Uknown fragment		150.047	151.04				

B

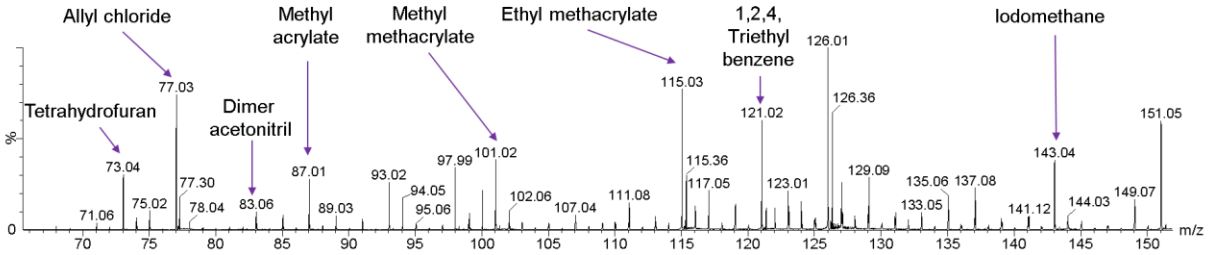

C

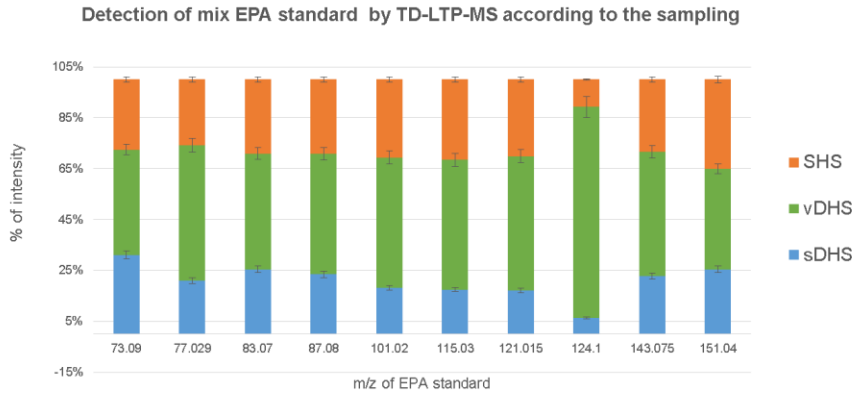

Figure 57: Sampling comparison by analysis of EPA mix. A Table of detected ion of EPA mix. B. Spectra of EPA by vDHS analysed by TD-LTP-MS. B.. C. comparison of sampling SHS, vDHS and DS.

In conclusion for further experiment the sampling vDHS will be favour as this dynamic sampling is the most efficient for adsorption/concentration of VOCs on a large range of molecule.

Chapter IV: Adsorbent membrane disc

Sorbent materials have a wide range of physical forms as tube, needle and fiber. Nonetheless, only a few disc membrane, flat sheet, or cylinder form sorbent materials for VOCs capture are commercially available in the market and no multiple bed adsorbent disc are available for these forms. Due to the difficulty of supply, only four membranes were investigated (Figure 58). Among them a Tenax disc membrane (Buchem, e: 1.5mm, d: 47mm), C18 disc membrane (Empore e: 0.5mm d: 47mm), flat sheet PDMS membrane (cat no: 751-624-16; Goodfellow, Cambridge Limited, e: 0.45mm) and Sorbstar cylinder (Action Europe, France, l: 2cm, d: 2mm). Sorbstar is a sorbent silicon-based polymeric phase with a density of 1.12 g/cm3. Considering the polarity of each sorbent, Tenax disc here is classified as bipolar and all the others (PDMS, C18 and Sorbstar) are apolar.

Figure 58: Adsorbent membrane. A. C18, Tenax TA like disc membrane. B. PDMS flat sheet. C. Sorbstar cyclinder membrane.

Sorbent comparison.

To appreciate each sorbent, 5µL of EPA standard solution were directly deposited onto the different membranes and analysed by TD-LTP-MS. The obtain spectra is presented in Figure 59, A. The temperature of TD was set at 250°C for the TX, at 260°C for the PDMS and 220 °C for the Sorbstar.

Each experiment was done in triplicate. The selected ion are listed in Figure 59, B; and their detection are compared according to the membrane (Figure 59, C).

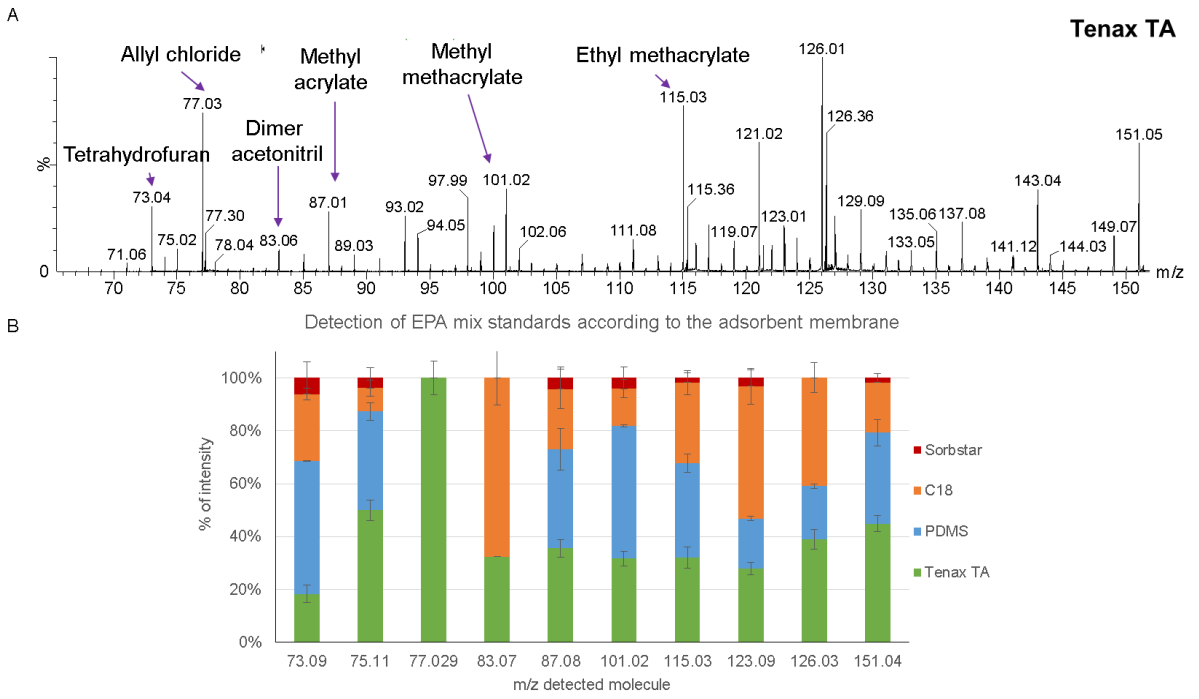

Figure 59: Comparison of adsorbent membrane. A. spectrum of EPA from TX membrane. B.. Detection of EPA standard according the membrane for direct sampling analyse by TD-LTP-MS

Concerning the Sorbstar sorbent, it showed the less VOCs capture efficiency. It's explained by the fact that no optimization of sampling or desorption system were done for cylinder form. Furthermore this adsorbent induce a patient discomfort when it's directly sample from the skin breast. Concerning the C18 disc membrane, it allowed the detection of polar compound such as methacrylate and acetonitrile. However C18 membrane is the thinnest, less supple and much more breakable sorbent used, then it has be found to be not well suitable for the experiment set up. PDMS membrane custom disc allowed the detection of polar compound, with high intensity, sometime higher than TX as for ethyl methacrylate, methyl methacrylate. Concerning the detection by TX, this membrane allow the detection all selected compound with the highest intensity. It's the only one which permit the detection of m/z 77.09.

In conclusion, the TX membrane was selected for the further experiment considering its bipolarity and the detection of a large range of VOCs class.

Tenax TA disc membrane.

Tenax TA is a porous polymer resin based on 2,6-diphenylene-oxide. It is the most widely used adsorbent resins for use with Purge and Trap Thermal Desorption for applications such as trapping VOCs in air and liquids. Here TENAX®-Discs contains only fibers from the known polymer TENAX® TA. The discs are not porous and can adsorb various polar and non-polar compounds. Important note, the values of the breakthrough volume data of molecule such as alcohols, glycols, alkenes, aldehydes, ketones, halogens, amines, aromatics, terpenes and water investigated on TENAX beads (https://www.sisweb.com/index/referenc/tenaxta.htm) shall be different from the values for the discs, but they provide an idea of the adsorbed compounds.

I. Tenax TA membrane conditioning and storage:

Conditioning is critical for successful sample extraction. Each sorbent requires conditioning or pre-treatment to prepare the sorbent to retain analytes and discard any residual artefact. Conditioning here involves the continuous flow of a high purity carrier gas (either nitrogen or helium) while the disc membrane is heated at elevated temperatures and under controlled atmosphere using high purity gases containing less than 1 ppm of oxygen. If possible the membrane disc should be conditioned 25 to 50 degrees higher than the temperature at which it will be desorbed the adsorbed molecules. In case of TX TA the maximum temperature is 330 °C. After complete conditioning time, controlled atmosphere must be maintained through the adsorbent resin during this cooling cycle which take 5 to 10 minutes cooled to room temperature. Here the membrane is placed within a membrane holder (Merck Millipore support inox 25mm or Pall, In line filter holder 47mm) connected to a heater hose (Hillesheim, H900 series) controlled by electronic compact controller (HT 63 series). After complete cooling, the carrier gas is turned off and the membrane is seal in a glass petri dish until use. If possible it is highly recommended to use fresh membrane conditioned within the past two days. Verification of the background membrane is always performed before sampling.

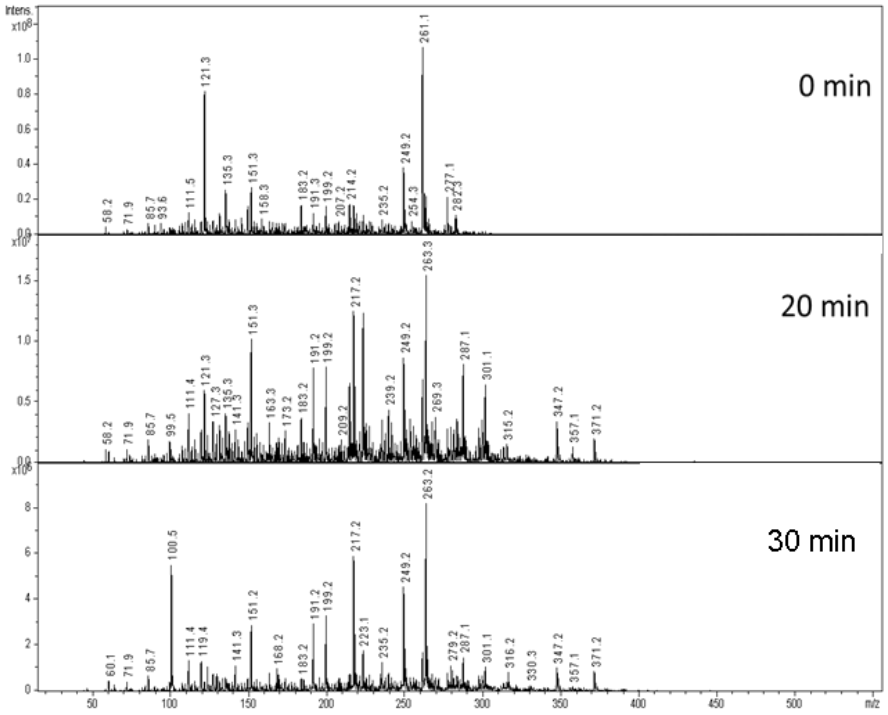

Figure 60: Spectra of conditioning TX membrane according time. The used sweep gas was nitrogen supply by the mass spectrometer at 2L/min.

The conditioning temperature was investigated in the case of TX TA disc membrane and as recommended by the supplier the optimal temperature was set at 330°C. Conditioning time was also investigated (0, 20 and 30 minutes) as presented in Figure 60. At 0 min, the obtained spectra of TX membrane present two major ion at m/z121 and m/z 261 with a global intensity of 10^8. After twenty minutes the signal intensity decrease (10^7) and the previous base pics tends to diminsh. After thirty minutes, the signal had diminish of 2 exponent with the apparition of ambaint background contamination ion (m/z 217, 263), already reported previously. The optimal time for conditioning is in accordance with the supplier, 30min of conditioning (Figure 60).

Chapter V: Patent

All these developments have led to a patent in the technical field related to an analytical system for analysis of adsorbed VOCs onto an adsorbent membrane. The patent was deposited the 20th May 2020 with the reference number FR 2005155. The deposited system (Figure 61) is a combination of vDHS and TD-LTP-MS system. The system allows the online conditioning, sampling and analysis of a disc membrane. This 3 in 1 configuration consist in a heating system fed by nitrogen for the membrane conditioning or the TD for analysis, The second part is a cylinder membrane holder with two entrance, in one way it allows the VOCs sampling onto the membrane using an aspiration system and in the other way, it allows the conditioning of the membrane with a gaseous internal standard The last part is the focalized exit directly toward the MS inlet for the ambient ionization of the desorbed VOCs with the LTP source. This system allows the drastic diminution of external contamination and responds to the miniaturization trend by the diminution of the heater system.

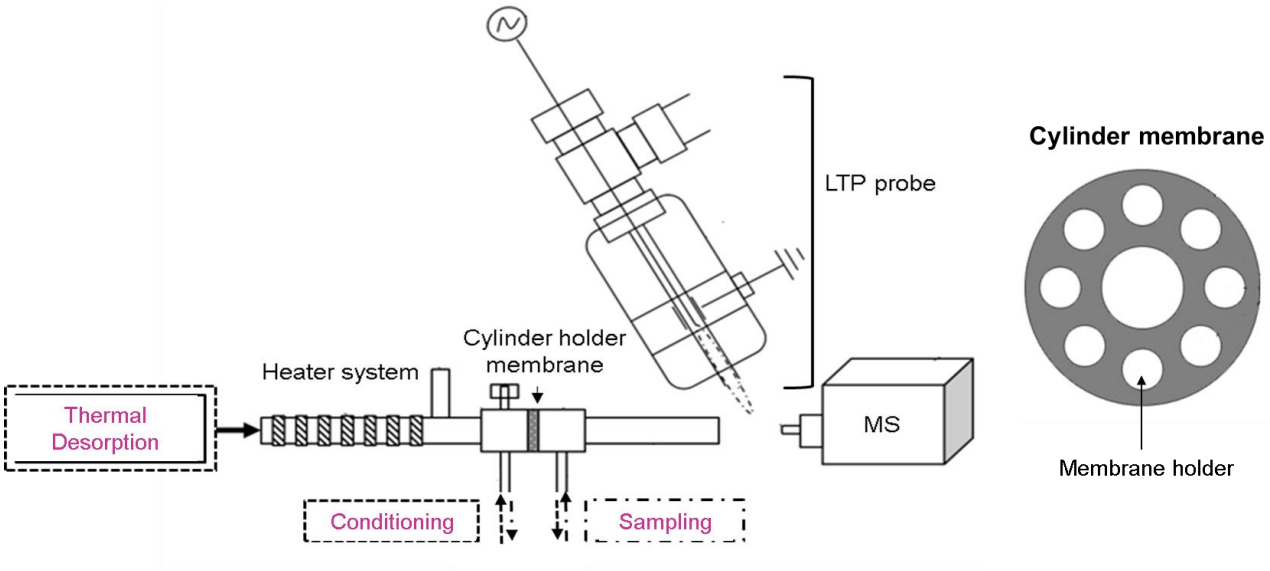

Figure 61: Schematic representation of deposit system. The heater system fed by nitrogen allow conditioning and thermal desorption of the membrane. The membrane is contained into a rotate cylinder with two entrance, one for the conditioning of internal standard onto the membrane and a second for the sampling.

Part three: Application of TD-LTP-MS for analysis of VOCs adsorbed onto a disc membrane.

Based on to the numerous developments carried out, our TD-LTP-MS system responds to a need for a rapid, sensitive, real and quasi real-time analysis of VOCs. In order to establish a fingerprint-based diagnosis from model discrimination groups, the TD-LTP-MS system has been applied to biological samples (Figure 62).

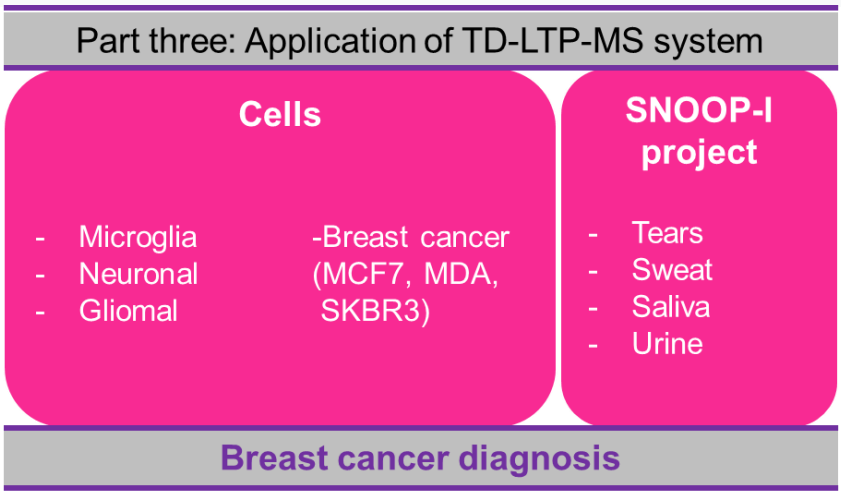

Figure 62: Different application of TD-LTP-MS for BC discrimination. The system is applied to cell VOcs discrimination and for BC discrimination in SNOOP-I project context.

The system was first assayed on cell lines of different cancer types to confirm the efficiency of the TD-LTP-MS to discriminate cell identities based their emitted VOCs. Subsequently, the cancer model discrimination group was based on the specific cell VOCs fingerprint. To assess the sensitivity of the system, three BC cell lines were compared. Finally, the system has been applied to its final purpose, the SNOOP-I projet. The project aims to diagnose BC through the analysis of adsorbed VOCs onto a disc membrane.Four biofluids (*e.g.* sweat, urine, saliva and tears) collected from five volunteer patients, were subjected to the TD-LTP based diagnosis system.

Chapter I: TD-LTP-MS system applied for VOCs cell line discrimination

Building on the systemic analysis assayed on standard, the vDHS-TD-LTP-MS system was applied to biological samples. In this context, the system was first tested for *in vitro* analyzes in positive and negative mode on cell lines. These VOCs analyses could indicate discriminant molecular and tumorigenic features of a tumor cell line. For this purpose, NCH82 (glioblastoma), BV2 (microglia), CHM3 (microglia), MV2 (microglia), DITNC1 (neuronal), MCF-7 (BC), SKBR-3 (BC) and MDA (BC) cell llines were subjected to vDHS-TD-LTP-MS for VOCs analysis.

For all experiment TX TA disc was used as adsorbent membrane, vDHS as sampling method and TD-LTP-MS as the analytical system in line with a QTOF premier. All collected LTP-MS data were processed using the Model Builder software (Waters) to evaluate the statistically significant VOCs patterns differences between samples.

VOCs based cell line discrimination:

We compared the MCF7 (BC) NCH82 (glioblastoma), CHM3 (microglia), BV2 (microglia), C6 (glioma) and DITNC1 (neuronal) cell lines.This set was selected to provide a first comparison between healthy and cancer cell VOCs patterns. Here microglia and neuronal cell lines were selected to have a non- cancerous VOCs signature, and NCH82, C6 and MCF7 for cancerous VOCs signature. These three latest allow us to appreciate the system ability of discriminating cancers of different origines. Cells were then subjected to VOCs analysis using the vDHS-TD-LTP-MS system in both positive and negative ion mode.

Cell lines and cultures

All the celll lines were grown according to the supplier recommendations in order to preserve their characteristics after several passages. MCF7, NCH82 and C6 were grown in DMEM high-glucose medium (Sigma-Aldrich) supplemented with 10% fetal bovine serum (Sigma-Aldrich), 100 units/ml penicillin and 100µg/ml streptomycin (Sigma-Aldrich). CHME3, DITNC1 microglia cell lines were maintained in DMEM medium supplemented with 10 % of exosome-depleted FBS media, Hepes 10 mM, L-

glutamine 2 mM and penicillin-streptomycin 1%. All the cells were incubated under standard conditions at 37 °C in a humidified atmosphere containing 5% of CO_2. BV2 microglia cell line was cultivated in RPMI 1640 medium supplemented with 10 % of exosome-depleted FBS media, L-glutamine 2 mM and penicillin-streptomycin 1% in T75 cm2 culture flask (Sarstedt, Nümbrecht, Germany). This cell line was seeded in 75 cm^2 culture flasks, and expanded until reaching a 80%-100% confluence.

Sampling and TD-LTP-MS analysis.

After trypsinization, cells were collected and washed twice with Dulbecco's phosphate-buffered solution. 200µL of suspended cells (25,000 cells/µl) in PBS were transferred into a 2mL vial for headspace sampling. TX membrane disc was placed into the vial cap and exposed to the cell VOCs headspace. vDHs was applied with 0.5bar of aspiration for 1 hour at 37.5 °C to avoid triggering oxidative stress. Then, the VOCs adsorbed were thermally desorbed by the TD system with an adjusted temperature of 250°C and analyzed using LTP-MS coupled to the QTOF premier. The setting parameters were: sweep gas 2L/min at 250°C, distance HM 5mm for TD system and for the LTP probe: the He flow was set at 354mL/min and the power 4kV and 24.34kHz.The distance between the LTP probe and the MS inlet was 4mm. No capillary voltage was applied on the QTOF premier and the ion guide was set to 2.7. The quad settings was m/z 100, Dwell time 60, Ramp time 10. The mass range was set at m/z 50 to 500.

Data analysis:

The raw data obtained from the LTP-MS/MS analysis were processed using Model Builder software (waters) to evaluate the statistical difference between the VOCs patterns of different samples. After normalization, Principal Component Analysis (PCA) was performed. The first 30 seconds time slot of each analysis was selected to build the model. The mass range was set to 50 to 500 Da with a limit of intensity of $2.00E^2$. Ion *m/z* 217.1 was excluded since it was classified as background. One spectrum per burn was applied in order to reinforce the model accuracy and balance the low sample number The classification was cross-validated by excluding 20% of sample. The parameters were the same for poitive and negative mode.

Results in positive mode

The MS spectrum from NCH82, MCF7 and DMEM was first compared to appreciate discriminative markers prior to data analysis. Three ions were found to be BC-specific, *i.e.* m/z 233.2, m/z 239.2 and m/z 242.3 (Figure 63, A). A model was then design based on CHM3, BV2, NCH82, MCF7 data. After processing, all cell lines were discriminated by their VOCs with an explanation up to 90% with the three first components (Figure 63, B, C). Concerning the two microglia cell lines, similar VOCs fingerprint were found. Indeed, the two microglia samples are positioned within the same area, despite coming from different species (mice, human). VOCs microglia were discriminated from other groups by the m/z *239.2*. The specific VOCs of NCH82 were m/z 114.1, m/z 126.1, and the specific VOCs of MCF7 were m/z 115.2, m/z 242.3, m/z 233.3. This last ion could be the -1-(2.6.6-trimethylcyclohex-2-ylazulene)-1-carbonitrile, molecule already reported in BC cell line analysis[145]. Thereby, the designed model enables the discrimination of cell lines from different pathologies, and furthermore, cell lines from similar pathologies but from different species.

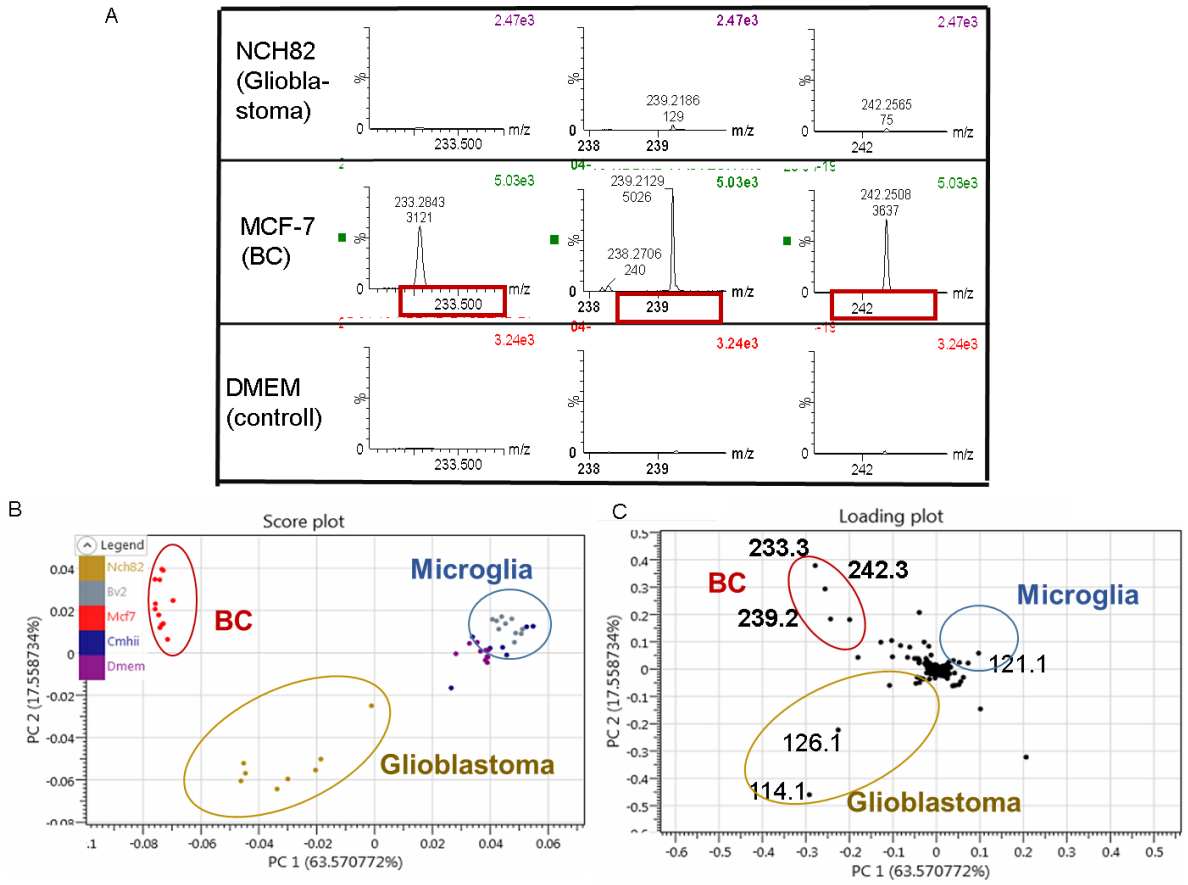

Figure 63: VOC s cell line discrimination in positive mode. A. Acquired spectra from NCH82, MCF-A and DMEM. %. The model was validated by cross validation excluding 20% of class, the classification rate is 93.92 %. B. Score plot of the two first component. C.Loading plot of the two first component. It highlights ion discriminative groups such as 233.3 and 242.3 for BC and 114.1 for glioblastoma cells.

Results in negative mode

To appreciate the versatility of LTP ionisation, VOC model based on negative ion mode acquisition was designed for the discrimination between BC, glioma and neuronal cell lines. The same method as described above was applied (i.e. sampling, analytical method). The spectra comparison of C6, MCF7 and DMEM feature some discriminative ions including m/z 92.8, m/z 205.2 and m/z 255.1(Figure 64, A). A model was determined based on MCF7, C6 and DITNC1 triplicate data. For BC, discriminant ions found were m/z 205.2; m/z 238.1 and m/z 249.9 whereas glioma was essentially discriminated by the m/z 92.8. Neuronal cell lines were discriminated by the ion m/z 255.1. This discrimination is well represented by the score plot based on the two first PCs in Figure 64, C. This model enables the VOCs-based discrimination of these cell lines in negative mode, with an explanation of up to 89% and 98% with two and three-components, respectively.

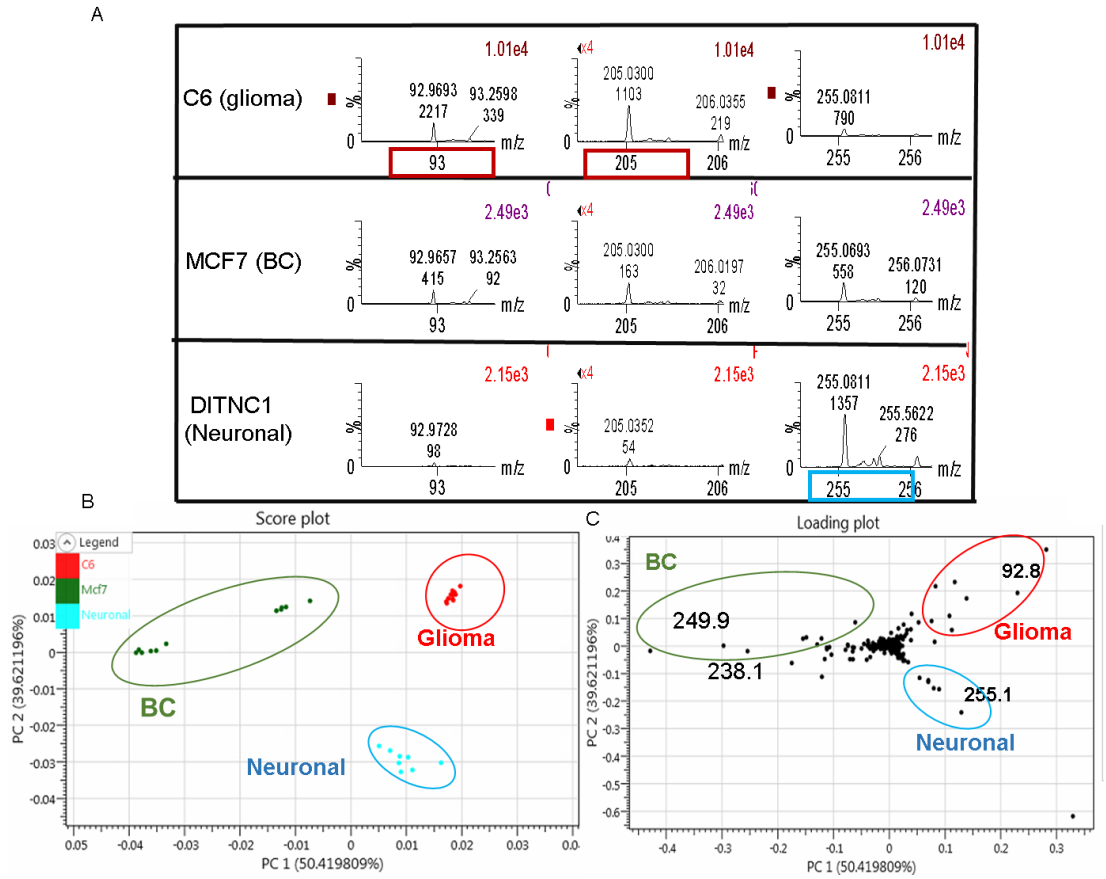

Figure 64: VOCs cell line discrimination in negative mode. A. Acquired spectra from C6, MCF-7 and DITNC1. B. Score plot of the two first component loading plot of the two first component. C. The model was validated by cross validation excluding 20% of class and the two first component explained up to 90% the group variability.

By these experiment the system have shown its efficiency to descriminate cell from their emmited VOCs, highiliting a healthy and deases VOCs fingerprint. In addition the vDHS-TD-LTP-MS enable the discrimination of cell line of different pathology as glioma and breast cancer by their VOCs. In order to appreciate the sentivity of the system and its efficacity in discrimination, cell lines from same pathology with different subtype of BC was investigated.

VOC based BC cell lines discrimination:

VOCs-based cell lines discrimination studies have already been reported using BC cell lines. In line with these experiments, three BC cell lines (MCF7, MDA, and SKBR3) were assayed in order to appreciate the ability of the system to discriminate cell lines from the same pathology with different subcellular types (Table 6). Indeed, these cell

lines present different receptors and mutation profiles, thus the detection of VOC content variations is highly expected. VOC differences between these cell lines were already reported[145,142]. The main chemical groups described for MCF7 cells were alkanes, ketones and alcohols. MDA cells are mainly represented by alcohols.

Table 6: Recapitulative table of cell line characteristics.

Cell line	Estrogen receptor	Progesterone receptor	HER2	Cancer subtype
MCF-7	+	+	-	Luminal A
SKBR3	-	+	+	HER2 +
MDA-MD231	-	-	-	Triple negative

Cell lines and cultures

The MCF7 and MDA cell lines were maintained according to the supplier recommendations in order to preserve their characteristics after several passages. They were grown in DMEM high-glucose medium (Sigma-Aldrich) supplemented with 10% fetal bovine serum (Sigma-Aldrich), 100 units/ml penicillin and 100µg/ml streptomycin (Sigma-Aldrich). SKBR3 was grown in Mcoy medium (Sigma-Aldrich) supplemented with 10% fetal bovine serum (Sigma-Aldrich), 100 units/ml penicillin and 100µg/ml streptomycin (Sigma-Aldrich). All cells were grown in T75 cm^2 culture flask (Sarstedt, Nümbrecht, Germany).

Sampling and TD-LTP-MS analysis

The cells were prepared as explained above and at similar sample concentrations. vDHs was applied with 0.5bar of aspiration for 1 hour at 37.5 °C to avoid oxidative stress. Then, the adsorbed VOCs were analysed by TD-LTP-MS using the same parameters as described above.

Data analysis:

The raw data obtained from the TD-LTP-MS were processed by Model Builder software. PCA and Linear component analysis (LDA) were done onthe first 30 seconds of each analysis. The mass range was set to 50 to 300 Da with a limit of intensity of $2.00E^2$. The ions m/z 217 and 261 and m/*z* 246 were considered as contaminants or background. One spectrum per sample was applied.

Results

The following acquisition of the MS spectra in positive mode demonstrates the specific molecular signature of cellular subtype (Figure 65), as shown by the ion measured at m/z 158.1.

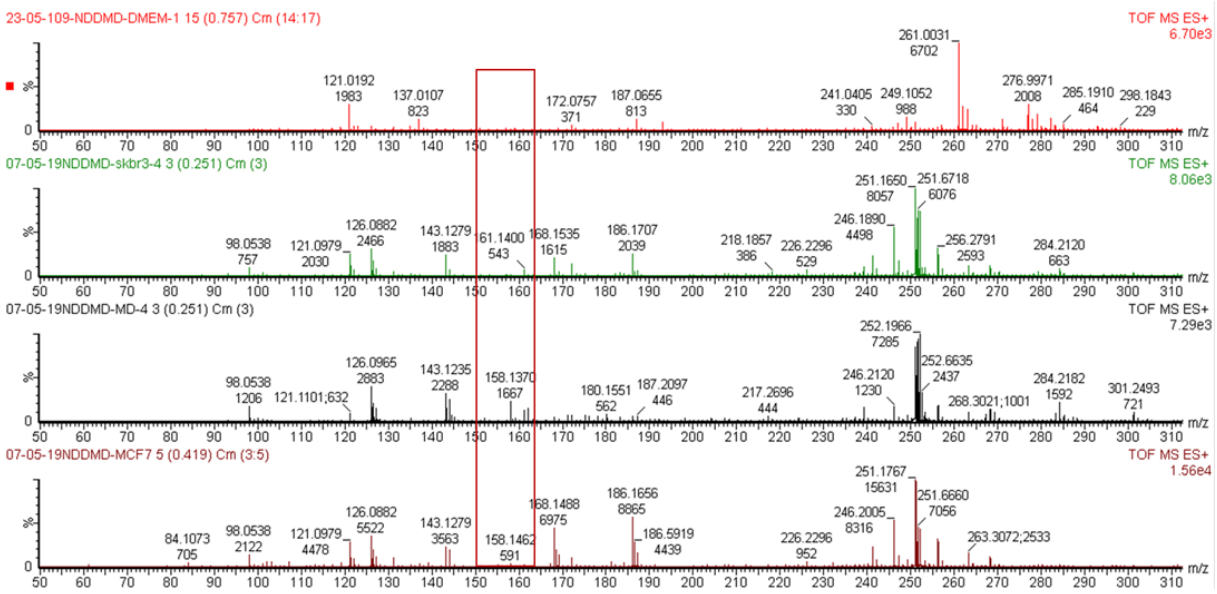

Figure 65: Spectra of VOCs cell line (MCF7, MDA, and SKBR3) collected from vDHS-TD-LTP-MS.

The results of the PCA-LDA generated from spectra acquired from 18 incubated TX membrane are summarized in Figure 66. The confusion matrix presents a good attribution group (Figure 66, A), with classification rate of 77% and 82 %, with and without outliers, respectively. Nonetheless, three MDA data were misclassified in SKBR3 samples group. Despite this discrepancy, the two and three first principal components (PCs) explained 68% and 82 % of the variance for the positive mode acquisition (Figure 66, B). Good separation was observed between the three groups, and discriminant ions (Figure 66, C) were highlighted, such as the m/z 158.1; m/z 126.1, m/z 161.1 for MDA, the m/z 175.1 and m/z 143.15 for SKBR-3. For MCF-7, the specific ions are the m/z 186.5; m/z 168.1 and m/z 187.1. Finally, LDA analysis was also designed for an optimal appreciation of BC cell line discrimination (Figure 66, D).

A

Confusion matrix:

	mcf7	mda	skbr3	Outlier	Total
mcf7	5	0	0	1	6
mda	0	3	3	0	6
skbr3	0	0	6	0	6
Total	5	3	9	1	18

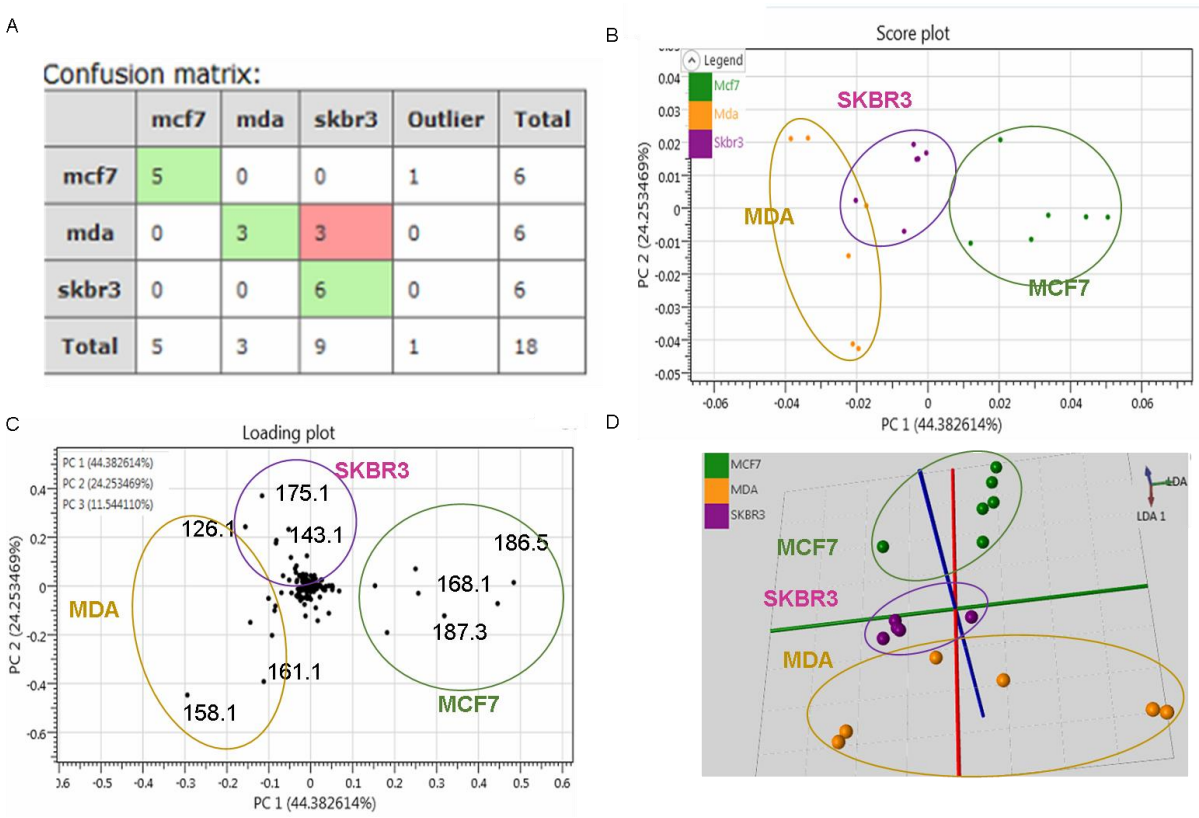

Figure 66: PCA-LDA model discrimination of three BC cell line (MCF7, SKBR3 and MDA). A. Confusion matrix of BC cell line (n=18). The model was cross validated excluding 20% of class, 77% specificity with outlier. B. Score plot of the two first component. C. Loading plot of the two first component. D. Linear Discriminant Analysis representation.

The misclassification of MDA from the matrix confusion could be explained by a molecular profile resembling to SKBR3. MDA and SKBR3 are both receptor-negative, with a different presence in HER2 presence. Their differences is reflected by ions m/z 175.1 and m/z 143.15, which could be assigned as the2-nanonone. This ketone was already reported as a BC biomarker as it is significantly increased in a cancers. The variance group of MDA-SKBR3 and MCF7 is explained by molecular subtype differences such as their receptor profiles (MCF7: luminal A; MDA: triple-negative).

Chapter II: SNOOP-I project based on volunteer subjects

All the development carried out during this thesis aimed at setting up a system for non-invasive, rapid, costless and quasi-real-time diagnosis. Since we are willing to analyse VOCs from membrane disc, all biofluid sample could be investigated as VOCs sources. In this context, tears and saliva samples were investigated by direct sampling without pre-concentration, while skin/sweat was collected by direct sampling with pre-concentration. Finally urine analysis was based on headspace sampling pre-concentrated method. The analysis of different biofluids of the same patient should overcome the heterogeneous presence of VOCs across samples, and lead to an improved detection of VOCs biomarkers in comparison to an analysis of a single sample type. Above all, a combination of VOCs data should provide a multimodal and sensitive VOCs fingerprint discrimination, thus should further increase the specificity and sensitivity of diagnosis. All the BC discrimination models were based on 5 volunteer patients (Table 7).

Table 7: Recapitulative table of volunteer patients

N°Pt	Prelevement date	Cancer stage	Subtype	Age	Ethnie	Initial diagnostic date of BC	Breast cancer side	Stage of deases	Treatment
287845	10/09/2019	metastatic	RH+ et HER2 negatif	49	caucasian	01/04/2017	right breast - os	undectable dease-remission	hormonotherapy by Arimidex
300586	10/09/2019	precoce	RH+ et HER2 negatif	53	caucasian	15/01/2019	leflt breast	detectable	chimiotherapy by carboplatine gemzar
224670	10/09/2019	None		26	caucasian				
359641	10/09/2019	None		25	caucasian				
235486	10/09/2019	None		27	caucasian				

BC diagnosis based on emanated VOCs from skin.

The concept of the incubated membrane incubated membrane on breast/mammary of cancerous patients for BC diagnosis was developed to offer a new diagnostic tool easy to implement, painless, costless and sensitive. For all experiments, TX membranes were used for skin incubation. The protocol was first tested on animal patients, as a proof-of-concept, and then transposed to human volunteer patients.

I. Animal patients

The concept was tested on animal patients from the pet clinic, in collaboration with OCR and Dr. Sebastien Olivier. The animal patients were two dogs and one cat presenting an advanced BC stage. Before the deposit of the membrane, the area (cancerous mammary) was cleaned using chlorixidine prior the fixation of the TX disc membranes (d: 14mm, t: 1.5mm) by straps and incubated in contact with the cleaned area overnight. The membranes were then stored at -80°C until analysis. All the membranes were analysed with the TD-LTP-MS system with the same parameters as previously described. In all cases, the based peak ion measured at m/z 317.28 (Figure 67) seems to be specific of the advanced BC stage.

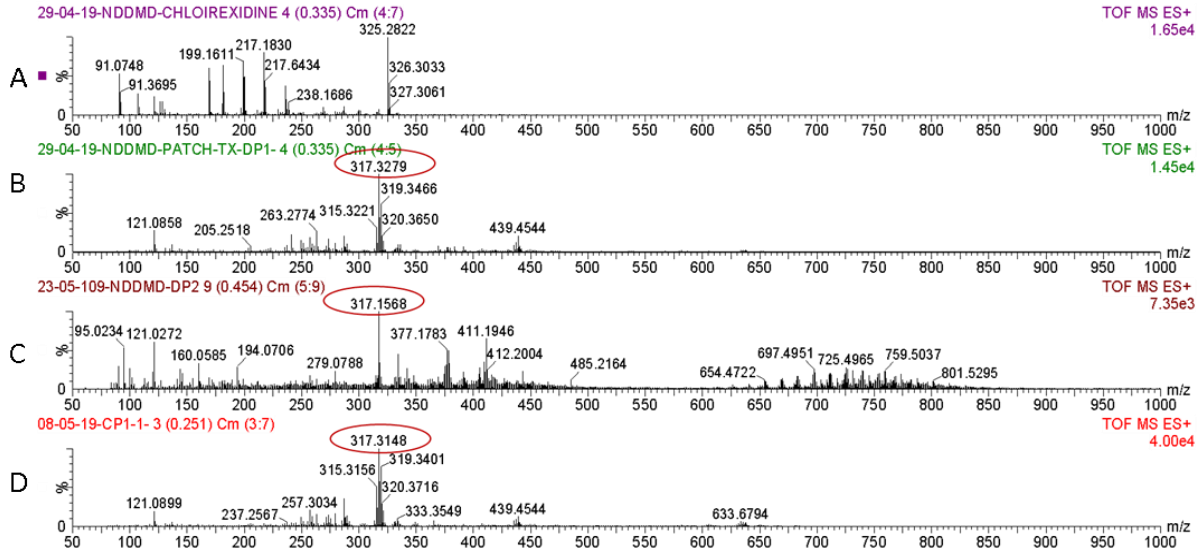

Figure 67: Collection of spectra obtained by TD-LTP-MS. A. Spectra of chlorixidine. chlorixidine was spotted onto the membrane and then analysed. B. Spectra of DP1 patch. C. Spectra of DP2 patch. D. Spectra of CP1 patch.

Further MS/MS experiment was done on the m/z 317 discriminative ion (Figure 68), but no identification was possible. This lack of identification is explained by the non-certitude of that this ion is not a fragment implying that the ion could not be identified and the used database could be incompatible with the ionization method. Furthermore if the ion is not in $[M+H]^+$ form shit of mass has to be consider.

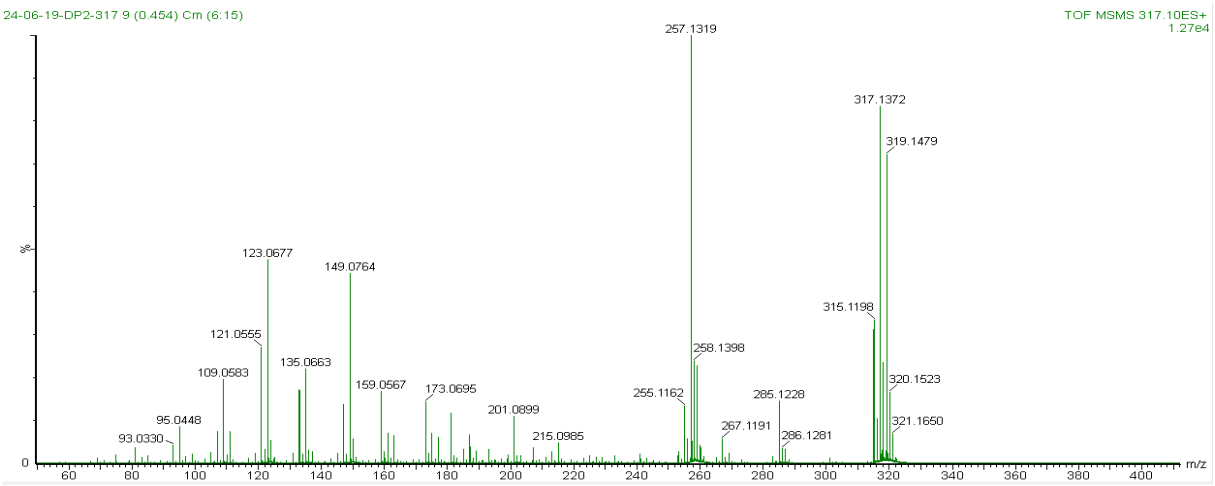

Figure 68: MS² spectra of the m/z 317.1 ion observed Figure 62.

This first application of the method showed the efficiency of the TX membrane to capture VOCs from skin/sweat and to detect ions which can be used as a BC specific signature.

II. Human patient

Based on the previous results, the developed strategy was extended to volunteer human patients included in a study managed by Dr. Nawale Hajjaji from the COL. Two sampling area, axillary fossa and nipple regions, were investigated as the profiles of human skin volatiles vary greatly with the sampling site. The axillary region is a particularly important source of diverse VOCs, which have been suggested to be useful as individual markers[146]. Nipple region has been selected for its proximity to the tumor region and then is the most likely to be a source of cancer-specific VOC fingerprints.

So far, one collect was obtained from BC human patient with cancer on the right side. TX membranes were left for incubation at two different regions, the nipple (left, L and right, R) and on the axillary fossa (left and right) for 9 hours. After incubation, the membranes were stored at -80°C until their analysis by the TD-LTP-MS system. The comparative data according the side (L or R) will allow us to validate the sensitivity of the system to detect BC tumor side. Then the two regions will be compared in order to select the one which has the most pathological specific molecular profile. All collected LTP-MS data were processed as previously described. Models were designed for cancer side discrimination, one for the incubation at the axillary fossa and another for

the nipple. Finally, spectra from axillary and nipple regions were compared to select the optimal sampling area for further experiments.

Axillary fossa

Data acquired form axillary fossa were processed by OMB builder model for PCA (Figure 69). 13 sample data were used to create the model and, after cross-validation, none of the sampled were misclassified (Figure 69, A). The loading plot from the PC 1 (Figure 69,B) highlights the discriminant ions between L and R with a variation explanation of 54%, and further separation was represented on the score plot of the two first PCs (88%) (Figure 69, C). The most discriminating VOCs were detected at m/z 87.4, m/z 105.4, m/z 204.3, m/z 258.28 and m/z 284.8. Even if the method enables the discrimination between R and L axillary fossa (Figure 69, C). The VOCs were probably not due to the pathology, considering that different metabolomics profiles were already described between L and R axillary sampling, and the sampling area was not close enough to the tumor environment to reflect the environment. For this reason, other membranes were incubated on the skin of cancerous masse, to get more representative samples.

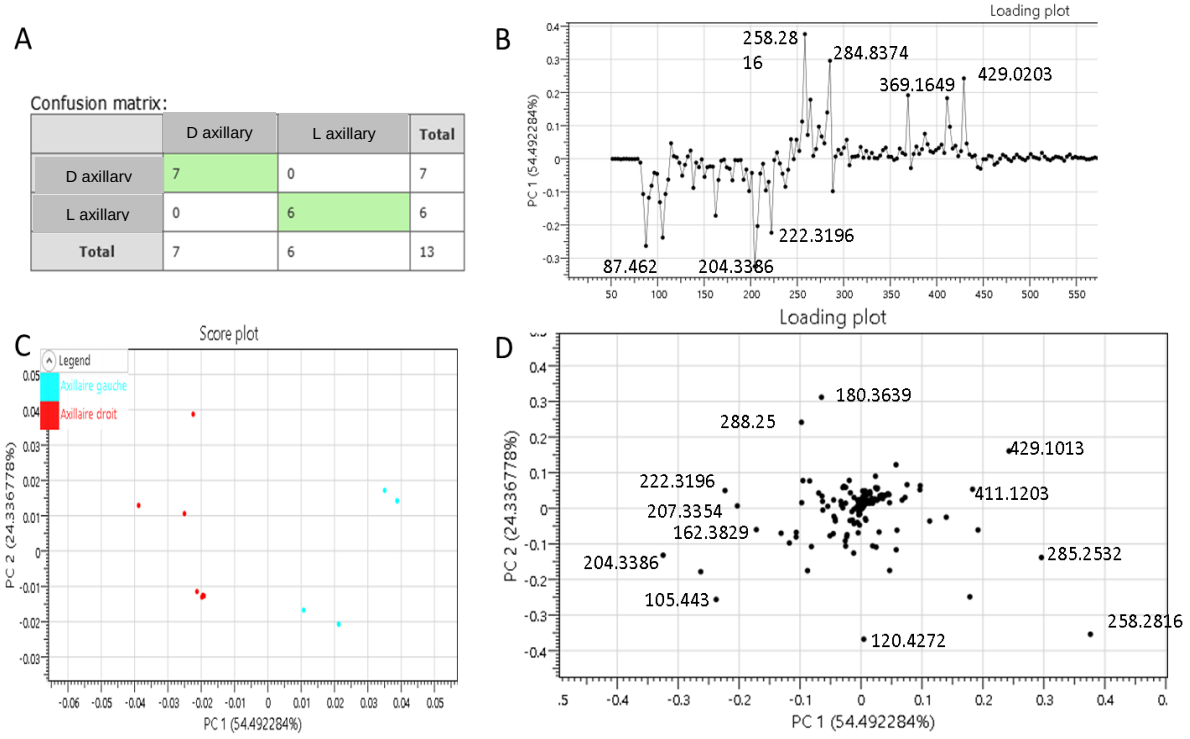

Figure 69: Model Of membrane incubated on axillary fossa of BC human patient. A. Confusion matrix of VOCs axillary fossa n=13 (7 right, 6 left) was taken to build the model. The model was validated by cross validation excluding 20% of class. B. Loading plot of first component of PCA analysis. C. Score plot of the two first component. D. Loading plot of the two first component.

Nipple

Without any data processing, the spectra clearly show differences and similarities between L and R as m/z 185.1, m/z 195.1 and m/z 93.0840, m/z 105.0, m/z 137.1 respectively (Figure 70).

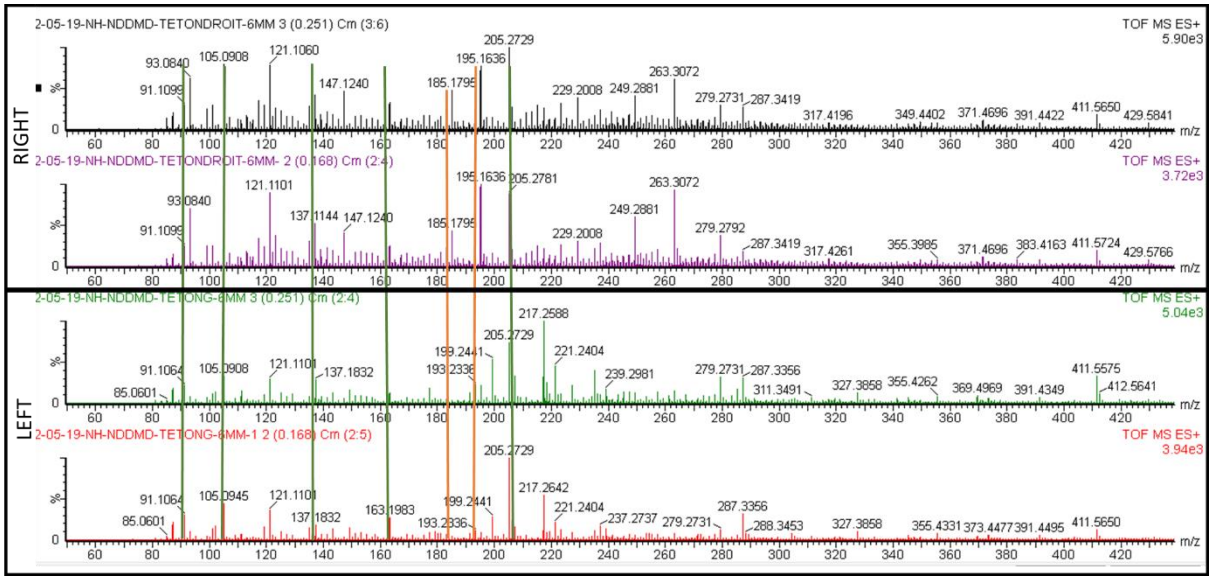

Figure 70: Spectra of membrane incubated on nipple BC patient during 9 hour. The green line highlight the common ions and the orange line highlight the discriminant VOCs.

Further identification attempted by MS^2 were assayed on ions m/z 195.1 and 205.2, (Figure 71).

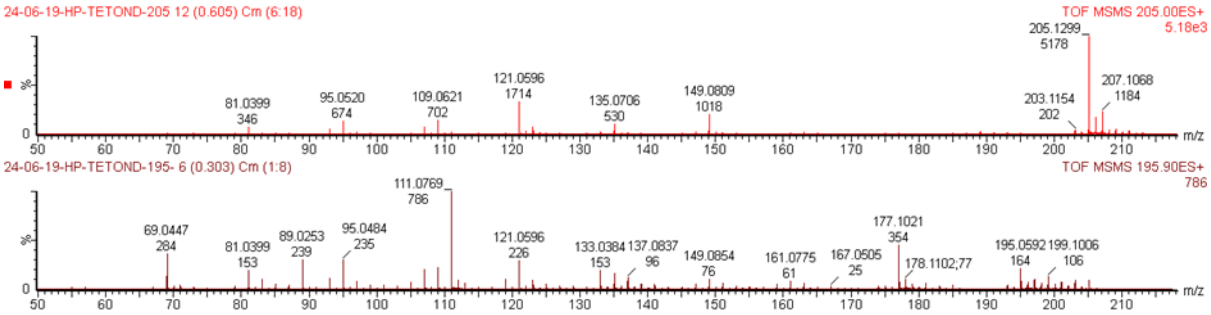

Figure 71: MS^2 spectra of parent ion m/z 205.2 and 195.1, ion observed in Figure 65.

A PCA model was also built based on the 22 samples data (Figure 72). Same PCA model parameters were kept. The PCA classification was cross-validated and confusion matrix verified (Figure 72, A). This model has discriminated BC breast side (cancer was present on the right side). The loading plot of PC1 highlighted discriminant ion of the breast side. The top part of loading plot represents the cancerous side, while the lower one the healthy side, discriminated mostly by ions measured at m/z 185.17

and m/z 195.16 (Figure 72, B, D). After PCA and establishment of a discrimination model (Figure 72, C, E), the used system enabled accurate breast tumor detection.

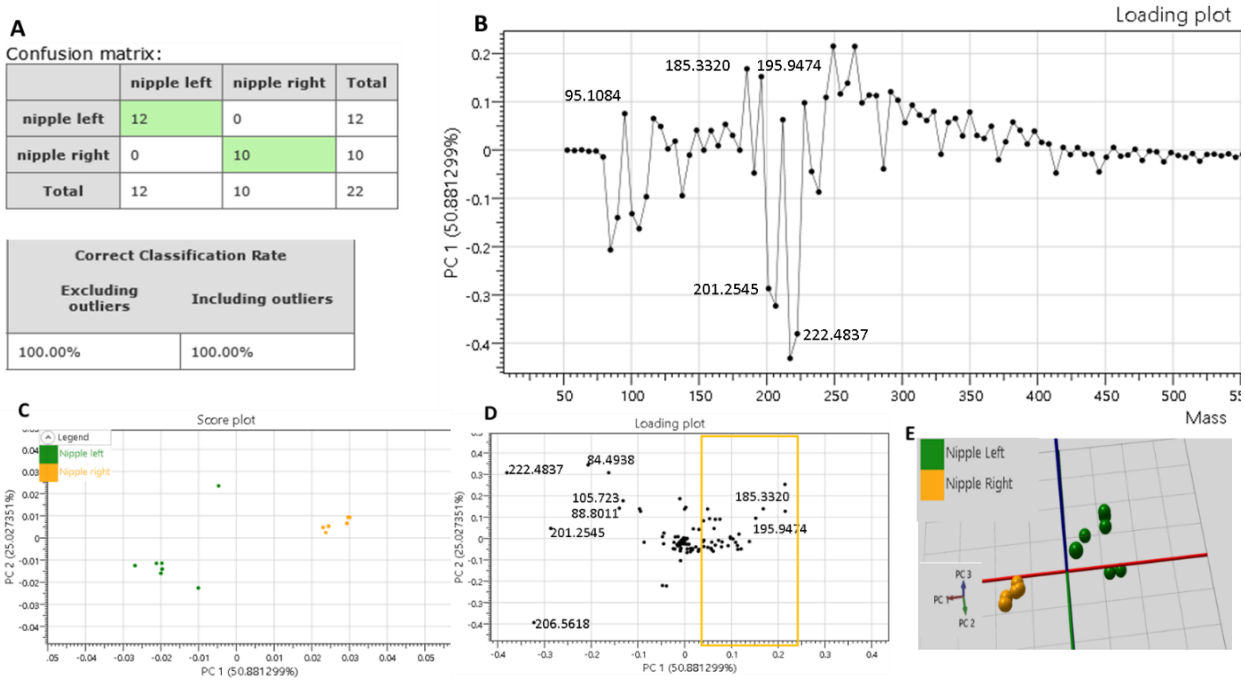

Figure 72: Model of membranes incubated on nipple of BC human patients. A. Confusion matrix of VOCs axillary fossa n=22 (10 right, 12 left) was taken to build the model. The model cross validated excluding 20% of class. B. Loading plot of first component of PCA analysis. B. Loading plot of first component of PCA analysis. C. Loading plot of the two first component. D. Score plot of the two first components. The yellow square highlight the specific BC VOCs. E. 3D representation of PCA analysis. The model explain the discrimination group at 88%.

Sampling area:

Data obtained from axillary fossa and nipples are compared to evaluate the more appropriate region to be investigated. Similarities were found between nipple and axillary fossa spectra, such as m/z 105.0, m/z 163.1, m/z 205.2 and m/z 287.3. However, previously discriminating VOCs from one model were not found in the other. For instance VOCs, measured at m/z 185.1 and m/z 195.1 in the nipple model were only present in this context (Figure 73).

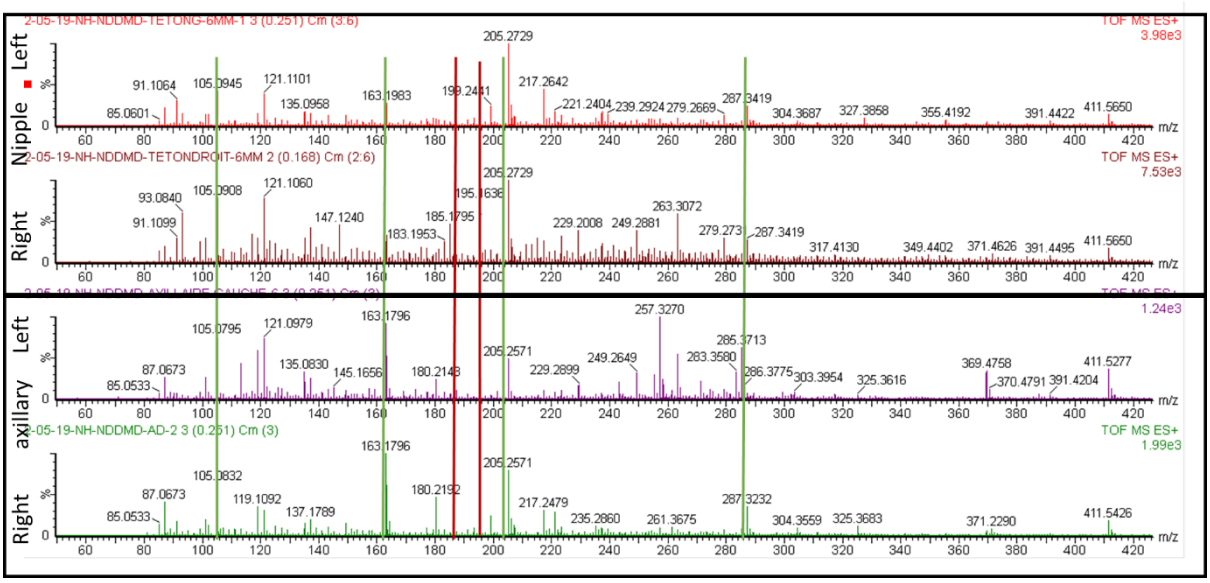

Figure 73: Comparison of sampling area. The red line highlight the different ion and the green the similar detected ion according to the sampling area.

Regarding the BC diagnosis from the membrane incubated onto the skin of BC patients, the concept was validated from animal to human patients. We have demonstrated that after 9 hours of TX skin incubation, BC specific VOCs can already be detected. Concerning the incubation area, nipple was chosen in order to have an incubation as close as possible from the tumor site.

Skin/sweat as source for BC diagnosis

After validating the patch design and sampling area, the SNOOP-I protocol was further assayed on 5 volunteer human patients; two harbouring BC and three non-cancerous (Table 7).

Sampling and LTP-MS analysis

The designed TX disc membrane patch was put on the left breast, on the left side for the non-cancerous patients, and on the tumor breast side for the cancerous patient. The patch consists of a Melipore band-aid with three TX membranes (d: 14mm, e: 1.5mm). The patch was kept overnight (>9 hours), collected the morning and stored in a sealed dish at -80°C to avoid any sample degradation. The three membranes were detached from the patch just before the TD-LTP-MS analysis. Same settings of TD-LTP-MS were kept (see above).

Data analysis:

Three raw data of each patient were processed by Model Builder software (waters) to evaluate the statistical difference between the sample patterns of VOCs. After normalization, PCA was performed. The first 30 seconds window of each analysis was selected to build the model. The mass range was set from 50 to 500 Da, with a limit of intensity of $2.00E^2$. One spectrum per sample was used in order to average each acquisition and decrease the intragroup variability. This intra-group variability should disappear with the increase in cohort patient numbers. The classification was cross-validated by excluding 20% of sample.

Results:

The MS spectra acquired in positive mode (healthy and cancer) are presented Figure 74, A. They provided the specific molecular group signatures, reflecting the physio pathological state. Ions revealing this discrimination included the m/z 101.5, m/z 119.05 for cancer and the m/z 309.07 for a healthy patient. Results of multivariate PCA analysis generated from acquired spectra of the 5 patches were summarized in Figure 74, B, C, D,E. The discriminant ions highlighted by the score plot (Figure 74, B) were in accordance with those selected from the MS spectra. A good separation between groups was observed based on score and loading plot of the two first PCs (72%) (Figure 74, C, D). Among the discriminative ion groups, m/z 101.0, m/z 119.0, m/z 237.0 and m/z 345.1 were cancer group-specific, and m/z 309.0 healthy group-specific. The m/z 101.05 could be assigned to cyclohexanol[147] molecule already reported as BC-specific VOC. Huang and collaborators suggested that cyclohexanol was generated by endogenous hydrocarbon metabolism. Hydrocarbons can be metabolized to aldehydes or ketones via alcohol dehydrogenase (ADH) and cytochrome P450 activity.

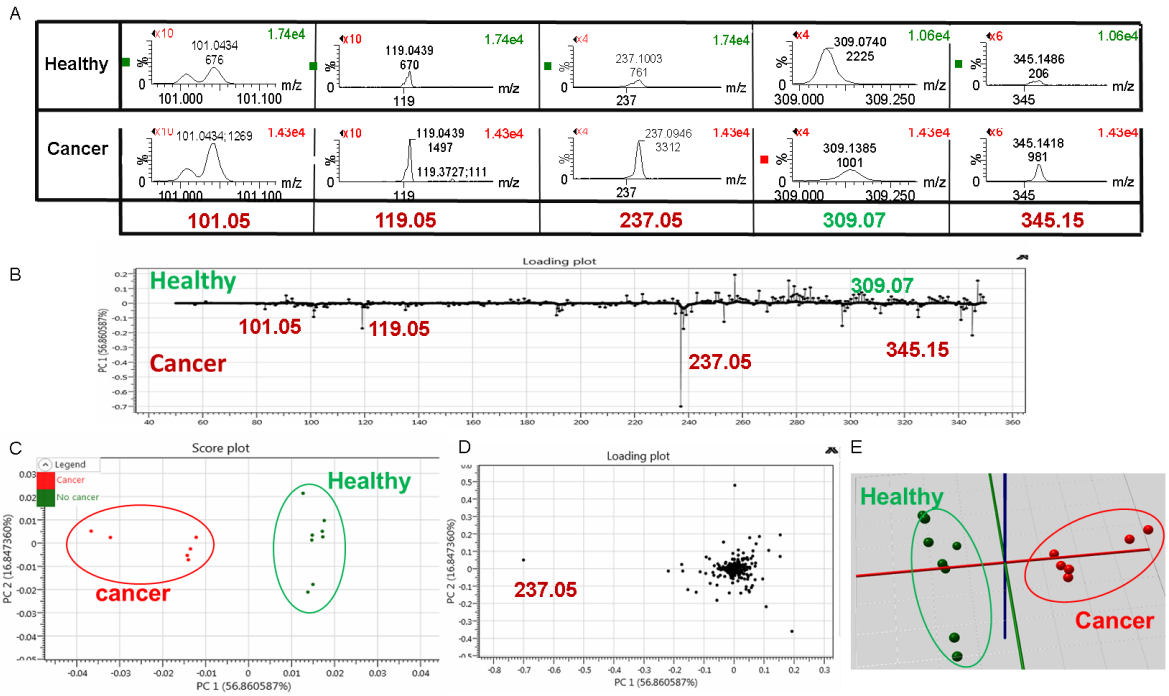

Figure 74: Data obtained from Patch analysis by TD-LTP-MS. A. Spectra of discriminant ion group between healthy and cancer. B. Loading plot of first component of the built model. C. Score plot of the two first component. D. Loading plot representation of the two first component. 90%of the variability is explained by this model E. 3D representation of discrimination group model. With the three first component the model is explained up to 95%.

Excellent cross-validation results were obtained using the 20% outpatient method with 100% correct classification rates, with and without outliers, in the positive mode. PCA classification model of cancer and healthy patient shown in Figure 74, enables the fingerprint discrimination of VOCs adsorbed onto a membrane from skin /sweat sample.

Tears as source for BC diagnosis

Tear is a body fluid exposed to both internal and external environment, containing a high amount of molecular information, which could be useful for diagnosis, prognosis and treatment of ocular surface diseases. To date, no VOCs analysis from tears have been reported. Nonetheless, few have been conducted through proteomics and lipidomics analysis[65]. In summary, tears are considered as another promising biofluid for diseases associated biomarkers discovery. Stimulated or un-stimulated sampling changes the metabolomic profil and eye side collection does not impact the tear pattern[148].

Sampling and LTP-MS analysis:

A swab purchased from Fl medical was used to collect non-stimulated tears (no electric choc) sample (3 µL) from the lower meniscus of left eye. This sampling is quick, easy to and non-invasive. The tear sample was directly stored at -80°c to avoid any sample degradation. Collected swab were then cut to keep only the cotton part (adsorbent part). The swab was placed within the membrane holder for thermal desorption, and the desorbed VOCs were analysed by LTP-MS. The TD system setting was 220°C, with a N_2 flow of 2L/min. Same settings were kept for the LTP-MS coupling.

Data analysis:

Raw data of each patient were processed by Model Builder software (waters) to evaluate the statistical difference between the patterns of VOCs related to sample. After normalization, PCA was performed. The first 30 seconds of each analysis was selected to build the model. The mass range was set from 50 to 500 Da, with a limit of intensity of $2.00E^2$. One spectrum per scan was used in order to decrease the intragroup variability. This intra-group variability should disappear with the increase in cohort patient number. The classification was cross-validated by excluding 20% of sample.

Results

The MS acquisition of tears and from swab in positive mode clearly dshows the specific molecular signatures of the physiological *versus* pathological states (Figure 75, A). Ions revealing this discrimination included the m/z 287.1 and m/z 304 for cancer, and 285.1 for a healthy subject. Multivariate PCA results generated from spectra acquired of the 5 swabs are summarized in Figure 75, B, C, D, E. The first and two first PC explain 65%, 77% of the variance for the positive mode acquisition (Figure 75, C). Among the discriminating ions m/z 256.1, m/z 287.1 and m/z 304.1 are cancer group-specific and m/z 285.1 healthy group-specific. The explanation of variance up to 86% leading to a good group separation and easy appreciation, as represented in the Figure 75, B for 2D representation or in Figure 75, C for 3D representation.

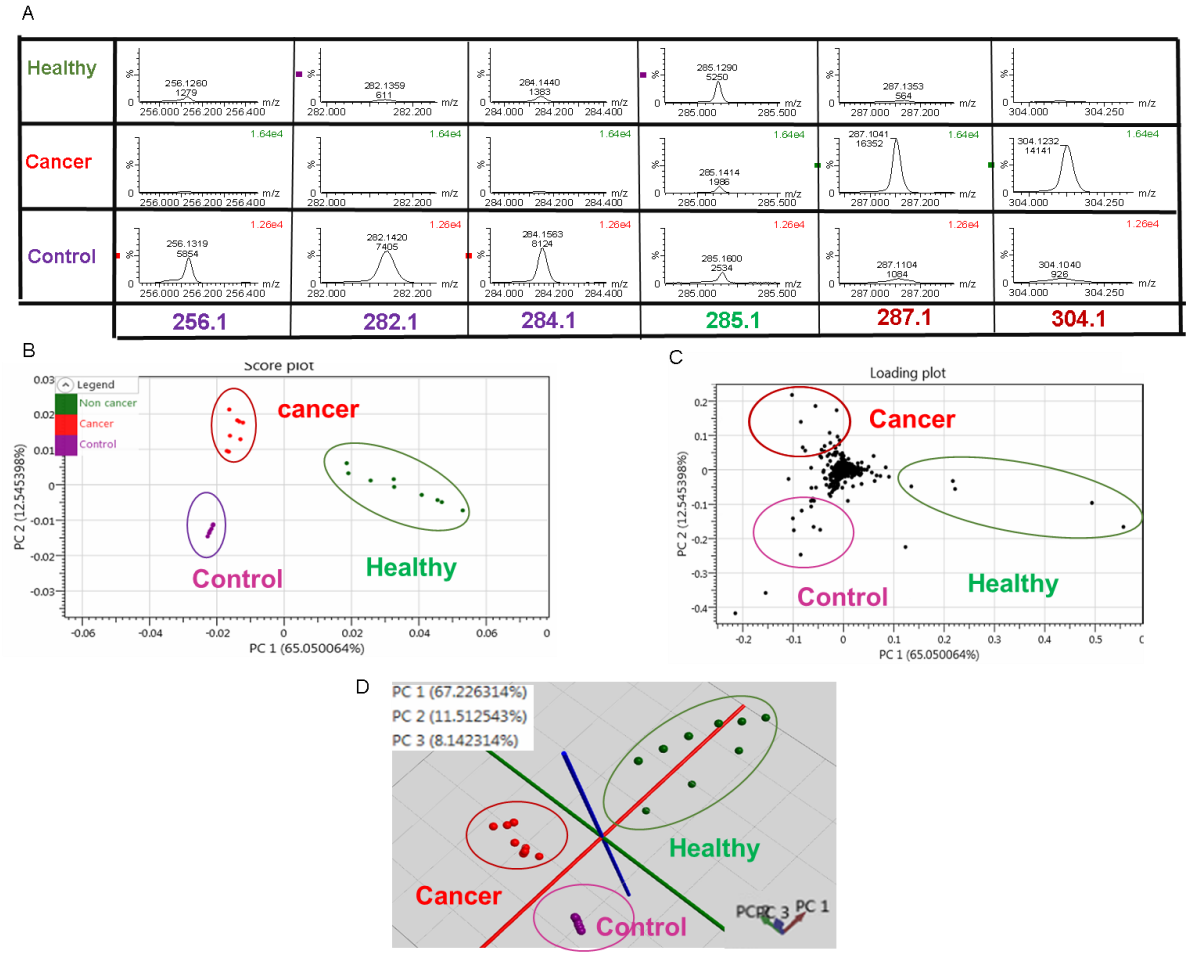

Figure 75: Data obtained from tears analysis by TD-LTP-MS. A. Spectra of discriminant ion group between healthy, cancer and control (clean swab).B. PCA score plot representation by the two first component. 77%of the variability is explained by this model. C. PCA Loading plot of the two first component. D. PCa 3D representation of discrimination group model. With the three first component the model is explained up to 86%.

The PCA classification model based on tears analysis enables the fingerprint discrimination of VOCs adsorbed onto a membrane for BC diagnosis.

Urine as source for BC diagnosis

Urine biofluid is also a major non-invasive, unlimited source of VOCs, and consequently a promising source of cancer biomarker. Recent urine-based studies are reported as a simplified model for comparing localized and metastatic breast cancer, in which the same tumor cells are injected into different sites (mammary pad versus iliac artery)[149]. The groups were able to discriminate cancer *versus* healthy and even metastatic *versus* local cancers for BC). Ketones, sulfur compounds and volatile

phenols were the chemical functions with the highest contribution for the metabolomics volatile profiles of the BC group.

Sampling and LTP-MS analysis

Early morning first urine samples from each subject were collected in sterile 50 mL falcon tubes, after maintaining the subjects in overnight fasting conditions. Samples were labelled, centrifuged at 5,000 g for 10 min at 4 °C, filtered through 0.45 µm filters and stored at −80 °C until further analysis. 200 µl of urine sample were transferred into 2 mL HS glass vial (Thermo Fisher, USA). The VOCs from the urine samples obtained from healthy controls and patients were extracted using the vDHS-sampling.

The sample vial was then incubated at 60 °C with continuous stirring at 800 rpm and continuous aspiration at 0.5bar. The TX membrane disc was exposed to the HS of the vial for 45 minutes in order to allow sufficient VOCs adsorption. After incubation, the TX was inserted into the holder, thermally desorbed at 250 °C and analysed by LTP-MS.

Data analysis:

Four raw data of each patient were processed by Model Builder software (waters) to evaluate the statistical differences between the VOCs patterns related to samples. After normalization, PCA-LDA was performed. The first 30 seconds of each analysis was taken to build the model. The mass range was set from 50 to 500 Da, with a limit of intensity of $2.00E^2$. One spectrum per sample was used in order to average each acquisition and decrease the intragroup variability. This intra-group variability should disappear with the increase in cohort patient numbers.

Results:

Results of the multivariate analysis using PCA from the generated spectra acquired from the sixteen TX membrane are summarized in Figure 76. The first PC explain 73% of the variance for the positive mode acquisition. Good separation is observed among the scores for the healthy and cancer groups, as shown in score and loading plot defined by the first two PCs (93%). PCA classification model of cancer and healthy patient (shown in Figure 76, B, C) enables the fingerprint discrimination of urine adsorbed VOCs. Among the discriminative ion groups, m/z 114.37, m/z 146.6 and m/z 227.1 are cancer group-specific and m/z 121.37 healthy group-specific.

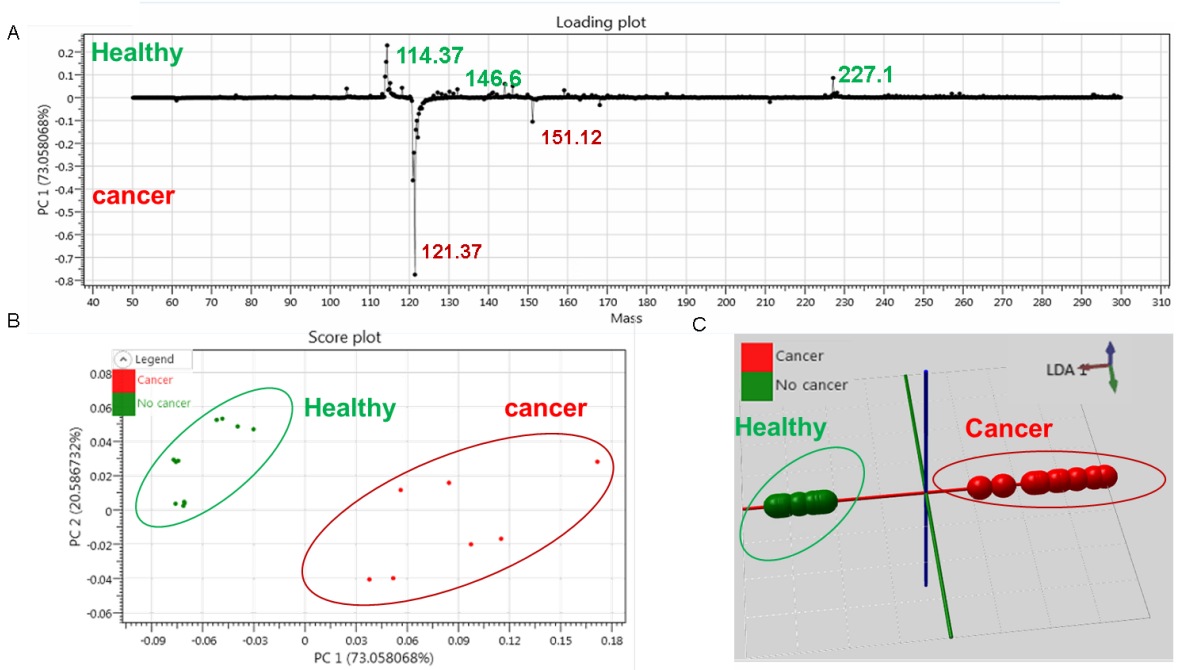

Figure 76: PCA-LDA urine model obtained by TD-LTP-MS. A. Score plot representation of the two first component. 93%of the variability is explained by this model. B. Loading plot of the two first component. C. 3D representation of discrimination LDA group model. With the three first component the model is explained up to 98%.

The features extracted using PCA were subjected to supervised analysis using linear discriminant analysis (LDA). Better discrimination can be observed from LDA analysis with groups defined prior to PCA. (Figure 76, C).

Saliva source of BC fingerprint diagnosis

Salivary transcriptomic, proteomic[150] and lipidomics studies have already established the basic groundwork and proven feasibility of saliva-based cancer diagnostics and ascertain the basis for continued biomarker research. It was established that saliva is particularly useful for diagnosis of cancer such as neck and head cancer[52,63]. The sampling consist of the direct swab of the mouth mucus. Unfortunately, some sample was contaminated by liptstick, showing the paramount importance of sampling method and standardization. The sample contamination have a direct impact on the MS spectra observable by over intensity of the lipstick compound as polymer making hard any comparison with the other acquired data even after reduction of this background. In this context, another type of sampling method was proposed for whole saliva collection. The sampling consists of the collected of an average of 3mL of unstimulated whole saliva in 10mL glass tube. The patient has to be *a jeun*, and before collection the mouth

is rinse with water. After collection, the samples were immediately stored at −80 °C. Nonetheless, no other experiment were assayed.

The developed TD- LTP-MS analytical system was implemented for VOC analysis of biological sample. By vDHS- TD-LTP-MS, cell lines from different and same pathologies were differentiated by their VOCs profiles. Designed PCA model allowed the VOCs-based differentiation of physiological states between healthy and disease cell lines. The cell fingerprint investigation was followed by analysis of three BC cell lines with different cellular subtypes. The PCA model highlights some VOCs apparently in relation with progesterone and oestrogen receptors status, such as the already reported 2- nonanone BC biomarker. Considering the suitability of the system for membrane VOCs analysis, different biofluids such as tears, skin/sweat, urine and saliva were collected from a volunteer patient cohort. Direct sampling was proceeded for tears and saliva, while skin/sweat and urine were pre-concentrated. Of note, sample collection (*e.g.* sampling, storage) remains an important source of variability. Overall, PCA/LDA model designed by tears, skin/sweat and urine data analysis enables BC fingerprint discrimination.

Conclusion and perspectives

The aim of this thesis was the development of a low temperature plasma mass spectrometry system (LTP-MS) for the analysis of volatile organic compound onto a membrane to respond to the need of a rapid, sensitive and non-invasive diagnosis. In opposition with breath sampler and sensor, mass spectrometry techniques respond to the demand of VOCs mixture detection and identification from all human biofluids if it's coupled to the right sampling method, analytical system and data processing.

In this context, a non-thermal plasma source based on dielectric barrier discharge was developed and coupled to MS for VOC cancer pattern discrimination for diagnosis purpose. The home-made LTP probe enables the simultaneous desorption and ionization of volatile small molecules from liquid, solid and gaseous sample. The combination of the probe versatility and the high sensitivity provided by MS is in perfect adequation for a rapid, affordable, non-invasive quasi and real-time system diagnosis. To achieve this goal, analytical system and sampling methods were developed. The sampling development has led to the establishment of a vacuum based dynamic headspace sampling method (vDHS) for an optimal adsorption onto a Tenax TA disc membrane. Improvement of analytical system has been made by the addition of another desorption process. Indeed the binding strength between the sorbent and the targeted molecule is too strong to be only broken by the desorption induced by the LTP. Thereby a thermal desorption (TD) unit has been implemented to the developed system. The TD-LTP system consists of a heating horse to heat the gas which induce the thermal desorption. Two control valves to manage the gas pressure, a membrane holder to focus the exit holder to the MS inlet and a LTP probe to ionise the desorbed VOCs. In order to enhance the robustness of the system, a 3D printed source holder was designed to permit the LTP probe position modulation (angle, x, y and z), to support the heating system and to maintain the exit of the membrane exit holder membrane in front of the MS inlet. Analysis of standard has led to the validation of the robust, sensitive, reproducible vDHS-TD-LTP-MS system. The system enables the VOCs identification of different classes of molecules such as hydrocarbons, ketones, amines, nitriles, esters, ethers, alcohols. Polar and apolar molecule with high or low boiling points were also detected.

Further improvements are required including planned including the size reduction of the TD unit in accordance with the deposit patent FR 2005155. The deposit 3 in 1 system allows membrane conditioning, dynamic vacuum sampling and thermal desorption a perfect combination to diminish conditioning variation, handling contamination and to inssure reproducibility.

The set up offer a rapid costless and non-invasive VOCs analytical system based on adsorbent disc. Thereby the versatile system was applied on *in vitro* and *in vivo* analysis for BC diagnosis.

The vDHS-TD-LTP-MS system was first applied to discriminate different cell lines based on multivariate statistical analysis. All the data were processed by model builder software (waters) which enables principal component analysis (PCA) and linear discriminant analysis (LDA). Models were designed in negative and positive ion mode and demonstrated the efficiency of the system by highlighting VOCs pattern of healthy cells (microglia and neuronal) and cancerous cells (gliomal, breast cancer). Further investigation were performed on BC cell lines analysis (MCF7, SKBR3 and MDA) for subtype cell differentiation. The acquired models has led to the grouping of SKBR3 and MDA (ER-, PR-) and the clear separation of MCF7 (ER+, PR+). Discrimination of MCF7 and SKBR3 were also appreciated by the detection of the 2-nonanone which has already been described as a putative BC biomarker. These analyses gave a glimpse of specific metabolic processes and metabolic pathways of BC tumor cells. Although, the metabolic pathways of compounds remains unclear. It is established that the accumulation of reactive oxygen species (ROS) can lead to the production of hydrocarbons and oxygen free radicals, leaking from the mitochondria into the cytoplasm. Also, cytochrome P450 can be upregulated by ROS in tissues and catalyses the oxidation of organic chemicals and the peroxidation of polyunsaturated fatty acids (PUFAs) resulting in the production of straight chained alkanes.

Besides fundamental analysis, the developments aimed to diagnose BC from VOCs human patients, in the context of SNOOP-I project. In this purpose tears, skin/sweat, urine and saliva samples were collected from 5 volunteer patients (cancerous=2, healthy=3). Tears and saliva were collected on sterile swab by direct sampling without concentration whereas skin/ sweat samples were pre-concentrated onto TX patch for 9 hours. Urine samples were also pre-concentrated on TX disc membrane by vacuum based dynamic headspace sampling (vDHS). All the sorbents were submitted to TD –

LTP-MS analysis at 220 or 250°C according to the adsorbent used (swab, TX). PCA/LDA models based on tears, urine, skin/sweat sample enables the discrimination groups between healthy and cancerous patients. In all models, the two first principal' components explained the variation up to 75% with a maximum at 96% for urine model. The classification was validated through the high rate specificity (>85%). Numerous discriminant ions were highlighted including the cyclohexanol, which has been reported as BC biomarker.

Even if the PCA and LDA allow cancer group discrimination; detection remains challenging. Most of the data analysis software enable identifications based on analytes separation which require a retention time which is missing in our rapid LTP-MS system. The second impediment is the acquisition of only MS spectra data, as our analysis is based on fingerprint analysis. Fragmentation data obtained by MS/MS analysis is also an asset for compound identification.

However, mass spectrometer offering high mass resolution with a minimum of 18 000 FWHM can overcome the need of separation. Unfortunately, the different used mass spectrometer including the 3D IT and the QTOF premier provide mass resolution of 6000 and 8000 FWHM in V mode respectively. Additionally, the mass accuracy in the mentioned mass spectrometer is also too weak for a direct compound identification based on the only measured mass. Moreover, in the case of ambient plasma ionization process, additional fragmentations, adducts formation, ozonolysis has to be taken into account for compound identification.

Nevertheless, the compound identification is slightly eased by the emerged databases and data analysis software. However their programming language (e.g. R, python, java) render them laborious to use. To date, metabolomics databases containing reported VOCs are now available including HMDB, phenol explorer, cancer odor database, ECMDB and mVOC.2. Among the data analysis software, Xomics, metabolomics center.ca are currently used. Also, few platform propose metabolic pathway such as SMPDB (small molecule pathway database).

The first trial of BC group discrimination performed from five volunteer patients has proven the efficiency of the system to diagnose BC based on the detection of VOCs extracted from biofluids. This validation step led to the establishment of a patient cohort for the BC diagnosis in collaboration with the Dr Nawale HAJJAJI, the Pr Nicolas PENEL and the Pr Eric LARTIGAU from the Oscar Lambret Center (COL). The

research cohort is register as follow: research code : OMERIC-1904, N° IdRCB : 2019-A02235-52. The aim of the cohort study is the appreciation of omic's profiles evolution associated with the resistance of Palbociclib (kinase inhibitor) in patients treated for metastatic breast cancer (OMERIC). In this context, tears, saliva, urine, skin/sweat and breath are collected. The inclusion criteria are woman over 18 years old with advanced BC (metastasis or unresectable disease), hormone receptors positive and HER2 negative and showing an indication for hormone therapy and CDK4 / 6 inhibitor. The excluded criterion are neoadjuvant or adjuvant treatment for localized BC and metastatic BC beyond the 4th line. Samples will be taken when patient come to the COL for treatment. Tumor tissue will be removed at the start of treatment and at progression. Biospecimens (e.g. saliva, exhaled breath, sweat, tears, urine) will be collected before the cycle 1 day 1 (C1J1), in the cycle 2 day 1 (C2J1), at the 1st reassessment (M3) and after the progression. Apart from the assessments, the therapeutic management and follow-up of the patients will be carried out according to the usual procedures of the COL.

All in all, TD-LTP-MS system all along the thesis have shown that BC diagnosis was successfully achieved based on the adsorbed VOCs analysis onto a disc membrane. Consequently, it's a rapid, affordable, sensitive, versatile, non-invasive, real and quasi-real-time analytical system for the detection of diseases related specific VOCs pattern.

The developed TD-LTP-MS was found to be an efficient analytical tool in the case of clinical research. However, the device can also be used in other field of applications including the quality control and the flavour analysis. Investigation was done on beers which were distinguished by their brewing process. It includes triple, blond, brown and IPL beers.

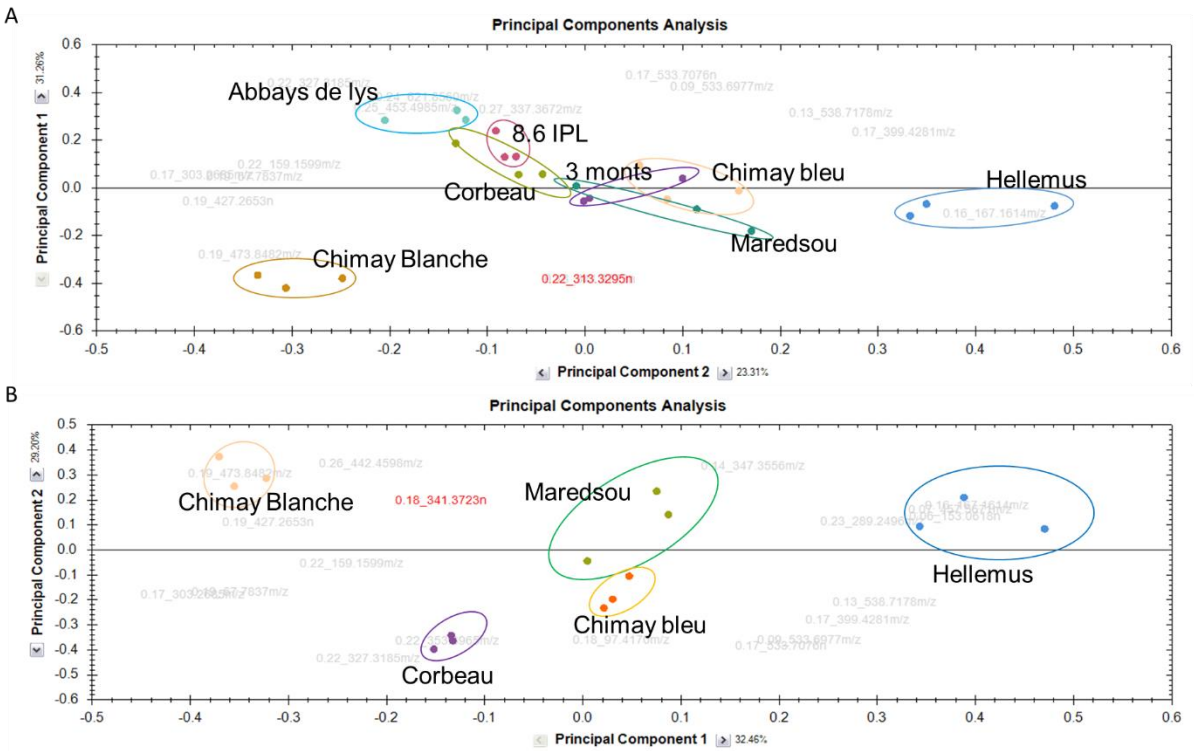

Figure 77: Analysis of beer by vDHS-TD-LTP-MS. 200µl of beer sample were incubated into 2mL glass and submit to headspace sampling based on vacuum for 40 min at 60°. A. PCA representation of all tested beer (n=8). B. PCA representation of triple beer discrimination.

After VOCs analysis by vDHS-TD-LTP of height beers (Abbays de lyse, IPL, Corbeau, 3 Monts, Chimay blanche, Chimay bleu, Maredsou and Hellemus) model discrimination enables the VOCs beer discrimination (Figure 77, A). This separation go further by the VOCs differentiation of triple fermentation beer from different and same brewer (e.g. Chimay, Corbeau and Hellemus) (Figure 77, B) showing the efficiency of the rapid discriminative TD-LTP-MS system.

Additionally, the relation between taste and color in candies were also investigated, to prove the influence of dyes on candy taste considering that all candies re made with dye. The dragibus candies were then submitted to vDHs-TD-LTP for color discrimination based on their specific VOCs (Figure 78).

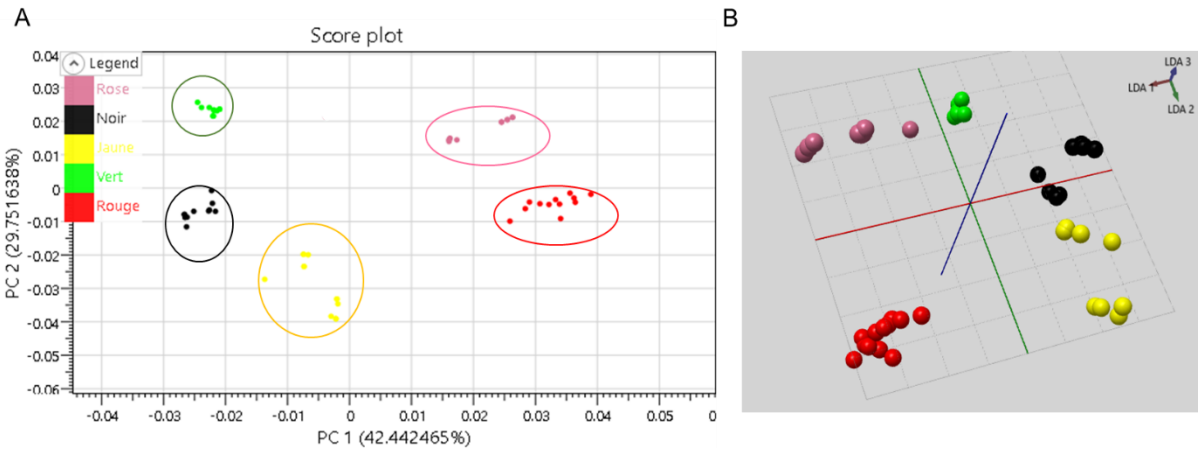

Figure 78: Analysis of Dragibus by vDHS-TD-LTP-MS. Sample were weight and suspended in 200µl of MeOH into 2mL glass and submit to headspace sampling based on vacuum for 40 min at 60°C. A. Score plot PCA representation of dragibus separation. The two first PC explained the variation up to 71%. A. 3D LDA representation of discrimination group color.

The discriminative model explained the VOCs variation by 70% with the two first component. The seperation is well representated on the score plot Figure 78, A and the 3D LDA representation inFigure 78, B. This assay has shown the sentivity of our system to discriminates VOCs groups.

These investigations have proven that the LTP-MS could also be used for control quality of food and beverage.

The LTP-MS offers also the possibility of direct *in vivo* analysis and could open frontiers for a direct rapid, sensitive, precise and accurate analysis of samples in their native environment. The LTP-MS system, enables the *in vivo* and real-time surface analyses of biological tissues without any sample preparation. Sample are therefore in their original state allowing the deciphering of the underlying biological mechanisms. In this context direct analytical system was applied on transgenic mouse spontaneously generating breast carcinoma C3(1)/SV40 T-antigen. The sacrified mouse was placed under the MS inlet, and was moved according to the analised tissue. The LTP probe was directly toward to the sample to analyse the conjonctive tissue, fat, guts and tumor. The Figure 79 represents the samples discrimination explained up to 88% by the two first PCs. This promising application could allow the real time VOCs pattern detection for real time discrimination of healty and disease samples.

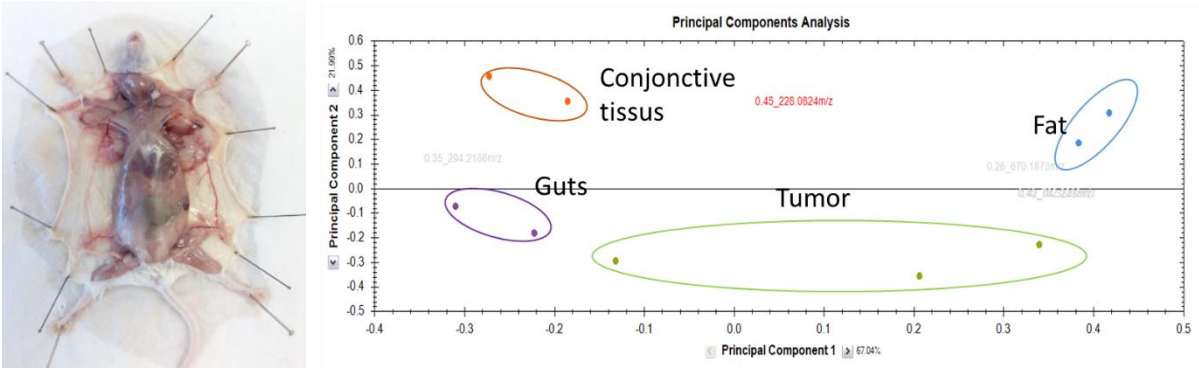

Figure 79: PCA-In vivo analysis of transgenic mice by LTP-MS. The LTP as directly toward to the sample for direct ionisation/desorption. The PCA model explained with the 2PCs up to 88%.

Tremendous applications is offered by the versatile LTP-MS system. First the LTP-MS offer the possibility of real time analysis directly from *in vivo* sample for direct diagnosis into surgery room as SPIDER MASS technique developed at the PRISM laboratory.
Secondly it could be applied for quasi real time analysis of all sample state by TD-LTP-MS system. Analysis purpose could be towards to control quality or cancer or diseases diagnosis.
For instance, the system could be applied as a tool to diagnose the ongoing COVID-19 pandemic. The current testing strategies rely on nasopharyngeal swabs and reverse transcription polymerase chain reaction test (RT-PCR). These techniques are time consuming, with debatable accuracy, remain questionable in terms of sensitivity and can be cost-prohibitive, especially for developing countries. The TD-LTP-MS system have the potential of fast, reliable, non-invasive and versatile VOCs screening tools for accurate identification of symptomatic and asymptomatic carriers to monitor the infection spread efficiently. Even if exhaled breath and saliva samples are currently used for VOCs diagnosis, these samples should be considered as high risk sources in terms of biological hazard. Urine, tears and skin/sweat sample, on the contrary, have the potential of providing an *a priori* safer sample type for diagnosis purpose. Surprisingly, to date, only few VOCs SARS-2 – CoV-2 study were conducted to this purpose[151]. The results of this pilot study supports the implementation of SARS-2 – CoV-2 VOC diagnostic as an approach which could offer an alternative to currently deployed tools, with the tremendous potential advantages of speed, sensitivity, accuracy, non-invasiveness and portability. Moreover, it could inform on processes occurring within the organism for a better understanding of how the virus is metabolized.

References

1. Bray, F. *et al.* Global cancer statistics 2018: GLOBOCAN estimates of incidence and mortality worldwide for 36 cancers in 185 countries. *CA. Cancer J. Clin.* **68**, 394–424 (2018).
2. Wild, C. P. The global cancer burden: necessity is the mother of prevention. *Nat. Rev. Cancer* **19**, 123–124 (2019).
3. Coleman, C. Early Detection and Screening for Breast Cancer. *Semin. Oncol. Nurs.* **33**, 141–155 (2017).
4. Peter C. Fong, M.D., David S. Boss, M.Sc., Timothy A. Yap, M.D., Andrew Tutt, M.D., Ph.D., Peijun Wu, Ph.D., Marja Mergui-Roelvink, M.D., Peter Mortimer, Ph.D., Helen Swaisland, B.Sc., Alan Lau, Ph.D., Mark J. O'Connor, Ph.D., Alan Ashworth, Ph.D., James, P. . New England Journal Medicine. *N. Engl. J. Med.* **361**, 123–134 (2009).
5. Zeeshan, M., Salam, B., Khalid, Q. S. B., Alam, S. & Sayani, R. Diagnostic Accuracy of Digital Mammography in the Detection of Breast Cancer. *Cureus* **10**, (2018).
6. Lee, C. H. *et al.* Breast Cancer Screening With Imaging: Recommendations From the Society of Breast Imaging and the ACR on the Use of Mammography, Breast MRI, Breast Ultrasound, and Other Technologies for the Detection of Clinically Occult Breast Cancer. *J. Am. Coll. Radiol.* **7**, 18–27 (2010).
7. Jaiswal, K. *et al.* Delays in diagnosis and treatment of breast cancer: A safety-net population profile. *JNCCN J. Natl. Compr. Cancer Netw.* **16**, 1451–1457 (2018).
8. Biomarkers - Latest research and news | Nature. Available at: https://www.nature.com/subjects/biomarkers. (Accessed: 13th June 2020)
9. Silva, C., Perestrelo, R., Silva, P., Tomás, H. & Câmara, J. S. *Breast cancer metabolomics: From analytical platforms to multivariate data analysis. A review*. *Metabolites* **9**, (2019).
10. Zhang, A., Sun, H., Yan, G., Wang, P. & Wang, X. Metabolomics for Biomarker Discovery: Moving to the Clinic. *Biomed Res. Int.* **2015**, (2015).
11. Colomer, R. *et al.* Biomarkers in breast cancer: A consensus statement by the Spanish Society of Medical Oncology and the Spanish Society of Pathology. *Clin. Transl. Oncol.* **20**, 815–826 (2018).
12. Budczies, J. *et al.* Comparative metabolomics of estrogen receptor positive and estrogen receptor negative breast cancer: Alterations in glutamine and beta-alanine metabolism. *J. Proteomics* **94**, 279–288 (2013).
13. Patti, G. J., Yanes, O. & Siuzdak, G. Metabolomics: the apogee of the omic triology NIH Public Access. *Nat Rev Mol Cell Biol* (2012). doi:10.1038/nrm3314
14. Schrimpe-Rutledge, A. C., Codreanu, S. G., Sherrod, S. D. & McLean, J. A. Untargeted Metabolomics Strategies—Challenges and Emerging Directions. *J. Am. Soc. Mass Spectrom.* (2016). doi:10.1007/s13361-016-1469-y
15. Metabolomics in Pharmaceutical Research and Development: Metabolites, Mechanisms and Pathways - PubMed. Available at: https://pubmed.ncbi.nlm.nih.gov/19152212/. (Accessed: 13th June 2020)
16. Cumeras, R. Volatilome Metabolomics and Databases, Recent Advances and Needs.

Curr. Metabolomics **5**, 79–89 (2017).

17. Broza, Y. Y., Mochalski, P., Ruzsanyi, V., Amann, A. & Haick, H. Hybrid Volatolomics and Disease Detection. *Angew. Chemie - Int. Ed.* **54**, 11036–11048 (2015).

18. Phillips, M. *et al.* Volatile markers of breast cancer in the breath. *Breast J.* **9**, 184–191 (2003).

19. Kuschner. 乳鼠心肌提取 HHS Public Access. *Physiol. Behav.* **176**, 139–148 (2017).

20. Li, W. *et al.* VOC biomarkers identification and predictive model construction for lung cancer based on exhaled breath analysis: Research protocol for an exploratory study. *BMJ Open* **9**, 1–4 (2019).

21. Amann, A. *et al.* The human volatilome: Volatile organic compounds (VOCs) in exhaled breath, skin emanations, urine, feces and saliva. *J. Breath Res.* **8**, (2014).

22. Martínez-Jarquín, S. & Winkler, R. Low-temperature plasma (LTP) jets for mass spectrometry (MS): Ion processes, instrumental set-ups, and application examples. *TrAC Trends Anal. Chem.* **89**, 133–145 (2017).

23. Hanahan, D. & Weinberg, R. A. Hallmarks of cancer: The next generation. *Cell* **144**, 646–674 (2011).

24. Nicholson, J. K. & Lindon, J. C. Metabonomics. **455**, 1054–1056 (2008).

25. Kennedy, A. D. *et al.* Metabolomics in the clinic: A review of the shared and unique features of untargeted metabolomics for clinical research and clinical testing. *J. Mass Spectrom.* **53**, 1143–1154 (2018).

26. Gorrochategui, E., Jaumot, J., Lacorte, S. & Tauler, R. Data analysis strategies for targeted and untargeted LC-MS metabolomic studies: Overview and workflow. *TrAC - Trends Anal. Chem.* **82**, 425–442 (2016).

27. Kim, K. J. *et al.* A MALDI-MS-based quantitative analytical method for endogenous estrone in human breast cancer cells. *Sci. Rep.* **6**, 4–10 (2016).

28. Martineau, E., Tea, I., Akoka, S. & Giraudeau, P. Absolute quantification of metabolites in breast cancer cell extracts by quantitative 2D 1H INADEQUATE NMR. *NMR Biomed.* **25**, 985–992 (2012).

29. Cífková, E. *et al.* Correlation of lipidomic composition of cell lines and tissues of breast cancer patients using hydrophilic interaction liquid chromatography/electrospray ionization mass spectrometry and multivariate data analysis. *Rapid Commun. Mass Spectrom.* **31**, 253–263 (2017).

30. Hilvo, M. *et al.* Novel theranostic opportunities offered by characterization of altered membrane lipid metabolism in breast cancer progression. *Cancer Res.* **71**, 3236–3245 (2011).

31. Wang, L. *et al.* 1H-NMR based metabonomic profiling of human esophageal cancer tissue. *Mol. Cancer* **12**, 1 (2013).

32. Tenori, L. *et al.* Serum metabolomic profiles evaluated after surgery may identify patients with oestrogen receptor negative early breast cancer at increased risk of disease recurrence. Results from a retrospective study. *Mol. Oncol.* **9**, 128–139 (2015).

33. Manuscript, A. the Detection of Breast Cancer. **686**, 57–63 (2012).

34. Huang, S. *et al.* Novel personalized pathway-based metabolomics models reveal key

metabolic pathways for breast cancer diagnosis. *Genome Med.* **8**, 1–14 (2016).

35. Tsutsui, H. *et al.* High-throughput LC-MS/MS based simultaneous determination of polyamines including N-acetylated forms in human saliva and the diagnostic approach to breast cancer patients. *Anal. Chem.* **85**, 11835–11842 (2013).

36. Cala, M., Aldana, J., Sánchez, J., Guio, J. & Meesters, R. J. W. Urinary metabolite and lipid alterations in Colombian Hispanic women with breast cancer: A pilot study. *J. Pharm. Biomed. Anal.* **152**, 234–241 (2018).

37. Giannoukos, S., Agapiou, A., Brkić, B. & Taylor, S. Volatolomics: A broad area of experimentation. *J. Chromatogr. B Anal. Technol. Biomed. Life Sci.* **1105**, 136–147 (2019).

38. De Lacy Costello, B. *et al.* A review of the volatiles from the healthy human body. *J. Breath Res.* **8**, (2014).

39. Amann, A., Mochalski, P., Ruzsanyi, V., Broza, Y. Y. & Haick, H. Assessment of the exhalation kinetics of volatile cancer biomarkers based on their physicochemical properties. *J. Breath Res.* **8**, (2014).

40. Kramer, C. *et al.* Prediction of blood:air and fat:Air partition coefficients of volatile organic compounds for the interpretation of data in breath gas analysis. *J. Breath Res.* **10**, (2016).

41. Manuscript, A. Europe PMC Funders Group Prediction of blood : air and fat : air partition coefficients of volatile organic compounds for the interpretation of data in breath gas. **10**, 1–17 (2016).

42. Calenic, B. *et al.* Oxidative stress and volatile organic compounds: Interplay in pulmonary, cardio-vascular, digestive tract systems and cancer. *Open Chem.* **13**, 1020–1030 (2015).

43. Boots, A. W. *et al.* The versatile use of exhaled volatile organic compounds in human health and disease. *Journal of Breath Research* (2012). doi:10.1088/1752-7155/6/2/027108

44. Leung, T. *et al.* Cytochrome P450 2E1 (CYP2E1) regulates the response to oxidative stress and migration of breast cancer cells. *Breast Cancer Res.* **15**, (2013).

45. Shirasu, M. & Touhara, K. The scent of disease: Volatile organic compounds of the human body related to disease and disorder. *J. Biochem.* **150**, 257–266 (2011).

46. He, J., Zou, Z. & Yang, X. Measuring whole-body volatile organic compound emission by humans: A pilot study using an air-tight environmental chamber. *Build. Environ.* **153**, 101–109 (2019).

47. Unal, B., Karaveli, F. S., Pestereli, H. E. & Erdogan, G. Determination of HER2 gene amplification in breast cancer using dual-color silver enhanced in situ hybridization (dc- SISH) and comparison with fluorescence ISH (FISH). *Asian Pacific J. Cancer Prev.* **14**, 6131–6134 (2013).

48. Park, S. *et al.* Characteristics and outcomes according to molecular subtypes of breast cancer as classified by a panel of four biomarkers using immunohistochemistry. *Breast* **21**, 50–57 (2012).

49. Prokop-Prigge, K. A., Thaler, E., Wysocki, C. J. & Preti, G. Identification of volatile organic compounds in human cerumen. *J. Chromatogr. B Anal. Technol. Biomed. Life Sci.* **953**–**954**, 48–52 (2014).

50. Phillips, M. *et al.* Volatile biomarkers in the breath of women with breast cancer. *J. Breath Res.* **4**, (2010).

51. Mangler, M. *et al.* Volatile organic compounds (VOCs) in exhaled breath of patients with breast cancer in a clinical setting. *Ginekol. Pol.* **83**, 730–736 (2012).

52. Taware, R. *et al.* Volatilomic insight of head and neck cancer via the effects observed on saliva metabolites. *Sci. Rep.* **8**, 1–10 (2018).

53. Cavaco, C. *et al.* Screening of salivary volatiles for putative breast cancer discrimination: an exploratory study involving geographically distant populations. *Anal. Bioanal. Chem.* **410**, 4459–4468 (2018).

54. Shigeyama, H., Wang, T., Ichinose, M., Ansai, T. & Lee, S. W. Identification of volatile metabolites in human saliva from patients with oral squamous cell carcinoma via zeolite-based thin-film microextraction coupled with GC–MS. *J. Chromatogr. B Anal. Technol. Biomed. Life Sci.* **1104**, 49–58 (2019).

55. Dormont, L., Bessière, J. M. & Cohuet, A. Human Skin Volatiles: A Review. *J. Chem. Ecol.* **39**, 569–578 (2013).

56. Riazanskaia, S., Blackburn, G., Harker, M., Taylor, D. & Thomas, C. L. P. The analytical utility of thermally desorbed polydimethylsilicone membranes for in-vivo sampling of volatile organic compounds in and on human skin. *Analyst* **133**, 1020–1027 (2008).

57. Silva, C. L., Perestrelo, R., Silva, P., Tomás, H. & Câmara, J. S. Implementing a central composite design for the optimization of solid phase microextraction to establish the urinary volatomic expression: a first approach for breast cancer. *Metabolomics* **15**, 1–13 (2019).

58. Porto-Figueira, P., Pereira, J., Miekisch, W. & Câmara, J. S. Exploring the potential of NTME/GC-MS, in the establishment of urinary volatomic profiles. Lung cancer patients as case study. *Sci. Rep.* **8**, 1–11 (2018).

59. Batty, C. A., Cauchi, M., Lourenço, C., Hunter, J. O. & Turner, C. Use of the analysis of the volatile faecal metabolome in screening for colorectal cancer. *PLoS One* **10**, 1–14 (2015).

60. Dharmawardana, N., Woods, C., Watson, D. I., Yazbeck, R. & Ooi, E. H. A review of breath analysis techniques in head and neck cancer. *Oral Oncol.* **104**, 104654 (2020).

61. Schon, S., Theodore, S. J. & Güntner, A. T. Versatile breath sampler for online gas sensor analysis. *Sensors Actuators, B Chem.* **273**, 1780–1785 (2018).

62. Del Nogal Sánchez, M., Hernández García, E., Pérez Pavón, J. L. & Moreno Cordero, B. Fast analytical methodology based on mass spectrometry for the determination of volatile biomarkers in saliva. *Anal. Chem.* **84**, 379–385 (2012).

63. F. Streckfus, C. Salivary Biomarkers to Assess Breast Cancer Diagnosis and Progression: Are We There Yet? *Saliva and Salivary Diagnostics* (2019). doi:10.5772/intechopen.85762

64. Martin, H. J. *et al.* Volatile organic compound markers of psychological stress in skin: A pilot study. *J. Breath Res.* **10**, 46012 (2016).

65. Böhm, D. *et al.* Comparison of tear protein levels in breast cancer patients and healthy controls using a de novo proteomic approach. *Oncol. Rep.* **28**, 429–438 (2012).

66. Zhou, L. & Beuerman, R. W. Tear analysis in ocular surface diseases. *Prog. Retin.*

Eye Res. **31**, 527–550 (2012).

67. Dewulf, J., Van Langenhove, H. & Wittmann, G. Analysis of volatile organic compounds using gas chromatography. *TrAC - Trends Anal. Chem.* **21**, 637–646 (2002).

68. Vyviurska, O., Zvršková, H. & Špánik, I. Distribution of enantiomers of volatile organic compounds in selected fruit distillates. *Chirality* **29**, 14–18 (2017).

69. Uozumi, T. & Hirotsu, T. Development of an early cancer detection method using the olfaction of the nematode caenorhabditis elegans. *Yakugaku Zasshi* **139**, 759–765 (2019).

70. McCulloch, M. *et al.* Diagnostic accuracy of canine scent detection in early- and late-stage lung and breast cancers. *Integr. Cancer Ther.* **5**, 30–39 (2006).

71. Thuleau, A. *et al.* A new transcutaneous method for breast cancer detection with dogs. *Oncol.* **96**, 110–113 (2019).

72. Institut Curie DOSSIER DE PRESSE 2017. (2017).

73. Tothill, I. E. & Turner, A. P. F. Biosensor : an overview. 108–123 (2003). doi:10.1201/9781351074933

74. Fu, X. *et al.* Ultra-fast and highly selective room-temperature formaldehyde gas sensing of Pt-decorated MoO3 nanobelts. *J. Alloys Compd.* (2019). doi:10.1016/j.jallcom.2019.05.145

75. Yang, S. *et al.* Zn doped MoO 3 nanobelts and the enhanced gas sensing properties to ethanol. *Appl. Surf. Sci.* (2017). doi:10.1016/j.apsusc.2016.10.021

76. Qin, H., Cao, Y., Xie, J., Xu, H. & Jia, D. Solid-state chemical synthesis and xylene-sensing properties of A-MoO3 arrays assembled by nanoplates. *Sensors Actuators, B Chem.* (2017). doi:10.1016/j.snb.2016.11.081

77. Bohli, N., Belkilani, M., Casanova-Chafer, J., Llobet, E. & Abdelghani, A. Multiwalled carbon nanotube based aromatic volatile organic compound sensor: Sensitivity enhancement through 1-hexadecanethiol functionalisation. *Beilstein J. Nanotechnol.* **10**, 2364–2373 (2019).

78. Devkota, J., Ohodnicki, P. R. & Greve, D. W. SAW sensors for chemical vapors and gases. *Sensors (Switzerland)* **17**, 13–15 (2017).

79. Shen, C. Y. & Liou, S. Y. Surface acoustic wave gas monitor for ppm ammonia detection. *Sensors Actuators, B Chem.* (2008). doi:10.1016/j.snb.2007.12.061

80. Liu, L., Morgan, S. P., Correia, R., Lee, S. W. & Korposh, S. Multi-Parameter Optical Fiber Sensing of Gaseous Ammonia and Carbon Dioxide. *J. Light. Technol.* (2020). doi:10.1109/JLT.2019.2953271

81. Liu, L. L. *et al.* A reflection-mode fibre-optic sensor for breath carbon dioxide measurement in healthcare. *Sens. Bio-Sensing Res.* (2019). doi:10.1016/j.sbsr.2018.100254

82. Afsari, A. & Sarraf, M. J. Design of a hydrogen sulfide gas sensor based on a photonic crystal cavity using graphene. *Superlattices Microstruct.* (2020). doi:10.1016/j.spmi.2019.106362

83. Rezende, G. C., Le Calvé, S., Brandner, J. J. & Newport, D. Micro milled microfluidic photoionization detector for volatile organic compounds. *Micromachines* (2019). doi:10.3390/mi10040228

84. ethanol, nitrous oxide (anesthesia), 13 carbon compounds. b. Analysis of specific endogenous compounds,. 1–38

85. Smith, D., Španěl, P., Herbig, J. & Beauchamp, J. Mass spectrometry for real-time quantitative breath analysis. *Journal of Breath Research* **8**, (2014).

86. Španěl, P. & Smith, D. Progress in SIFT-MS: Breath analysis and other applications. *Mass Spectrom. Rev.* **30**, 236–267 (2011).

87. Smith, D. & Španěl, P. SIFT-MS and FA-MS methods for ambient gas phase analysis: Developments and applications in the UK. *Analyst* **140**, 2573–2591 (2015).

88. Davey, N. G., Krogh, E. T. & Gill, C. G. Membrane-introduction mass spectrometry (MIMS). *TrAC - Trends in Analytical Chemistry* (2011). doi:10.1016/j.trac.2011.05.003

89. Johnson, R. C., Cooks, R. G., Allen, T. M., Cisper, M. E. & Hemberger, P. H. Membrane introduction mass spectrometry: Trends and applications. *Mass Spectrom. Rev.* **19**, 1–37 (2000).

90. Davey, N. G., Bell, R. J., Krogh, E. T. & Gill, C. G. A membrane introduction mass spectrometer utilizing ion-molecule reactions for the on-line speciation and quantitation of volatile organic molecules. *Rapid Commun. Mass Spectrom.* **29**, 2187–2194 (2015).

91. Baumbach, J. I. Process analysis using ion mobility spectrometry. *Anal. Bioanal. Chem.* **384**, 1059–1070 (2006).

92. Pietrzak, D. & Bieliński, D. M. Application of multi-capillary column – ion mobility spectrometry (MCC-IMS) in rubber chemistry and technology. *Int. J. Ion Mobil. Spectrom.* **21**, 1–9 (2018).

93. Hernández-Mesa, M. *et al.* Ion mobility spectrometry in food analysis: Principles, current applications and future trends. *Molecules* (2019). doi:10.3390/molecules24152706

94. Jünger, M. *et al.* Ion mobility spectrometry for microbial volatile organic compounds: A new identification tool for human pathogenic bacteria. *Appl. Microbiol. Biotechnol.* (2012). doi:10.1007/s00253-012-3924-4

95. Perl, T. *et al.* Determination of serum propofol concentrations by breath analysis using ion mobility spectrometry. *Br. J. Anaesth.* **103**, 822–827 (2009).

96. Westhoff, M. *et al.* Ion mobility spectrometry for the detection of volatile organic compounds in exhaled breath of patients with lung cancer: Results of a pilot study. *Thorax* **64**, 744–748 (2009).

97. Fernández, F. M. & Garcia-Reyes, J. F. Ambient mass spectrometry. *Anal. Methods* **9**, 4894–4895 (2017).

98. Farré, M. & Barceló, D. *Ambient Ionization Techniques*. *Comprehensive Analytical Chemistry* **68**, (Elsevier, 2015).

99. Takáts, Z., Wiseman, J. M. & Cooks, R. G. Ambient mass spectrometry using desorption electrospray ionization (DESI): instrumentation, mechanisms and applications in forensics, chemistry, and biology. *J. Mass Spectrom.* **40**, 1261–1275 (2005).

100. Takáts, Z., Wiseman, J. M., Gologan, B. & Cooks, R. G. Mass spectrometry sampling under ambient conditions with desorption electrospray ionization. *Science (80-.).* (2004). doi:10.1126/science.1104404

101. Otles, S. & Hazal Ozyurt, V. Direct Analysis in Real Time Mass Spectrometry. *Ambient*

Mass Spectrosc. Tech. Food Environ. 95–104 (2019). doi:10.1201/9781315146836-5

102. Pitman, C. N. & LaCourse, W. R. Desorption atmospheric pressure chemical ionization: A review. *Anal. Chim. Acta* (2020). doi:10.1016/j.aca.2020.05.073

103. Ratcliffe, L. V. *et al.* Surface analysis under ambient conditions using plasma-assisted desorption/ionization mass spectrometry. *Anal. Chem.* **79**, 6094–6101 (2007).

104. Na, N., Zhao, M., Zhang, S., Yang, C. & Zhang, X. Development of a Dielectric Barrier Discharge Ion Source for Ambient Mass Spectrometry. *J. Am. Soc. Mass Spectrom.* **18**, 1859–1862 (2007).

105. Harper, J. D. *et al.* Low-Temperature Plasma Probe for Ambient Desorption Ionization. *Anal. Chem.* **80**, 9097–9104 (2008).

106. Bee-DiGregorio, M. Y., Feng, H., Pan, B. S., Dokoozlian, N. K. & Sacks, G. L. Polymeric sorbent sheets coupled to direct analysis in real time mass spectrometry for trace-level volatile analysis—a multi-vineyard evaluation study. *Foods* **9**, (2020).

107. Yew, J. Y. Natural product discovery by direct analysis in real time mass spectrometry. *Mass Spectrom.* **8**, (2019).

108. Harper, J. D. *et al.* Low-temperature plasma probe for ambient desorption ionization. *Anal. Chem.* **80**, 9097–9104 (2008).

109. Kogelschatz, U. *et al.* Dielectric-Barrier Discharges . Principle and Applications To cite this version : *J. Phys. Iv* (1997).

110. Adamovich, I. *et al.* The 2017 Plasma Roadmap: Low temperature plasma science and technology. *Journal of Physics D: Applied Physics* (2017). doi:10.1088/1361-6463/aa76f5

111. Lim, D. K. *et al.* Non-destructive profiling of volatile organic compounds using HS-SPME/GC–MS and its application for the geographical discrimination of white rice. *J. Food Drug Anal.* **26**, 260–267 (2018).

112. Ziuzina, D. & Misra, N. N. Cold Plasma for Food Safety. in *Cold Plasma in Food and Agriculture: Fundamentals and Applications* 223–252 (Elsevier, 2016). doi:10.1016/B978-0-12-801365-6.00009-3

113. Martínez-Jarquín, S., Herrera-Ubaldo, H., de Folter, S. & Winkler, R. In vivo monitoring of nicotine biosynthesis in tobacco leaves by low-temperature plasma mass spectrometry. *Talanta* **185**, 324–327 (2018).

114. Albert, A., Kramer, A., Scheeren, S. & Engelhard, C. Rapid and quantitative analysis of pesticides in fruits by QuEChERS pretreatment and low-temperature plasma desorption/ionization orbitrap mass spectrometry. *Anal. Methods* **6**, 5463–5471 (2014).

115. Mirabelli, M. F., Gionfriddo, E., Pawliszyn, J. & Zenobi, R. A quantitative approach for pesticide analysis in grape juice by direct interfacing of a matrix compatible SPME phase to dielectric barrier discharge ionization-mass spectrometry. *Analyst* **143**, 891–899 (2018).

116. WANG, S., WANG, Z., HOU, K.-Y. & LI, H.-Y. Thermal Desorption Low Temperature Plasma Ionization Mass Spectrometry for Rapid and Sensitive Detection of Pesticides in Broomcorn. *Chinese J. Anal. Chem.* **45**, 175–182 (2017).

117. Wu, A. S. *et al.* Porcine intact and wounded skin responses to atmospheric nonthermal plasma. *J. Surg. Res.* **179**, e1–e12 (2013).

118. Daeschlein, G. *et al.* Skin decontamination by low-temperature atmospheric pressure plasma jet and dielectric barrier discharge plasma. *J. Hosp. Infect.* **81**, 177–183 (2012).

119. Šimončicová, J., Kryštofová, S., Medvecká, V., Ďurišová, K. & Kaliňáková, B. Technical applications of plasma treatments: current state and perspectives. *Appl. Microbiol. Biotechnol.* **103**, 5117–5129 (2019).

120. Winkler, R. & Rosas-Román, I. Contrast Optimization of Mass Spectrometry Imaging (MSI) Data Visualization by Threshold Intensity Quantization (TrIQ). (2020). doi:10.26434/chemrxiv.12312251

121. Nørgaard, A. W., Kofoed-Sørensen, V., Svensmark, B., Wolkoff, P. & Clausen, P. A. Gas chromatography interfaced with atmospheric pressure ionization-quadrupole time-of-flight-mass spectrometry by low-temperature plasma ionization. *Anal. Chem.* **85**, 28–32 (2013).

122. Garcia-Reyes, J. F. *et al.* Detection of explosives and related compounds by low-temperature plasma ambient ionization mass spectrometry. *Anal. Chem.* (2011). doi:10.1021/ac1029117

123. Wiley, J. S., Shelley, J. T. & Cooks, R. G. Handheld low-temperature plasma probe for portable 'point-and- shoot' ambient ionization mass spectrometry. *Anal. Chem.* **85**, 6545–6552 (2013).

124. Wiley, J. S. INSTRUMENTATION, APPLICATIONS AND FUNDAMENTALS OF PLASMA IONIZATION OF ORGANIC MOLECULES FROM SURFACESs. *Thesis* 228 (2013).

125. Wolf, J. C. *et al.* A Radical-Mediated Pathway for the Formation of [M + H]+ in Dielectric Barrier Discharge Ionization. *J. Am. Soc. Mass Spectrom.* **27**, 1468–1475 (2016).

126. Miekisch, W. *et al.* Impact of sampling procedures on the results of breath analysis. *J. Breath Res.* (2008). doi:10.1088/1752-7155/2/2/026007

127. Liu, H., Xu, B., Wei, K., Yu, Y. & Long, C. Adsorption of low-concentration VOCs on various adsorbents: Correlating partition coefficient with surface energy of adsorbent. *Sci. Total Environ.* (2020). doi:10.1016/j.scitotenv.2020.139376

128. Borusiewicz, R. & Zięba-Palus, J. Comparison of the effectiveness of Tenax TA® and Carbotrap 300® in concentration of flammable liquids compounds. *J. Forensic Sci.* **52**, 70–74 (2007).

129. Pawliszyn, J. Theory of Solid-Phase Microextraction. in *Handbook of Solid Phase Microextraction* (2012). doi:10.1016/B978-0-12-416017-0.00002-4

130. Pawliszyn, J. Theory of solid-phase microextraction. *Journal of Chromatographic Science* (2000). doi:10.1093/chromsci/38.7.270

131. Kędziora, K. & Wasiak, W. Extraction media used in needle trap devices—Progress in development and application. *J. Chromatogr. A* **1505**, 1–17 (2017).

132. Truong, T. V. *et al.* Trace Analysis in the Field Using Gas Chromatography-Mass Spectrometry. *Sci. Chromatogr.* **6**, 13–26 (2014).

133. Martínez-Jarquín, S., Moreno-Pedraza, A., Guillén-Alonso, H. & Winkler, R. Template for 3D Printing a Low-Temperature Plasma Probe. *Anal. Chem.* **88**, 6976–6980 (2016).

134. Martínez-Jarquín, S. & Winkler, R. Design of a low-temperature plasma (LTP) probe with adjustable output temperature and variable beam diameter for the direct detection of organic molecules. *Rapid Commun. Mass Spectrom.* **27**, 629–634 (2013).

135. Ateacha, D. N., Kuhlmann, C. & Engelhard, C. Rapid screening of antimalarial drugs using low-temperature plasma desorption/ionization Orbitrap mass spectrometry. *Anal. Methods* **11**, 566–574 (2019).

136. Benassi, M. *et al.* Petroleum crude oil analysis using low-temperature plasma mass spectrometry. *Rapid Commun. Mass Spectrom.* (2013). doi:10.1002/rcm.6518

137. Jafari, M. T. Low-temperature plasma ionization ion mobility spectrometry. *Anal. Chem.* (2011). doi:10.1021/ac1022937

138. Kuklya, A. *et al.* Low-Temperature Plasma Ionization Differential Ion Mobility Spectrometry. *Anal. Chem.* (2015). doi:10.1021/acs.analchem.5b02077

139. Cai, Y., Kingery, D., McConnell, O. & Bach, A. C. Advantages of atmospheric pressure photoionization mass spectrometry in support of drug discovery. *Rapid Commun. Mass Spectrom.* (2005). doi:10.1002/rcm.1981

140. Nørgaard, A. W., Vibenholt, A., Benassi, M., Clausen, P. A. & Wolkoff, P. Study of Ozone-Initiated Limonene Reaction Products by Low Temperature Plasma Ionization Mass Spectrometry. *J. Am. Soc. Mass Spectrom.* **24**, 1090–1096 (2013).

141. Valadbeigi, Y., Ilbeigi, V., Michalczuk, B., Sabo, M. & Matejcik, S. Study of Atmospheric Pressure Chemical Ionization Mechanism in Corona Discharge Ion Source with and without NH 3 Dopant by Ion Mobility Spectrometry combined with Mass Spectrometry: A Theoretical and Experimental Study. *J. Phys. Chem. A* (2019). doi:10.1021/acs.jpca.8b11417

142. Silva, C. L., Perestrelo, R., Silva, P., Tomás, H. & Câmara, J. S. Volatile metabolomic signature of human breast cancer cell lines. *Sci. Rep.* (2017). doi:10.1038/srep43969

143. Gong, X., Shi, S. & Gamez, G. Real-Time Quantitative Analysis of Valproic Acid in Exhaled Breath by Low Temperature Plasma Ionization Mass Spectrometry. *J. Am. Soc. Mass Spectrom.* **28**, 678–687 (2017).

144. Albert, A. & Engelhard, C. Chemometric optimization of a low-temperature plasma source design for ambient desorption/ionization mass spectrometry. *Spectrochim. Acta - Part B At. Spectrosc.* (2015). doi:10.1016/j.sab.2014.08.034

145. Lavra, L. *et al.* Investigation of VOCs associated with different characteristics of breast cancer cells. *Sci. Rep.* (2015). doi:10.1038/srep13246

146. Penn, D. J. *et al.* Individual and gender fingerprints in human body odour. *J. R. Soc. Interface* **4**, 331–340 (2007).

147. Huang, Y., Li, Y., Luo, Z. & Duan, Y. Investigation of biomarkers for discriminating breast cancer cell lines from normal mammary cell lines based on VOCs analysis and metabolomics. *RSC Adv.* (2016). doi:10.1039/c6ra03238a

148. Alanazi, S. A., Aldawood, M. A., Badawood, Y. S., El-Hiti, G. A. & Masmali, A. M. A comparative study of the quality of non-stimulated and stimulated tears in normal eye male subjects using the tear ferning test. *Clin. Optom.* **11**, 65–71 (2019).

149. Woollam, M. *et al.* Detection of Volatile Organic Compounds (VOCs) in Urine via Gas Chromatography-Mass Spectrometry QTOF to Differentiate Between Localized and Metastatic Models of Breast Cancer. *Sci. Rep.* (2019). doi:10.1038/s41598-019-38920-0

150. Zhang, L. *et al.* Discovery and preclinical validation of salivary transcriptomic and proteomic biomarkers for the non- invasive detection of breast cancer. *PLoS One* **5**, 1–7 (2010).

151. Jendrny, P. *et al.* Scent dog identification of samples from COVID-19 patients - A pilot study. *BMC Infect. Dis.* **20**, 1–7 (2020).

Summary
Breast cancer (BC) is the second most prevalent cancer in women. To date, early diagnosis is central in cancer care since it is directly related to the prognostic, evolution and survival of patients. For instance, the 5-year survival rate for BC drops drastically if the pathology is diagnosed at a later state, from 80% at stage II to 22% at stage IV for metastatic cancer. Analysis of Volatile Organic Compounds (VOCs) is a promising approach for achieving accurate and non-invasive molecular classification of cancer from exhaled breath and body fluids.Numerous VOCs strategies are time consuming, labour intensive with many steps of sample handling, whereas the ambient source Low temperature plasma (LTP) allows real-time analysis of VOCs from surfaces and complex matrices. LTP enables the ambient soft ionization and desorption of molecules from solid, liquid, and gaseous materials.
The main objective was the development of a LTP-MS system for the real and quasi-real time diagnosis of BC based on VOCs signature. The first attempt was the discrimination of cell lines from different pathology and BC cell lines (SKBR3, MCF7, MDA) according to their VOCs signature using Tenax TA disc as sorbent membrane. To capture VOCs from cell culture, a dynamic headspace sampling based on vacuum was performed for 40 minutes at 37°c in a 2ml glass vial. Data were processed using model builder (Waters) principal component analysis (PCA), which showed accurate, specific and sensitive model group discrimination and highlight two BC compounds 2-nonanone and cyclohexanol which their levels differ from BC cell line. The second objective was the application of the developed TD-LTP-MS system to study the VOCs from the BC and healthy patients. Urine, saliva, tears and skin/ sweat sample were collect in this context. Sampling with pre-concentration (urine, skin/sweat) and without pre-concentration (saliva, tears) allows the discrimination groups between healthy and cancerous patient. All these results have shown that VOCs can be used as a signature of cancers and coupled to a LTP-MS technology allows a rapid, costless, non-invasive real and quasi real time diagnosis of patients.

Résumé
Le cancer du sein est le deuxième cancer le plus répandu chez les femmes dans le monde. À ce jour, le diagnostic précoce est au cœur des soins contre le cancer car il est directement lié au pronostic, à l'évolution et à la survie des patients. Par exemple, le taux de survie à 5 ans pour cancer du sein diminue considérablement si la pathologie est diagnostiquée à un stade tardif, il passe de 80% au stade II à 22% au stade IV pour un cancer au stade métastatique. L'analyse des composés organiques volatiles (COV) est une approche prometteuse pour obtenir une classification moléculaire précise et non invasive du cancer à partir de l'air exhalé et des fluides corporels. Les nombreuses stratégies pour les COV prennent du temps et demandent de nombreuses étapes de manipulation des échantillons, tandis que la source ambiante plasma à basse température (LTP) permet une analyse en temps réel des COV à partir d surfaces et des matrices complexes sans aucune séparation préalable de l'échantillon. Le LTP permet simultanément une ionisation douce et une désorption de molécules à partir d'echantillon solides, liquides et gazeux. L'objectif principal était le développement d'un système LTP-MS pour le diagnostic en temps réel et quasi-réel du cancer du sein basé sur la signature des COVs.
La première tentative a été la discrimination des lignées cellulaires de différentes pathologies puis de mêmes pathologies (SKBR3, MCF7, MDA) en fonction de leur signature COV en utilisant le disque Tenax TA comme membrane adsorbent. La capture des COV à partir de culture cellulaire, c'est fait par un échantillonnage dynamique de l'espace de tête basé sur l'aspiration effectué pendant 40 minutes à 37 °C dans un vial en verre de 2 ml. Les données ont été traitées par analyse des analyse par composantes principal (APC) qui a montré une discrimination précise, spécifique et sensible des groupes cellulaire mettant ainsi en évidence deux composés connu et lié au cancer du sein le 2-nonanone et cyclohexanol.
Le deuxième objectif était l'application du système TD-LTP-MS développé pour étudier les COV émis de patient cancéreux et sain. Des échantillons d'urine, de salive, de larmes et de peau / sueur ont été collectés dans ce contexte. L'échantillonnage avec pré-concentration (urine, peau / sueur) et sans pré-concentration (salive, larmes) permet de distinguer les groupes entre patient sain et cancéreux. Tous ces résultats ont montré que les COV peuvent être utilisés comme signature de cancers et couplés à une technologie LTP-MS, il permet un diagnostic rapide, abordable, non invasif en temps réel et quasi en temps réel des patients.